Deposition, positioning and dynamics of H2A.Z in *Saccharomyces cerevisiae*

DISSERTATION ZUR ERLANGUNG DES DOKTORGRADES DER NATURWISSENSCHAFTEN (DR. RER. NAT.) DER FAKULTÄT FÜR BIOLOGIE UND VORKLINISCHE MEDIZIN DER UNIVERSITÄT REGENSBURG

vorgelegt von
Claudia Huber
aus Bogen

Mai 2012

Das Promotionsgesuch wurde eingereicht am: 22. Mai 2012

Die Arbeit wurde angeleitet von: Prof. Dr. Gernot Längst

Prüfungsausschuss:

Vorsitzender:	Prof. Dr. Christoph Oberprieler
1. Prüfer:	Prof. Dr. Gernot Längst
2. Prüfer:	Prof. Dr. Klaus Grasser
3. Prüfer:	Prof. Dr. Michael Thomm

Die vorliegende Arbeit wurde in der Zeit von Februar 2008 bis Mai 2012 am Lehrstuhl Biochemie III des Instituts für Biochemie, Genetik und Mikrobiologie der Naturwissenschaftlichen Fakultät III der Universität Regensburg unter Anleitung von Prof. Dr. Gernot Längst angefertigt.

Ich erkläre hiermit, dass ich diese Arbeit selbst verfasst und keine anderen als die genannten Quellen und Hilfsmittel verwendet habe.
Diese Arbeit war bisher noch nicht Bestandteil eines Prüfungsverfahrens.
Andere Promotionsversuche wurden nicht unternommen.

Claudia Huber

Regensburg, den 22. Mai 2012

“If you can find a path with no obstacles,

it probably doesn’t lead anywhere”

(Frank A. Clark)

Table of Contents

ABBREVIATIONS ..... **VII**

1 SUMMARY **1**

2 INTRODUCTION **3**

2.1 NUCLEOSOME STRUCTURE 3

2.1.1 Nucleosome positioning *4*

2.2 REGULATING FACTORS OF CHROMATIN 5

2.2.1 Posttranslational modifications of histones *6*

2.2.2 DNA methylation *7*

2.2.3 Chromatin remodeling *7*

2.2.4 Histone variants *9*

2.3 CHROMATIN DYNAMICS 11

2.3.1 Chromatin dynamics during replication *11*

2.3.2 Chromatin dynamics during transcription *12*

2.4 HISTONE VARIANT H2A.Z 13

2.4.1 Unique properties distinguish H2A.Z- from H2A-containing nucleosomes *15*

2.4.2 Splice isoforms of H2A.Z *18*

2.4.3 Specialized functions of H2A.Z *18*

2.4.4 H2A.Z specific posttranslational modification patterns associated with function *21*

2.4.5 Deposition of H2A.Z into pre-formed nucleosomes *22*

3 OBJECTIVES **27**

3.1 MECHANISMS OF H2A.Z DEPOSITION 27

3.2 *IN VITRO* AND *IN VIVO* POSITIONING DIFFERENCES OF HISTONE VARIANTS 27

3.3 NOVEL ROLES FOR THE H2A C-TERMINAL TAIL IN NUCLEOSOME STABILITY, MOBILITY AND BINDING OF LINKER HISTONE H1 28

4 RESULTS **29**

4.1 DEPOSITION OF H2A.Z IN *SACCHAROMYCES CEREVISIAE* 29

4.1.1 Preliminary analysis of selected genomic regions *29*

4.1.2 Known H2A.Z binding sites can be mapped using Chromatin Endogenous Cleavage analysis (ChEC) *31*

4.1.3 Core histones are enriched at promoters when they are expressed constitutively *33*

4.1.4 H2A.Z is depleted within the ORF region rather than enriched at the promoter *38*

4.1.5 H2A.Z depletion from coding regions might correlate with transcription levels at the respective genes *40*

4.1.6 The H2A.Z deposition pattern is established independently of the SWR complex *44*

4.1.7 ChIP analysis of the SWRc influence *45*
4.2 DYNAMICS AND POSITIONING OF VARIANT NUCLEOSOMES 49
4.2.1 Variant and canonical nucleosomes show similar dynamics during thermal sliding *49*
4.2.2 Positioning differences of variant nucleosomes in vitro *50*
4.2.3 ChEC shows in vivo nucleosome positioning differences *55*
4.2.4 The INO80 complex contributes to nucleosome positioning in vivo *56*
4.3 HISTONE H2A C-TERMINUS REGULATES CHROMATIN DYNAMICS, REMODELING AND HISTONE H1 BINDING 58
4.3.1 Influence of the H2A C-terminal tail on nucleosome assembly and mobility *58*
4.3.2 Truncations of the H2A C-terminus affect nucleosome remodeling *59*
4.3.3 The C-terminus of H2A interacts with linker histone H1 ..... *61*

5 DISCUSSION 63

5.1 MECHANISMS OF H2A.Z DEPOSITION 63
5.1.1 Transcription is crucial for the establishment of H2A.Z enrichment patterns *63*
5.1.2 The H2A.Z enrichment pattern is established independently of the SWR complex *66*
5.1.3 Explaining ChEC and ChIP discrepancies *67*
5.2 DYNAMICS AND POSITIONING OF VARIANT NUCLEOSOMES 69
5.2.1 In vivo nucleosome stability might depend on more than pure histone content *69*
5.2.2 H2A.Z influences nucleosome positioning in vitro and in vivo *70*
5.2.3 The INO80 complex influences nucleosome positions *73*
5.3 HISTONE H2A C-TERMINUS REGULATES CHROMATIN DYNAMICS, REMODELING AND HISTONE H1 BINDING 74
5.3.1 Dynamics and nucleosome positioning are influenced by the H2A C-terminal tail . *74*
5.3.2 The H2A C-terminal tail is necessary for efficient chromatin remodeling *74*
5.3.3 The H2A C-terminus as a new targeting domain for H1? *75*

6 OUTLOOK 77

6.1 FURTHER EXPERIMENTS ON THE ROLE OF H2A.Z IN TRANSCRIPTION COMPETENT CHROMATIN STATES 77
6.2 *IN VIVO* POSITIONING OF H2A.Z 77
6.3 THE C-TERMINAL H2A TAIL AS A NEW FACTOR IN CHROMATIN REGULATION 78

7 MATERIAL 79

7.1 CHEMICALS 79
7.2 BUFFERS AND MEDIA 79
7.3 NUCLEIC ACIDS 83
7.3.1 Oligonucleotides *83*
7.3.2 Plasmids *92*
7.3.3 DNA probes for Southern Blot detection *94*
7.4 ENZYMES AND POLYPEPTIDES 95
7.5 ORGANISMS 95

7.5.1 Bacteria 95
7.5.2 Yeast strains 95
7.6 SOFTWARE AND ONLINE TOOLS 97
7.6.1 Software 97
7.6.2 Online tools 97
7.7 CONSUMABLES 98
7.8 APPARATUS 99

8 METHODS 101

8.1 DNA 101
8.1.1 Enzymatic manipulation of DNA 101
8.1.2 Purification of nucleic acids 102
8.1.3 Quantitative and qualitative analysis of nucleic acids 103
8.1.4 Formaldehyde crosslink 104
8.1.5 Preparation of nuclei 104
8.1.6 Chromatin Endogenous Cleavage (ChEC) 105
8.1.7 Unspecific endonuclease digestion (MNase) 106
8.1.8 Southern Blot, Hybridization and detection of radioactive probes 106
8.1.9 Chromatin Immuno Precipitation (ChIP) 108
8.1.10 Quantitative real-time PCR (qPCR) 109
8.2 MANIPULATION OF *ESCHERICHIA COLI* 110
8.2.1 Liquid culture 110
8.2.2 Glycerol stock 110
8.2.3 Preparation of chemically competent bacteria 110
8.2.4 Transformation of competent bacteria 110
8.3 MANIPULATION OF *SACCHAROMYCES CEREVISIAE* 111
8.3.1 Liquid culture 111
8.3.2 Glycerol stock 111
8.3.3 Preparation of competent yeast cells 111
8.3.4 Transformation of competent yeast cells 111
8.3.5 Establishment of knock out strains 112
8.3.6 Establishment of MNase fusion strains for histones expressed under the control of the H2A.Z promoter 112
8.4 PROTEIN-BIOCHEMICAL METHODS 112
8.4.1 Denaturing protein extraction from yeast cells 112
8.4.2 SDS-polyacrylamide gel electrophoresis 113
8.4.3 Coomassie staining of SDS polyacrylamide gels 113
8.4.4 Western blot, semi-dry 114
8.4.5 Immunodetection of proteins 114
8.4.6 Expression and purification of recombinant histones 115
8.4.7 Reconstitution of histone octamers 116
8.4.8 Chromatin reconstitution 117

8.4.9 Mobilization of nucleosomes 118

9 BIBLIOGRAPHY 121

APPENDIX 135

LIST OF PUBLICATIONS 135

CONFERENCES 135

ACKNOWLEDGMENTS – DANKSAGUNG 137

Abbreviations

Å	Ångström (10^{-10} m)
A	ampere
ACF	ATP-utilizing chromatin assembly and remodeling factor
Amp	ampicillin
APS	ammonium persulfate
ATP	adenosine 5’ triphosphate
bp	base pair(s)
BSA	bovine serum albumin
°C	degrees celcius
c	concentration
CDS	coding sequence
ChEC	chromatin endogenous cleavage
CHD	chromodomain
ChIP	chromatin immunoprecipitation
cpm	counts per minute
C-terminal	carboxy-terminal (end of a protein chain)
Da	Dalton
DMSO	dimethyl-sulfoxide
DNA	desoxyribonucleic acid
DTT	di-thiothreitol
dNTP	2-desoxyribonucleotide 5’ triphosphate
dsDNA	double stranded DNA
E. coli	*Escherichia coli*
EDTA	ethylene diamine tetra-acetate
EGTA	ethylene glycol tetraacetic acid
EMSA	electrophoretic mobility shift assay
EtBr	ethidium bromide
FACT	facilitates chromatin transcription
g	gram(s); relative centrifugal force
h	hour(s)
INO	inositol requiring
Ino80p	inositol requiring protein 80
IP	immunoprecipitation

IPTG	isopropyl-thiogalactoside
ISWI	imitation of switch
k	kilo
kb	kilo base pair(s)
kDa	kilo Dalton
l	liter(s)
LB	lysogeny broth (Luria-Bertani)
mg	milligram(s)
min	minute(s)
ml	milliliter(s)
M	molar (mol/l)
MNase	micrococcal nuclease
MW	molecular weight
MWCO	molecular weight cutoff
NFR	nucleosome free region
nm	nanometer(s)
NPS	nucleosome positioning sequence
N-terminal	amino-terminal (end of a protein chain)
OD_x	optical density at x nm
on	over night
ORF	open reading frame
PAA	polyacrylamide
PAGE	polyacrylamide electrophoresis
PBS	phosphate buffered saline
PCR	polymerase chain reaction
pH	negative decadic logarithm of $[H^+]$
Pol	DNA- or RNA polymerase
PTM	post-translational modification
qPCR	quantitative real-time PCR
rDNA	ribosomal DNA
RNA	ribonucleic acid
RNAPI/II/III	RNA-polymerase I/II/III
RP	ribosomal protein
rpm	rotations per minute
RT	room temperature
SAM	S-adenosyl-methionine
S. cerevisiae	*Saccharomyces cerevisiae*

SDS	sodium dodecyl sulfate
sec	second(s)
SNF	sucrose non-fermenting
SNF2H	SNF2 homologous protein
ssDNA	single stranded DNA
SWI	mating type switching
SWR	SWI/SNF related protein
Taq	*Thermus aquaticus*
TBE	Tris-borate-EDTA buffer
TCA	tri-chloro acetic acid
TE	Tris-EDTA buffer
TEMED	tetra-methyl-ethylene-diamine
Tris	tris(hydroxyl-methyl) amino methane
TSS	transcription start site
TTF1	transcription termination factor 1
U	Unit(s)
UV	ultraviolet
V	volt
vol	volume(s)
v/v	volume per volume
wt	wild type
w/v	weight per volume

The common one-letter-code is used for essential amino acids as well as for the bases occurring in DNA or RNA.

1 Summary

The histone variant H2A.Z exhibits specialized functions in a large number of organisms. It is generally found to be enriched in heterochromatic regions as well as at the promoters of most genes. The effects of differential expression during the cell cycle, an outstanding distinction between canonical and variant histones have so far not been examined. This study addressed the question whether S-phase coupled vs. constitutive expression can explain the observed incorporation patterns characteristic of H2A.Z. A second part of this work dealt with specific nucleosome positions occupied by variant nucleosomes.

Analysis of histone deposition via Chromatin Endogenous Cleavage (ChEC) showed that the characteristic enrichment of H2A.Z containing nucleosomes at promoters is dependent on the constitutive expression of the histone variant. Deposition patterns similar to H2A.Z were observed with canonical histones when they were expressed under the control of the H2A.Z promoter. In contrast, results showed that the SWR complex is not responsible for targeting H2A.Z to promoters. So far the SWR complex had been regarded as the only determinant for the establishment of H2A.Z deposition patterns. ChIP analyses showed that the increased promoter occupancy of H2A.Z containing nucleosomes depends on the transcription rate of a given gene. These findings led to the proposal of a model wherein H2A.Z gets incorporated into chromatin via untargeted replacement of H2A-H2B dimers with H2A.Z-H2B dimers across the genome in a Swr1p dependent manner. During transcriptional elongation, nucleosomes over coding regions are subsequently depleted of H2A.Z, which results in the higher H2A.Z density observed at promoters.

In addition to a predominant incorporation of the histone variant at certain loci, the specific positioning of variant containing nucleosomes might affect chromatin structure. *In vitro* analyses of nucleosome positioning in the presence of the histone variants H2A.Z and H3.3 showed that the incorporation of H2A.Z into recombinant histone octamers resulted in altered nucleosome positioning on short linear DNA fragments. Presence of H3.3 did not affect positioning and could not alter H2A.Z mediated positioning differences. For the first time ATP-dependent nucleosome remodeling machines could be shown to respond differently to canonical and variant nucleosome templates *in vitro*, suggesting they have the ability to interpret the histone content of nucleosomes in addition to the underlying DNA. Next, histone variant positioning was addressed *in vivo* using the ChEC method. ChEC experiments proofed to be a viable

tool to study *in vivo* nucleosome positions; differences in MNase cutting events mediated by H2A- or H2A.Z-MNase fusion proteins were observed at different genomic locations. Additional ChEC analysis revealed that the INO80 complex plays a role in the specific positioning of promoter nucleosomes, visualizing for the first time the *in vivo* effect of a chromatin remodeling complex on single nucleosomes.

A third part of the presented thesis investigated the role of the unique C-terminal tail of canonical histone H2A. *In vitro* experiments showed that C-terminal truncation mutants exhibited increased nucleosome mobility in thermal mobilization experiments. Chromatin remodeling by ISWI type chromatin remodeling enzymes was impaired with nucleosomes containing C-terminally truncated H2A mutants. Furthermore, it could be shown that the C-terminal tail of H2A acts as a recognition and binding site for linker histone H1. The results led to the conclusion that the H2A C-terminal tail has a bipartite function: it stabilizes the nucleosome core particle and mediates protein interactions that control chromatin dynamics and conformation.

2 Introduction

2.1 Nucleosome structure

Eukaryotic DNA is packed into the nucleus of each cell via several compaction steps. This compaction is achieved by the interaction of DNA with histones and non-histone proteins. The combination of DNA and proteins is commonly summarized under the term chromatin.

The basic repeating unit of chromatin is the nucleosome core particle (hereafter termed NCP) (Kornberg 1974; Olins et al. 1974), which consists of two molecules of each of the four core histones H2A, H2B, H3 and H4. High resolution crystal structure analysis showed that 147 bp of double stranded DNA are wrapped around the histone octamers in 1.7 turns resulting in a disk-like structure shown in **Figure 1** (Luger et al. 1997). The NCPs on a DNA strand are evenly spaced by the linker DNA whose length varies between organisms.

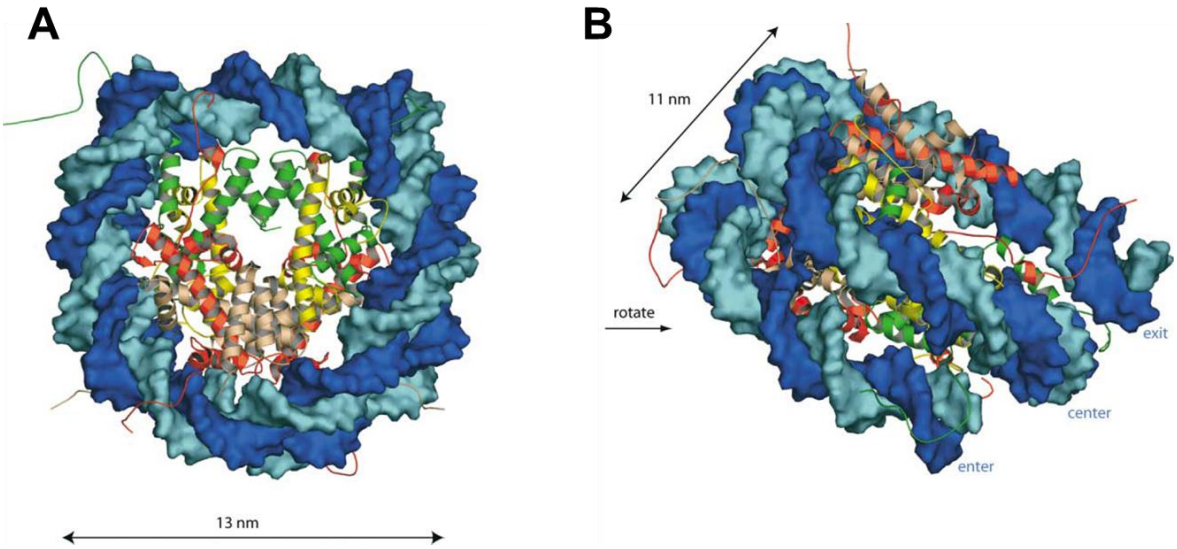

Figure 1: Atomic structure of a nucleosome core particle at a resolution of 2.8 Å. (A) Front view of a nucleosome core particle (NCP) reconstituted from recombinant histones. (B) The DNA strand makes 1.7 turns around the histone octamers, resulting in a disk-like structure. The DNA double helix is shown in shades of blue; histones are colored red (H2A), pink (H2B), green (H3) and yellow (H4) (modified from Khorasanizadeh 2004).

Each core histone can be functionally divided into two domains: the central histone fold domain responsible for histone-histone and histone-DNA interactions within the

nucleosome and the N- and C-terminal domains which serve as sites for posttranslational modifications (see section 2.2.1).
In addition to the four canonical histones, there is another conserved histone protein with specialized functions associated to chromatin: linker histone H1. It binds to NCPs at the DNA entry and exit sites and facilitates protection of the DNA as well as further compaction (Bednar et al. 1998; Maresca et al. 2006).
Very little is still known about structural chromatin organization levels beyond the "beads on a string" organization of NCPs. Further levels of compaction are achieved via poorly defined higher order structures, but there are several findings suggesting chromatin fibers are organized into large domains via potential interactions with the elusive "nuclear matrix" (reviewed in Cremer et al. 2004).

2.1.1 Nucleosome positioning

Several models describing nucleosome positioning are discussed in the field and the most important ones will be described in the following.
First, biophysical properties of the DNA itself – so called *cis*-factors – can determine nucleosome positions. Since histone-DNA interactions are exclusively ionic, an octamer cannot "read" the DNA sequence. However, certain sequence motifs have a high affinity for nucleosomes and are known as nucleosome positioning sequences (NPS). AA/TT/TA dinucleotide sequences with a periodicity of ~10 bp (Segal et al. 2006) in combination with repeating GC-rich dinucleotides offset by ~5 bp (Ioshikhes et al. 2006) are characteristic for NPSs. The reason for this is the energetic favorability for nucleosome formation at these sequences. Bending anisotropy and stacking energies of AA/TT/TA motifs allow DNA bending and nucleosome formation (Kaplan et al. 2010a; Kaplan et al. 2010b). In contrast, poly-AT motifs or AA/TT stretches which are incorrectly spaced have a low affinity towards nucleosomes and are defined as nucleosome excluding sequences.
Secondly, *trans*-factors can determine the location of histone-DNA interactions. Regulatory proteins like Reb1 in yeast (Hartley et al. 2009) or TTF-1 in mouse (Langst et al. 1998) occlude their binding sites and inhibit nucleosome formation at these locations. These factors direct the nucleosome to a different position and – preferentially at promoters – establish nucleosome free regions (NFR) (Badis et al. 2008). This may also explain why nucleosomes encompassing NFRs are usually very well positioned and serve as anchor nucleosomes (Raisner et al. 2005). For example, in yeast there is usually a NFR upstream of the transcription start site (TSS) which is flanked by two well-positioned nucleosomes that are followed by regularly placed nucleosomes. This spacing regularity however, decays with growing distance from the

TSS (Jiang et al. 2009; Rando et al. 2009). Chromatin remodeling machines can also serve as *trans*-factors for nucleosome positioning. A recent study in yeast showed that the RSC remodeling complex moved nucleosomes away from the predicted NPSs in order to form proper NFRs. This could explain discrepancies between sequence prediction models and steady-state average positions *in vivo* (Hartley et al. 2009).
For many years, a statistical positioning model has been used to explain the regularity of nucleosomes (Fedor et al. 1988; Kornberg et al. 1988). This theoretical model proposed that nucleosomes would slide along DNA until they encounter barrier elements. Only a small number of barriers would be required to direct nucleosomes over a large genomic region. This would minimize the limitations of DNA sequence to code for its own packaging. Additionally, it would be an energy saving, passive process at a thermodynamic equilibrium. Mathematical descriptions and physical calculations verified the possibility of such a positioning mechanism. The prediction of highly positioned nucleosomes followed by a decaying spacing regularity downstream of the anchor nucleosome fully correlates with experimental observations. But just recently, experimental evidence was generated which negates the model of statistical positioning. *In vitro* experiments failed to generate statistically positioned nucleosomes and showed that DNA sequence and *trans*-factors as described above determine nucleosome positioning (Zhang et al. 2011). It was also shown *in vivo* that a decrease in nucleosome density did not result in a reorganization of nucleosome positioning. In the statistical model the loss of nucleosomes would result in a redistribution of nucleosomes and an increased distance between them. This was neither observed in yeast nor mammalian cells, providing substantial experimental evidence against the statistical nucleosome positioning model (Celona et al. 2011).

2.2 Regulating factors of chromatin

The wrapping of the double helix around nucleosomes and the further compaction of chromatin into higher order structures by incorporation of linker histone H1, as well as non-histone proteins, render DNA mostly inaccessible for the cellular machinery. All DNA based processes – replication, transcription, repair and recombination - however, require access to DNA. In order to make this possible, cells have developed specific mechanisms to regulate chromatin: post-translational modifications of histones, methylation of the DNA, chromatin remodeling and the incorporation of histone variants.

2.2.1 Posttranslational modifications of histones

One level of chromatin variation which directly affects the primary organization level of chromatin – the nucleosome – is the covalent modification of the N-terminal histone tails that protrude from the nucleosome core particle. The combinatorial variety originating from the high number of modifications that can be realized within a single nucleosome led to the proposal of the so-called “histone code” (Strahl et al. 2000; Jenuwein et al. 2001). The modification patterns can serve as a differentiation map for establishing specialized chromatin domains as well as signals for a number of cellular processes.

Acetylation is observed with all four core histones at different lysine residues (reviewed in Vaquero et al. 2003). Generally acetylation is linked to activated genes; this may be due to the fact that upon acetylation, positive charges on the histone surface are lost and thus the histone-DNA interactions are weakened. The decreased binding affinity of nucleosomes could then result in higher mobility or easier disruption, both of which could positively regulate transcription. The establishment of this modification is carried out by histone acetyl transferases (HATs) utilizing acetyl-coenzyme A as a carrier. The removal of acetyl groups from lysine residues is catalyzed by histone deacetylases (HDACs).

Methylation is only observed at the arginine and lysine residues of H3 and H4. Functional involvement of methyl marks depends on the amino acid that is methylated. The modification of H3K4 is associated with active genes and facilitates transcription (Santos-Rosa et al. 2003), whereas H3K9 methylation is a mark of transcription repression and formation of heterochromatin and the methylation of H3K27 is seen in the silencing of Hox genes (Cao et al. 2002). Histone methyl transferases (HMTs) catalyze the transfer of methyl groups from S-adenosylmethionine (SAM) to lysine residues of H3, whereas the methylation of arginines is carried out by protein-arginine-methyltransferases (PRMTs) (reviewed in Vaquero et al. 2003).

All four core histones as well as linker histone H1 can be phosphorylated (reviewed in Vaquero et al. 2003). Phosphate groups are transferred to serine residues and can exclude the simultaneous modification of neighboring amino acids. Phosphorylation has different important roles in chromosome condensation and segregation (Guo et al. 1995).

The role of ubiquitination depends on the extent of the modification. Poly-ubiquitination is generally a signal for 26S proteasome mediated degradation, whereas mono-ubiquitination plays a role in transcription regulation (reviewed in Pickart 2001).

Furthermore, ADP-ribosylation, biotinylation and sumoylation are also observed with histones, but functions and interplay of all possible modifications remain unclear.

2.2.2 DNA methylation

A conserved mechanism of altering chromatin on the level of DNA is the covalent modification of DNA bases. Methyl groups are attached at the C-5 position of cytosines in the context of so called CpG islands (Hermann et al. 2004). The methyl groups lie within the major groove of the double helix where they are accessible for DNA-interacting proteins.

So far the most important function of CpG methylation is generally thought to be gene repression. By the addition of a methyl group, relatively large parts of DNA are occluded and proteins such as transcription factors are detained from binding at their respective recognition sites. At the same time, methyl groups can serve as signals or interaction platforms and thereby recruit other proteins responsible for further repression (reviewed in Hermann et al. 2004). Because cytosine methylation provides DNA with additional information that is not primarily encoded within its sequence, methylated cytosine is nowadays referred to as the 5th base of DNA.

2.2.3 Chromatin remodeling

Another way by which cells maintain their chromatin accessible in a specifically regulated fashion is the use of ATP-dependent chromatin remodeling complexes. The combinatorial variety of several hundred remodeling complexes results in diverse and tightly controlled expression patterns (Rippe et al. 2007). Chromatin remodelers are categorized according to their protein domains. They all contain two recA-like helicase domains and are therefore part of the helicase-like Superfamily 2 (SF2). Because of sequence similarity to *S. cerevisiae* Snf2 protein, they are further grouped into the Snf2 family of ATPases. (Eisen et al. 1995). Until now, 24 subgroups have been classified according to sequence homology within the helicase-like region (Flaus et al. 2006). The majority of Snf2 family members exhibit chromatin remodeling activity; however, not all proteins of this family are DNA translocases. For example, Rad54 and Rad51 promote strand pairing and Mot1 displaces the TATA binding protein from DNA (Flaus et al. 2006).The classification based on multi-sequence alignments is shown in **Figure 2 A+B**.

A different and more commonly used classification divides members of the Snf2 family into four subgroups. These subgroups are characterized by the domains flanking the ATPase domain: SWI/SNF family members contain a bromodomain, ISWI like proteins a SANT domain, members of the CHD domain have a chromodain and INO80 proteins have a characteristic split ATPase and HSA domain (**Figure 2C**).

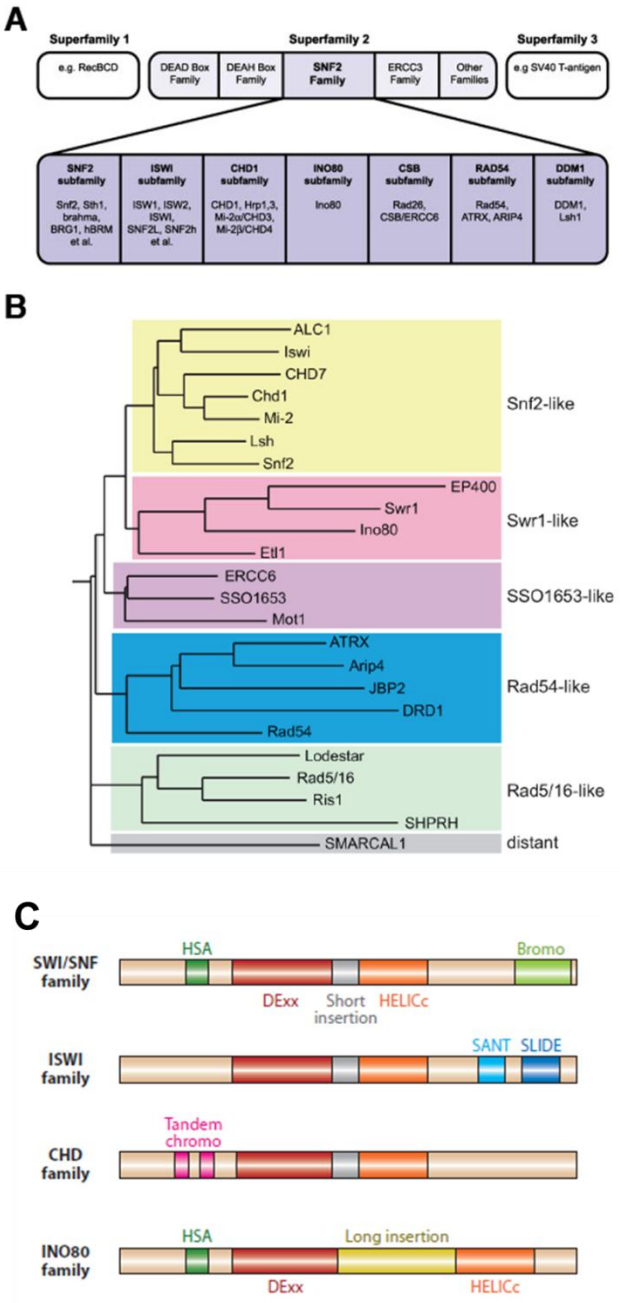

Figure 2: Chromatin remodeling complexes. (A) Remodelers belong to the SNF2 subfamily of the helicase-like Superfamily 2 (SF2). A hierarchical classification into further subgroups is shown (Lusser et al. 2003). (B) Relationships between subgroups is shown as a rooted tree, based on full-length alignments of the helicase region (Flaus et al. 2006). (C) The more commonly used classification according to domains flanking the ATPase domain (modified from Clapier et al. 2009).

All these ATPases are part of multi-subunit complexes of different content and complexities and either the characteristic ATPase domains and/or certain subunits are needed for different parts of the catalyzed reactions: nucleosome affinity, recognition of covalent histone modifications, the ATPase domain which hydrolyzes ATP to carry out the actual reaction by breaking distinct histone-DNA interactions and furthermore domains or subunits to regulate the ATPase activity and to interact with other proteins.

So far, all identified complexes consist of 2-12 subunits and their biological context concerning associated proteins results in an enormous variety of specialized functions (Lusser et al. 2003).

2.2.3.1 Remodeling mechanism

The sliding of nucleosomes along the DNA happens in all cases upon the hydrolysis of ATP, but the mechanisms by which sliding is realized depend on the enzyme complex. Members of the ISWI subfamily slide nucleosomes along the DNA without disrupting or displacing the octamer (Langst et al. 1999), whereas SWI/SNF complexes were shown to drastically decrease histone octamer DNA interactions (Narlikar et al. 2001).
Differences between the observed phenomena were convincingly explained and joined in the “loop-recapture-model” which suggests that the energy from ATP hydrolysis is used to detach small parts of DNA at the entry/exit sites of the nucleosomes. This stretch of unbound DNA can either be re-associated resulting in the original positioning (a phenomenon termed “DNA breathing”) or a loop of the unbound DNA can be propagated around the octamer, leading to a *cis*-translocation of the nucleosome (Strohner et al. 2005). The non-catalytic subunits of remodeling complexes can vary this reaction mechanism concerning the direction of translocation or the length of the loop and its propagation, establishing a mechanistic view, wherein the outcome of a remodeling reaction depends on both the underlying DNA as well as the type of remodeler itself (Rippe et al. 2007).

2.2.4 Histone variants

In most organisms the bulk of histones is made up of the four major histones. They share high sequence similarity and are strictly expressed in S-phase.
Non-allelic variants have been identified for all four core histones besides H4, differing considerably in their sequence, function and regulation (reviewed in Kamakaka et al. 2005; Boyarchuk et al. 2011) In contrast to their canonical counterparts, these variants are mostly encoded by a single copy gene They usually contain introns and are constitutively expressed over the cell cycle (Wu et al. 1982). Variant histones can be deposited onto DNA independently of replication (Ahmad et al. 2002). The observation that they exchange with canonical histones within existing nucleosomes has led to them being referred to as “replacement histones” (Brandt et al. 1979; Grove et al. 1984). Histone variants are highly conserved and have evolved specialized functions in crucial cellular mechanisms such as chromosome segregation, DNA repair and transcription regulation. An overview over known histone variants is given below. A

more detailed description about the main focus of this work, H2A.Z is presented in section 2.4.

Most known histone variants belong to the H2A family, among them: macroH2A, H2A.Bbd, H2A.X and H2A.Z (reviewed in Malik et al. 2003; Bernstein et al. 2006; Talbert et al. 2010). They share a considerably high sequence similarity, but especially the N- and the C-terminal domains show divergent sequences and lengths.

H2B variants are not well studied yet. The few variants that have been found, completely replace major H2B in specific tissues or during certain developmental stages. Concerning function, a rough overview has been generated, attesting them roles within chromatin fiber condensation and transcription repression, but the functional roles remain unclear (reviewed in Poccia et al. 1992).

More is known about H3 variants. They have different functions in chromosome segregation or are linked to transcriptionally active sites (Ahmad et al. 2002).

Histone H4 on the other hand is one of the slowest evolving proteins, therefore it is not surprising that no sequence variants of this histone are known. There are however several H4 genes that are constitutively expressed – like all known histone variants and unlike the canonical forms – but they do not differ in sequence (Akhmanova et al. 1996).

Table 1: Histone variant overview. The table is based on Bernstein and Hake (2006) and Talbert and Henikoff (2010)

Histone	Variant	Distribution	Localization	Function	Chaperone
H2A	H2A	Universal	Genomewide	Genome packaging	Nap1
	H2A.Bbd	Mammals	Xi exclusion	Spermatogenesis, gene activation?	Unknown
	H2A.X	Universal	Genomewide		FACT
	H2A.Z	Universal	Genomewide	DNA repair, genome integrity	Chz1, Nap1, SWR1
	macroH2A	Animals	Xi	Gene activation, silencing, chromosome segregation X-inactivation, gene silencing?	Unknown
H2B	H2B	Universal	Genomewide	Genome packaging	Nap1
	H2BFWT	Primates	Telomeres?	Testis specific functions	Unknown
	hTSH2B	Mammals	Basal part of the nucleus	Testis specific, activation of paternal genes?	Unknown
	spH2B	Human	Telomeres	Unknown	Unknown
H3	H3.1	Mammals	Not determined	Genome packaging	CAF-1
	H3.2	Widespread	Not determined	Genome packaging	Unknown
	H3.3	Universal	Genes, TFBS telomeres	Gene activation	HIRA, Daxx, DEK
	CenH3	Universal	Centromeres	Chromosome segregation	HJURP

	tH3	Mammals	Not determined	Testis specific functions	Nap2
H4	H4	Universal	Genomewide	Genome packaging	CAF-1

? = hypothesized; TFBS = transcription factor binding site; Xi = inactive X chromosome

2.3 Chromatin dynamics

The inhibitory structure of chromatin is reorganized upon cellular signals so that DNA-dependent processes like replication, transcription and DNA repair can take place. The following sections shortly describe nucleosome turnover during replication and transcription.

2.3.1 Chromatin dynamics during replication

Genome replication includes the duplication of the DNA as well as its re-organization into chromatin. The replication machinery destabilizes pre-existing nucleosomes in front of the replication fork which leads to their disruption (Sogo et al. 1986; Gasser et al. 1996). After polymerase passage, nascent DNA is rapidly re-packaged into chromatin (Gasser et al. 1996). Therefore, either histones from disrupted parental nucleosomes are recycled or newly synthesized histones are deposited in a process known as replication-dependent *de novo* nucleosome deposition (Groth et al. 2007). The distribution of old vs. new histones happens randomly and at a ratio of about 50% old and new on the parental and daughter strands (reviewed in Corpet et al. 2009). That way, specific post-translational histone modifications (PTMs) are preserved on the parental DNA and at the same time imparted on the daughter strands where they are propagated to newly synthesized histones.

For the ordered nucleosome turnover during replication, many factors are needed, including histone chaperones, chromatin remodelers and chromatin modifiers that establish specific PTMs. In addition to its role in transcription, the facilitates chromatin transcription (FACT) complex is implicated in the eviction of H2A-H2B dimers during replication via the activity of its Spt16 subunit (Stuwe et al. 2008). Asf1 could subsequently bind the C-terminus of H4 and split an $(H3\text{-}H4)_2$ tetramer into two dimers (English et al. 2006). However, whether the tetramer is indeed split or left intact is still not clear (reviewed in Corpet et al. 2009).

Through the activity of the chromatin assembly factor 1 (CAF-1), H3-H4 histones are deposited on the replicating DNA (Smith et al. 1989). CAF-1 is targeted to replication forks through the interaction with proliferating cell nuclear antigen (PCNA). Since this interaction requires CAF-1 phosphorylation by a replicative kinase, the tight interplay

between ongoing DNA replication and histone deposition is ensured (Gerard et al. 2006).

Depletion experiments have shown that chromatin remodeling complexes ACF, ISWI and INO80 are required for efficient replication. However, a direct connection of the remodelers and the replication machinery is still missing, so the question where these complexes exactly act during replication, remains an open question (reviewed in Corpet et al. 2009).

2.3.2 Chromatin dynamics during transcription

Transcription-coupled nucleosome turnover is predominantly observed at promoter regions at so-called “hot nucleosomes”. Usually, the presence of nucleosomes at promoter regions prevents transcription initiation (Lorch et al. 1987) but later studies have shown that promoter nucleosomes are disrupted in the course of transcriptional activation (Boeger et al. 2003; Reinke et al. 2003; Adkins et al. 2004). Through this nucleosome loss, binding sites for transcription initiation factors are exposed and the assembly of the transcriptional machinery can start. Loss of promoter nucleosomes is linked to the eviction activity of chromatin remodelers of the SNF/SWI family (Treand et al. 2006; Dechassa et al. 2010). However, not all promoters with high nucleosome turnover rates are adjacent to highly transcribed genes, suggesting that promoter nucleosome turnover is not solely caused by transcription, but multiple overlapping mechanisms may determine this phenomenon (Dion et al. 2007).

In addition to initiation, nucleosomes within coding regions are barriers for transcription elongation. This has been shown *in vitro*, where transcription of nucleosomal templates is slower than *in vivo* (Lavelle 2007). Consequently, nucleosomes in ORFs are also subjected to turnover, albeit to a smaller extent than promoter nucleosomes (Dion et al. 2007). Experiments in *Drosophila* showed that canonical H3 gets evicted from nucleosomes and replaced with H3.3 during transcription (Ahmad et al. 2002). In *S. cerevisiae* transcription leads to the eviction of nucleosomes from some genes and thus lowers their density over coding regions (Schwabish et al. 2004; Farris et al. 2005). The opposite was shown for *Physarum polycephalum* (Thiriet et al. 2005), so it cannot be surely postulated that there is a general transcription-coupled mechanism for histone turnover. The general idea is that nucleosomes are partially or completely disrupted during RNAPII passage and rapidly re-assembled behind the transcription machinery (Workman 2006) similar to the events during replication.

The passage of RNA polymerase through a nucleosome is facilitated by chromatin remodelers of the ISWI, INO80 and CHD family as well as so-called transcription elongation factors. *In vitro* studies have shown that the ISWI family possesses histone-

exchange capabilities (Bruno et al. 2003) and can overcome nucleosomal barriers during transcription elongation (Gaykalova et al. 2011). INO80 family members evict and exchange H2A-H2B dimers and can thus facilitate transcription through nucleosomal templates (Luk et al. 2010; Papamichos-Chronakis et al. 2011). Members of the CHD family co-localize with RNAPII and are implicated to participate in early elongation steps (Srinivasan et al. 2005). Moreover, CHD family proteins interact with the histone chaperone FACT and the RNAPII elongation factor DSIF (DRB sensitivity-inducing factor) (Simic et al. 2003)

The bi-functional FACT complex travels with elongating RNAPII and facilitates nucleosome disruption by removing one of the H2A-H2B dimers from an NCP (Orphanides et al. 1996). The acidic C-terminus of the Spt16 subunit plays a crucial role in the destabilization step (Belotserkovskaya et al. 2003). Additionally, FACT also exhibits nucleosome assembly activity (Belotserkovskaya et al. 2003), suggesting it takes part in the rapid re-assembly of NCPs behind the polymerase. The transcription elongation factor Spt6 was implicated in H4 deposition behind the transcription machinery (Kaplan et al. 2003). A cooperation of FACT and Spt6 could explain how a complete nucleosome is translocated during transcription. At the same time it is possible that at individual genes only the Spt16 subunit of FACT is utilized. This might explain discrepancies between studies reporting only the loss of H2A-H2B dimers vs. studies showing complete nucleosome disruption during RNAPII passage.

Previously, FACT had not been found at RNAPIII transcribed genes, which was consistent with data showing that RNAPIII transcribes genes without disrupting nucleosomes (Studitsky et al. 1997). Interestingly, more recent studies showed that FACT also facilitates RNAPIII transcription (Birch et al. 2009).

2.4 Histone variant H2A.Z

H2A.Z has been one of the most extensively studied histone variants over the last few years (reviewed in Draker et al. 2009; Svotelis et al. 2009).

H2A.Z diverged early during evolution and has acquired diverse functions. It has been shown that H2A.Z isoforms of different organisms, like mammals (H2A.Z), birds (H2A.F), sea urchins (H2A.F/Z), *Drosophila* (H2AvD), budding yeast (Htz1) and *Tetrahymena* (hv1) are closer related to each other than to canonical H2A forms of the same organism (Thatcher et al. 1994). Also *Drosophila* H2A.Z (H2AvD) seems to have emerged as a hybrid of the two mammalian H2A variants H2A.X and H2A.Z (Redon et al. 2002).

It is essential in such diverse organisms as *Tetrahymena thermophila* (Liu et al. 1996), *Xenopus laevis* (Ridgway et al. 2004), *Drosophila melanogaster* (Clarkson et al. 1999) and mice (Faast et al. 2001), whereas in budding yeast knockout cells are viable, but have changed gene expression patterns (Carr et al. 1994; Ridgway et al. 2004).
An overview over species specificity is presented in Table 2.

Table 2: H2A.Z nomenclature and function across different species. The table is based on Zlatanova and Thakar (2008).

Species	**Name of Z variant**	**Characteristic features**	**Biological function**
S. cerevisiae	Htz1p	Acetylated at lysine residues by NuA4 and by Gcn5	Transcription activation; repression of ~100 euchromatic genes; prevents spreading of silent chromatin; genomic stability and repair;
Trypanosoma	H2A.Z	Unique N-terminal extension	Essential gene; dimerizes with a novel H2B form which is also essential; absent from sites of active transcription
Tetrahymena	Hv1	Charge neutralization of the N-terminus via acetylation of lysine residues is critical for function and essential for viability	Essential gene; correlated with transcriptional competence
Arabidopsis	Four distinct variants: HTA4, -8, -9, -11	Z variants are more closely related to yeast and metazoan H2A.Z proteins than to other plants H2As	Absent from centromeric and pericentromeric repeats; present in mitotic chromosomes, required for high-level expression of the FLOWERING LOCUS C gene
C. elegans	Htz-1/H2A.Z	Highly homologous to yeast and human protein	Synthetically lethal with a TF critical for foregut development; recruited to foregut promoters at transcriptional onset

Drosophila	H2AvD	Hybrid between H2A.Z and H2A.X; the S residue of H2A.X becomes phosphorylated after DNA damage; acetylated by Tip60 complex	Essential for development; non-random distribution on polytene chromosomes; absent from highly transcribed regions; lost upon transcriptional activation; localizes to centromeric chromatin; required for heterochromatin formation; acetylation required for H2AvD removal from DSB sites
Xenopus	H2A.Z	Polyadenylated mRNA whose synthesis is uncoupled from DNA synthesis; mRNA is mainly detected during oogenesis and after mid-blastula transition	Essential for early development; key residues in the acidic patch on the nucleosome surface determine role in development
Mouse	H2Afz;H2Afv	Acetylated	Essential for early development; targeted to pericentric heterochromatin during embryo cell differentiation; role in spermatogenesis; contributes to the unique structure of the centromere
Human	H2A.Z; H2AF/Z	Two subvariants, up to three acetylated residues; mono-ubiquitylated	Enriched at promoter regions upstream and downstream of TSSs; binding level correlates with gene expression; enriched at insulators; marks the fraction of H2A.Z associated with gene silencing/ facultative hetero-chromatin

DSB = double strand break; TF = transcription factor; TSS = transcription start site

2.4.1 Unique properties distinguish H2A.Z- from H2A-containing nucleosomes

H2A.Z differs from H2A in large parts of its amino acid sequence and nucleosomes containing the variant exhibit unique physical properties. Both histones have a sequence identity of only 60% (Wu et al. 1981), with some differences within the

histone fold domain and the largest divergence in their C-terminal domains as depicted in **Figure 3A**.

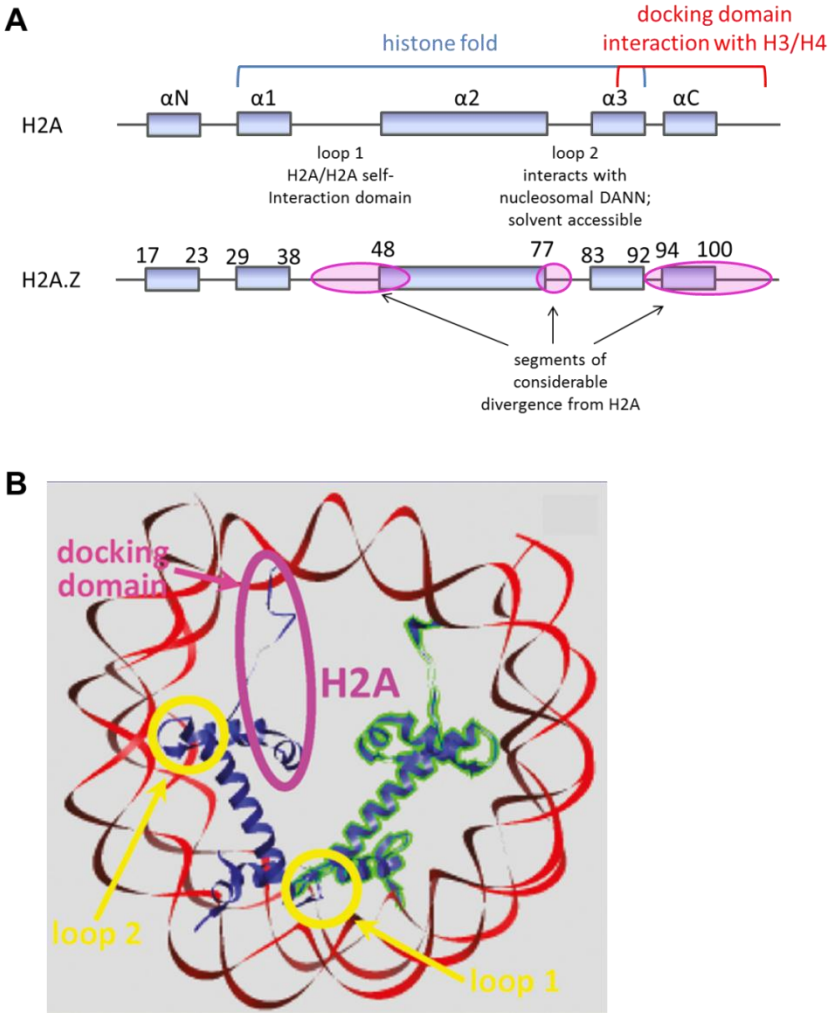

Figure 3: Schematic representation of the secondary structure of H2A and H2A.Z. (A) Blue rectangles represent the five α helices. Blue brackets mark the canonical histone fold domain, red brackets the docking domain. Pink ovals depict locations of considerable sequence divergence between H2A and H2A.Z. Numbers refer to the amino acid residue encompassing the secondary structure elements on H2A.Z (modified from Zlatanova et al. 2008). (B) Portions of the crystal structure of the nucleosome core particle, containing two H2A.Z molecules. Major regions of divergence are encircled in yellow and pink (modified from Thakar et al. 2009)

A comparative analysis of crystal structures revealed that the overall structures are very similar. Only slight differences were found in the $(H3\text{-}H4)_2$-tetramer docking domain (Suto et al. 2000) (**Figure 3B)**. The substitution of Glu 104 in H2A to Gly 106 in H2A.Z, and the resulting loss of three hydrogen bonds, was suggested to decrease the stability of H2A.Z-H3 interactions and consequently of the complete H2A.Z containing nucleosome. Two unique and highly conserved amino acid residues in a solvent accessible region of the docking domain are His 112 and His 114. In the structure analysis His 112 bound a manganese ion and His 114 stabilized this interaction.

Manganese, however, was present in the crystallization buffer and the authors suggested that *in vivo* they would expect either a copper or a zinc ion to be bound at this site. The presence of such a metal ion on the octamer surface could serve as a unique interaction site for other proteins. Subtle differences were also observed in the region forming the acidic patch on the surface of the nucleosome which is thought to serve as a specific interaction site for proteins *in vivo*. Different amino acid substitutions in the H2A.Z molecule result in an extension of this patch in the variant nucleosome.
In vivo studies later confirmed that the acidic patch was essential for the HP1 mediated formation of highly condensed chromatin fibers and this effect could not be observed with canonical nucleosomes (Fan et al. 2004). Interestingly parts of the acidic patch were also shown to be important for embryonic development. Studies in *Drosophila* identified regions in the C-terminus of H2A.Z that could not be replaced by the corresponding amino acids from H2A without resulting in lethality of *Drosophila* embryos (Clarkson et al. 1999). Similar studies in *Xenopus* observed the disturbance of correct mesoderm formation upon deletion or mutation of single amino acids lying within the acidic patch on the nucleosome surface (Ridgway et al. 2004). All three studies nicely demonstrated that the unique nucleosome surface mediated by H2A.Z incorporation has profound influences *in vivo*. In addition the distinct acidic patch of the H2A.Z C-terminal tail is also implicated in the deposition of the histone variant into chromatin, which is discussed in section 2.4.5.1.

Concerning the predicted destabilization, biochemical and biophysical analyses performed by different groups resulted in highly conflicting data. In accordance with the crystal structure analysis, a salt-dependent decrease of stability was shown by analytical ultracentrifugation (Abbott et al. 2001) of isolated yeast chromatin fibers (Zhang et al. 2005). A Fluorescence Energy Transfer approach on the other hand suggested that H2A.Z actually stabilizes the octamer (Park et al. 2004). Other groups found no significant influence of H2A.Z incorporation on salt-dependent nucleosome stability (Jin et al. 2007). Taken together, the influence of H2A.Z on the stability of the NCP remains unclear and since the abovementioned studies are non-uniform concerning the origin of tested nucleosomes and the applied methods, hardly any interpretation can be drawn from them.
The existence of hybrid nucleosomes, containing one molecule of H2A and one of H2A.Z has long been debated. First predictions from initial crystallization studies suggested that the existence of such nucleosomes was impossible because of potential steric clashes or the lack of self-stabilization between H2A and H2A.Z (Suto et al. 2000). Later studies from the same group negated this view (Chakravarthy et al.

2004) and the *in vivo* existence of heterotypic H2A/H2A.Z nucleosomes has been shown since (Luk et al. 2010; Weber et al. 2010), adding another level of nucleosome variation.

2.4.2 Splice isoforms of H2A.Z

The importance of the unique C-terminal tail of H2A.Z was recently highlighted by the identification of truncated H2A.Z versions with distinct C-termini.

In vertebrates, there are two H2A.Z proteins called H2A.Z-1 and H2A.Z-2 (Dryhurst et al. 2009; Eirin-Lopez et al. 2009) that exhibit a very similar functional specialization. The H2A.Z-2 gene was recently identified to produce a splice isoform with a characteristically truncated C-terminus, 14 amino acids shorter and differing at six sequence positions compared to the complete protein. The full length protein - H2A.Z-2.1 - is predominant in all tissues, levels of the truncated isoform – H2A.Z-2.2 – are preferentially elevated in brain, liver and skeletal muscle (Bonisch et al. 2012; Wratting et al. 2012). The shorter H2A.Z form was shown to weaken chromatin association of nucleosomes *in vitro* as well as *in vivo*, leading to the hypothesis that H2A.Z-2.2 containing nucleosomes could be more rapidly exchanged than nucleosomes containing full length H2A.Z (Bonisch et al. 2012). The absence of this isoform in lower vertebrate organisms suggests that truncated H2A.Z isoforms and the resulting effects on chromatin are potentially essential for mammalian evolution.

2.4.3 Specialized functions of H2A.Z

Several genome wide studies have mapped specific H2A.Z localizations and have generated a better understanding of its numerous specialized functions. Roles for H2A.Z have been attested to such diverse cellular pathways as transcription, heterochromatic silencing, chromosome segregation, genome stability as well as DNA repair and correct cell cycle progression in different organisms.

2.4.3.1 Functions in *Saccharomyces cerevisiae*

H2A.Z was shown to be preferentially incorporated into promoter nucleosomes of most yeast genes, but enrichment was not as pronounced at promoters of highly transcribed genes (Guillemette et al. 2005). In the same study it was suggested that the presence of H2A.Z at promoters establishes a chromatin structure that is important for transcription regulation. Unlike the variants H2A-Bdb and macro-H2A, H2A.Z was not observed to be clustered at certain chromosomal elements, it is however, depleted at RNAPI and RNAPIII genes, implicating a larger role in the regulation of RNAPII

transcribed genes (Zhang et al. 2005). Nevertheless, definite roles in transcriptional regulation are far from being well understood. It is known that H2A.Z functions in the recruitment of co-activators and TATA-binding proteins (Wan et al. 2009). The distinct biophysical properties of H2A.Z containing nucleosomes are thought to help poise promoters carrying such nucleosomes for transcriptional initiation, through recruitment of the transcriptional machinery or the loss of nucleosomes at regions that have to be accessible for the formation of the transcription complex (Albert et al. 2007). Contrary to its roles in transcription activation, H2A.Z also influences gene silencing. Studies on HMR and telomere silencing showed an interplay between H2A.Z and Sir1p where the presence of the histone variant strengthened Sir1p mediated silencing and overexpression could compensate SIR1 deletion, whereas H2A.Z deletion led to a total loss of HMR and telomere silencing (Dhillon et al. 2000).

Another interesting set of experiments was carried out to demonstrate the role of H2A.Z in DNA repair processes. Sites of persisting DNA double strand breaks (DSB) got rapidly enriched with H2A.Z molecules. Cells with a h2a.zΔ background were severely delayed in their ability to form ssDNA, usually part of the DSB-induced checkpoint activation, and failed to recruit the DSB to the nuclear periphery (Kalocsay et al. 2009).

Furthermore, H2A.Z has been assigned functions within cell cycle progression. Cells lacking H2A.Z exhibit slowed S-phase progression, possibly mediated by reduced induction kinetics of the two cell cycle regulatory genes CLN2 and CLB5 when H2A.Z is missing at their promoters (Dhillon et al. 2006). Although, the authors of the latter study discuss several other models, how lack of H2A.Z could lead to delayed replication phenotypes: the absence of H2A.Z from chromatin could lead to its compaction, thereby reducing the kinetics of all cellular processes that have to rely on accessible chromatin; without H2A.Z, recruitment of the replication machinery to replication origins might be impaired; furthermore, lack of H2A.Z could result in multiple chromatin- or DNA-damages that are recognized by S-phase checkpoints, therefore H2A.Z deletion may indirectly affect replication processes.

Mutation analyses in yeast revealed interactions of H2A.Z with subunits of the spindle position checkpoint, the kinetochore complex and genes required for microtubule stability which argued for the requirement of H2A.Z in chromosome stability and segregation (Krogan et al. 2004). However, the effects on chromosome transmission are not solely dependent on H2A.Z protein but were shown to depend on the specific acetylation of H2A.ZK14. This modification is function-specific since its absence does not affect transcription, telomere silencing or DNA repair. Function specific histone

modifications may explain the various H2A.Z functions in diverse pathways (Keogh et al. 2006).

2.4.3.2 Functions in other species

Unlike *S. cerevisiae*, where sites of centromere formation are defined by short DNA sequences, most eukaryotes regulate active centromeres via chromatin-based epigenetic mechanisms (Allshire et al. 2008). One example for a role of H2A.Z in centromere silencing is found in fission yeast. H2A.Z is not enriched at centromeres, but its deletion in *S. pombe* results in loss of centromeric silencing and defects in chromosome segregation (Hou et al. 2010). This effect does not rely on the presence of H2A.Z at centromeres, but on its regulative effect on CenH3 expression, the histone variant typically linked with centromere silencing.

Studies attesting a negative role to H2A.Z in transcription in plants (Smith et al. 2010) are in contrast with findings from *S. cerevisiae*. This highlights the species specificities of H2A.Z functions. In *Arabidopsis thaliana*, various environmental signals affect the FLOWERING LOCUS C (FLC). The intrinsic effectors controlling FLC represent many types of chromatin-based signals. H2A.Z has been shown to activate FLC, which leads to repression of premature flowering (Deal et al. 2007). A recent study by Kumar and colleagues demonstrated that H2A.Z is a key factor in the response of *Arabidopsis* to increased temperature. Hsp70 is a gene that gets increasingly expressed with rising temperature and phenotypes that expressed high levels of Hsp70 even at normal temperatures carried mutations in the ARP6 gene which is part of the H2A.Z depositing SWR complex (see section 2.4.5.1). Moreover, H2A.Z is lost from genes upon temperature increase. These observations led to the assumption that H2A.Z functions as a molecular thermostat in plants (Kumar et al. 2010).

Tetrahymena thermophila is an interesting organism to study H2A.Z involvement in temporal and spatial chromatin organization in nuclear development. Vegetative *Tetrahymena* cells have a transcriptionally active macronucleus and a transcriptionally inactive micronucleus. It was thought that H2A.Z was positively involved in transcription and would therefore only be present in the macronucleus. In a study by Stargell and colleagues, cells were treated with H2A.Z antibodies during all stages of the cell cycle and macro- and micronuclei were fractionated. Surprisingly, H2A.Z was found in the micronuclei during early stages of conjugation, right before micronuclei get transcriptionally active. The authors concluded from this that H2A.Z is not acquired in the active macronucleus, but rather establishes transcriptionally competent chromatin needed for the transition from the micro- to the macronucleus (Stargell et al. 1993).

During mouse development, H2A.Z was demonstrated to be expressed upon differentiation and was immediately incorporated at pericentric heterochromatin thus establishing a signal for the discrimination between facultative and constitutive heterochromatin (Rangasamy et al. 2003). A novel system of inducible RNA interference studies was used by the same group to examine genome stability in the absence of H2A.Z. The experiments revealed that defects in the chromosome segregation pathway were causing massive genome instability by a directly linked loss of HP1α upon H2A.Z depletion (Rangasamy et al. 2004).

Taken together, these examples show how diverse H2A.Z functions are. The fact that H2A.Z diverged early in evolution and has been strongly conserved in many organisms, might explain the sometimes contrasting roles observed among different species.

2.4.4 H2A.Z specific posttranslational modification patterns associated with function

Acetylation of H2A.Z seems to have the same importance for transcription coupled functions as it has on canonical histones. In yeast four N-terminal lysine residues (K3, K8, K10 and K14) have been identified with K14 being the preferred site for acetylation marks. In contrast, the C-terminus seems to be completely unmodified. Acetylated forms of H2A.Z are predominantly found at active genes whereas unacetylated H2A.Z is associated with promoters of inactive genes. The predominant H2A.Z-K14 acetylation is dependent on two histone-acetyltransferases (HATs): Gcn5 and interestingly Esa1 – a subunit of the NuA4 acetyltransferase which shares subunits with the SWR complex discussed below (Millar et al. 2006).

A second form of modification associated with a role of H2A.Z in transcription is ubiquitinylation. The covalent linking of ubiquitin to lysines K120 and K121 was observed in mouse and human cells. This modification was preferentially found within the inactive female X-chromosome, indicating its role in transcriptional silencing (Sarcinella et al. 2007).

Phosphorylation of the H2A.Z specific C-terminus at S137 was observed after radiation induced DSB. Cells lacking the phosphorylation site underwent apoptosis in early larval stages. Phosphorylation is dependent on the DNA damage checkpoint kinases ATR and ATM. Since the occurrence of phosphorylation spreads around the sites of DSB, it was suggested to serve as a recruiting signal for the DSB repair machinery (Madigan et al. 2002).

These examples highlight that the numerous functions of H2A.Z can be regulated by posttranslational modifications in addition to tissue and organism specific differentiations.

2.4.5 Deposition of H2A.Z into pre-formed nucleosomes

The deposition mechanisms which are responsible for creating and maintaining H2A.Z enriched regions within chromatin are intensively studied. Sequence differences in the C-termini of H2A and H2A.Z as well as N-terminal lysines have been found to be important for H2A.Z deposition (Millar et al. 2006; Jensen et al. 2011). In addition to sequence requirements within H2A.Z, cells also make use of so-called histone chaperones as well as ATP dependent chromatin remodelers to incorporate or evict histone variants. Two closely related multi-subunit complexes are tightly linked to H2A.Z and are introduced below in more detail: the SWR complex and the INO80 complex (**Figure 4**).

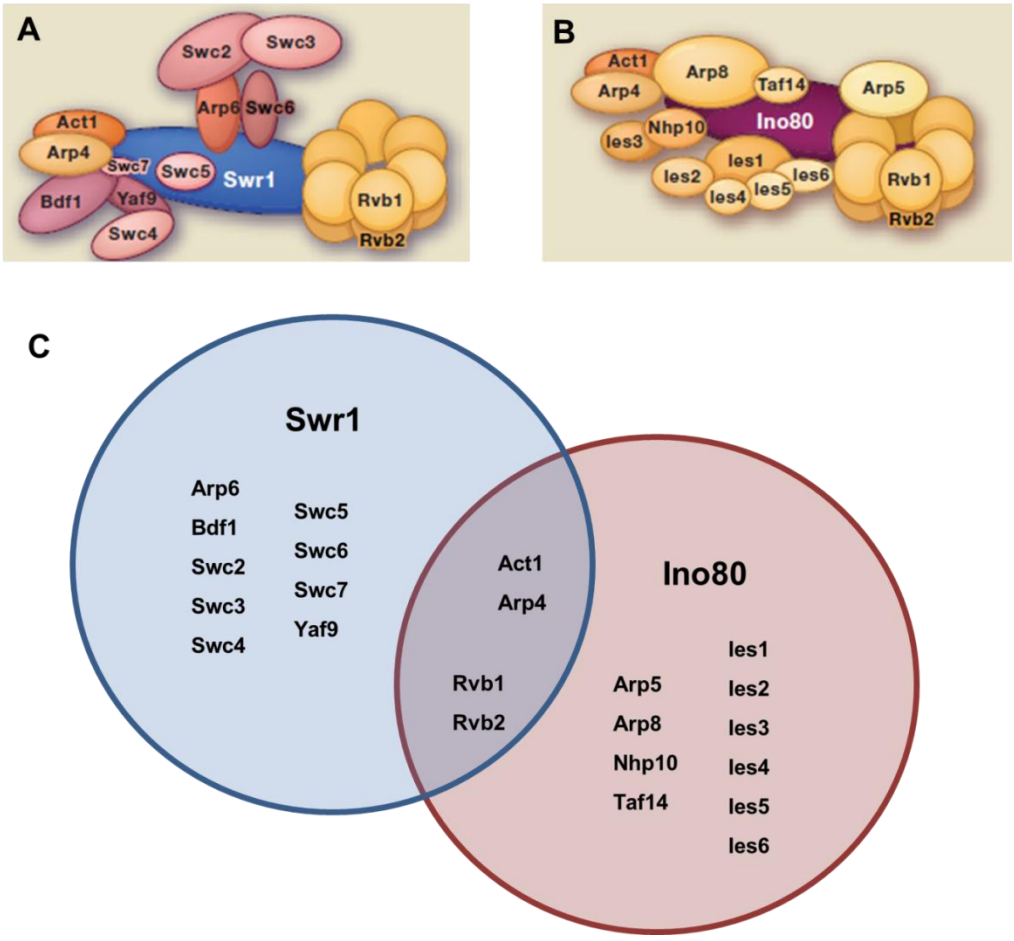

Figure 4: Chromatin remodeling complexes SWRc and INO80c from yeast. Schematic structural overviews of (A) the SWR complex and (B) the INO80 complex. (C) a scheme of the relatedness, highlighting the four subunits shared between both complexes.

2.4.5.1 The SWR complex

The specific exchange of H2A.Z for H2A has been found to be carried out by Swr1 protein related remodeling complexes by three independent laboratories (Krogan et al. 2003; Kobor et al. 2004; Mizuguchi et al. 2004).

Co-purification studies established its interaction with H2A.Z early on. In the absence of Swr1 protein (Swr1p), the association of H2A.Z with chromatin was drastically reduced and *in vitro* studies confirmed the ATP-dependent activity of the SWR complex (SWRc) to carry out the exchange of a H2A-H2B dimer for a H2A.Z-H2B dimer. Furthermore SWRc can either evict H2A-H2B dimers from nucleosomes and replace them with H2A.Z-H2B dimers or can provide H2A.Z-H2B dimers for incorporation during chromatin assembly.

It has been known for quite some time that H2A.Z is enriched around promoter regions of both active and inactive RNAPII transcribed genes (Guillemette et al. 2005; Raisner et al. 2005; Millar et al. 2006) in yeast whereas in higher eukaryotes this enrichment seems to be limited to active promoters (Schones et al. 2008) and usually this specific enrichment pattern is assigned to a strict targeting of the SWR complex. The mechanism by which SWRc itself is recruited to promoters is however, not fully understood, yet specific protein composition might be decisive for targeting. A functional crosstalk between the NuA4 histone acetyltransferase and the SWR complex seems to facilitate the eviction of H2A-H2B dimers from nucleosomes (Durant et al. 2007; Zhou et al. 2010). NuA4 acetylates N-terminal tails of H2A, H4 and H2A.Z poising them for the exchange reaction. The Bdf1 subunit of SWRc recognizes and binds acetylated tails of histones, recruiting the complex to nucleosome locations enriched for these posttranslational marks – usually promoter regions. Acetylation of H2A and H4 lysines at the same time activates the Swc2 subunit of SWRc facilitating ATP hydrolysis which is the start of the actual exchange reaction (Matangkasombut et al. 2003; Koerber et al. 2009; Altaf et al. 2010). Another subunit shared between SWRc and the histone acetyltransferase is the Yaf9 protein. Recently, the YEATS domain of Yaf9p has been shown to be required for H2A.Z deposition by SWRc as well as H2A.ZK14 acetylation by NuA4 (Wang et al. 2009). The deletion of YAF9 resulted in the typical loss of H2A.Z from chromatin, observed with not properly functional SWRc. Interestingly, the phenotypically moderate yaf9-3 mutant carrying an amino acid exchange in the conserved cleft only led to the loss of H2A.Z incorporation at some genomic loci, but retention of the histone variant at others. These data implicate a strong role for the Yaf9 YEATS domain in the function of SWRc but also show that there are qualitatively different functions within the protein domains.

In addition to its enzymatic activity of the complex, structural features of H2A.Z are also needed for proper SWRc function. Domain swap experiments have shown that the M6 region in the C-terminal acidic patch of H2A.Z is crucial for SWRc catalyzed deposition of H2A.Z into chromatin (Wu et al. 2005). A more recent study narrowed the essential region down to an extended patch of five acidic amino acid residues (DDELD) required for the H2A.Z-SWRc interaction (Jensen et al. 2011). This is another example for the importance of distinct structural and physical specifications that differentiate H2A.Z from its canonical counterpart.

2.4.5.2 The INO80 complex

The opposing reaction to the SWR complex mediated deposition of H2A.Z is carried out by a closely related protein complex containing Ino80p as the central ATPase subunit.

Upon its identification, first observations in yeast showed ino80Δ cells were highly sensitive to hydroxyurea and the alkylating agent methyl-methanesulfonate (MMS), implicating a role for the INO80 complex (INO80c) in DNA repair. INO80c also seemed to affect transcription as indicated by reduced levels of certain mRNAs upon INO80 deletion *in vivo* and through its nucleosome remodeling activity *in vitro*. Furthermore the complex exhibits 3'-5' DNA helicase activity through its Rvb1 and Rvb2 subunits which are related to bacterial RuvB (Shen et al. 2000). Another link to DNA repair could be made after the observation that INO80c localizes at DSBs in a mechanism depending on phosphorylated H2A.X (van Attikum et al. 2004). The involvement of INO80c in DNA repair has further been observed in *Arabidopsis thaliana* (Fritsch et al. 2004), suggesting a conservation of this function throughout different organisms.

In addition to transcription, INO80c has been shown to be essential for replication processes through ensuring progression of the replication fork (Papamichos-Chronakis et al. 2008; Shimada et al. 2008).

A link between INO80c and H2A.Z has first been made indirectly via an interaction between SWRc and INO80c in checkpoint adaption during DSB (Papamichos-Chronakis et al. 2006). But only recently the same group has convincingly demonstrated a direct interaction between INO80c and H2A.Z, showing that cells lacking Ino80p exhibit an aberrant localization and a genome wide increase of the H2A.Z levels (Papamichos-Chronakis et al. 2011). Furthermore they were able to characterize the specific eviction of H2A.Z-H2B dimers and replacement with H2A-H2B dimers via the ATPase activity of Ino80p *in vitro* and could link this effect to *in vivo* eviction of H2A.Z nucleosomes during transcription.

2.4.5.3 Histone chaperones linked to H2A.Z

In addition to H2A.Z specific chromatin remodeling complexes, some histone chaperones with a clear specificity for exchanging H2A-H2B dimers with H2A.Z-H2B dimers have been identified.

Nucleosome assembly protein 1 (Nap1) was among the proteins bound to H2A.Z in studies characterizing the SWR complex, but its role remained somewhat elusive since *in vitro* the SWRc catalyzed exchange reaction could be carried out efficiently in the absence of Nap1 (Mizuguchi et al. 2004). It was however, observed that the majority of unincorporated H2A.Z-H2B dimers were associated with Nap1, suggesting a role for the chaperone in providing the dimers for the SWRc catalyzed exchange reaction. Other *in vitro* experiments showed that Nap1 alone was capable of exchanging H2A-H2B dimers with H2A.Z-H2B dimers (Park et al. 2005). Nap1 isoforms between different organisms show significant sequence divergence but seem to have maintained a mostly uniform function.

The so-called chaperone for H2A.Z-H2B (Chz1) was also identified through co-precipitation with H2A.Z-H2B dimers (Luk et al. 2007). Chz1 binds to variant dimers with a higher preference than Nap1, but the two proteins have overlapping functions. Knockout of either one of these chaperones leads to binding of H2A.Z-H2B dimers by the other chaperone. In strains with deletions of both the CHZ1 and the NAP1 gene, other proteins that were part of either the FACT complex (Spt16, Pob3), the ISW1a complex (Isw1, Ioc3) or independent histone chaperones Fpr3 and Fpr4 which are not associated with H2A.Z in wt situations could compensate the chaperone functions.

These seemingly unspecific findings highlighting numerous non-exclusive H2A.Z chaperone functions of various proteins led to the assumption that chaperone disposal to the SWR complex is not highly specified, but can be fulfilled by diverse chaperone-H2A.Z-H2B complexes.

A more recent study provided some evidence that Nap1 and Chz1 indeed have independent functions and are more clearly divided in their influence on H2A.Z (Straube et al. 2010). The authors assigned the role of an import cofactor for H2A.Z-H2B dimers to Nap1 and showed that only Nap1 was responsible for maintaining a pool of soluble H2A.Z in the cytoplasm. Chz1 on the other hand is a protein strictly present in the nucleus and while it shares the function of providing SWRc with H2A.Z-H2B dimers with Nap1, it was indicated by the authors that Chz1 plays more specific roles in chromatin assembly than histone level maintenance.

2.4.5.4 Proposal of random H2A.Z deposition (targeted vs. random deposition)

In addition to a targeted deposition of H2A.Z, a model of random incorporation into chromatin has been proposed recently (Hardy et al. 2010). H2A.Z seems to be incorporated into the genome outside of the typical promoter enrichment sites and at non-transcribed loci, and transcription was shown to deplete genes of H2A.Z (Farris et al. 2005). It remains speculative whether this random incorporation is carried out by SWRc or chaperones or a combination of the two.

Interestingly, the recent development of the computational analysis tool Podbat (Positioning database and analysis tool) also revealed a Swr1p independent mode of H2A.Z deposition (Sadeghi et al. 2011). The authors analyzed all published genome wide data sets for H2A.Z in *Schizosaccharomyces pombe* and combined these data with histone marks and reported phenotypes. Surprisingly, they found that in *S. pombe* H2A.Z got incorporated into chromatin independently of the activity of Swr1p in the response pathways after DNA damage.

3 Objectives

3.1 Mechanisms of H2A.Z deposition

The DNA within a cell is highly compacted in order to fit into the nucleus of eukaryotic cells. Specific mechanisms to keep chromatin dynamic and accessible are required for the activity of all DNA dependent processes.

In addition to four canonical histones, a vast number of histone variants are able to exchange their canonical counterparts resulting in a large variety of nucleosomes that are associated with genomic DNA. H2A.Z – a prominent H2A variant first described over 30 years ago (West et al. 1980) – is the main focus of the presented work.

In the past, many publications reported an enrichment of H2A.Z within promoter regions of the genome. However, contradictory results in the literature have not pointed out a conclusive function of this histone variant at these specific regulatory sites of the genome. Different protein complexes were shown to be implicated in the deposition of H2A.Z in promoter regions. However, the basic fact that histone variants like H2A.Z are expressed independently of the cell cycle – unlike their canonical counterparts – had so far been disregarded. Thus the aim of this study was to determine what causes H2A.Z incorporation at specific elements of the genome and whether the deposition of this histone variant is related to the expression of the H2A.Z gene outside of the S-phase of the cell cycle.

3.2 *In vitro* and *in vivo* positioning differences of histone variants

The specific positioning of nucleosomes plays an important role in the regulation of chromatin. In general, DNA sequences that are occluded by nucleosomes are inhibitory for gene expression. Previous work showed that histone variant H2A.Z-containing nucleosomes can occupy different positions on DNA fragments *in vitro* (Huber, 2007).

The aim of this project was to show differences in the positioning and remodeling behavior of variant nucleosomes for a number of DNA substrates and remodelers *in*

vitro. In a second part, the observed positioning differences and the influence of remodeling enzymes should be analyzed *in vivo* by Chromatin Endogenous Cleavage.

3.3 Novel roles for the H2A C-terminal tail in nucleosome stability, mobility and binding of linker histone H1

H2A is the only core histone that contains an additional flexible C-terminal extension besides the N-terminal tail. Whereas the functions of N-terminal histone tails have been investigated in numerous studies, very little is known about the function of the H2A C-terminal tail.

In this project, the role of the H2A C-terminus on nucleosome stability, mobility in ATP-dependent remodeling reactions and on the binding of linker histone H1 *in vitro* was addressed in cooperation with the group of Robert Schneider at the Max-Planck Institute of Immunobiology, Freiburg.

4 Results

4.1 Deposition of H2A.Z in *Saccharomyces cerevisiae*

H2A.Z has been shown to be enriched at promoters compared to the respective open reading frames in several genome wide studies (Guillemette et al. 2005; Raisner et al. 2005; Zhang et al. 2005; Albert et al. 2007). H2A.Z containing nucleosome positions were a first focus point of the presented study. During early analyses the question arose whether positioning is influenced by the constitutive expression of histone variants. Surprisingly, differences of expression timing between canonical and variant histones had so far been disregarded in all published studies.

Chromatin Endogenous Cleavage (ChEC) (Schmid et al. 2004) was used to investigate the location of DNA binding proteins *in vivo*. This method allows the study of cleavage events from a MNase fusion protein of interest over a large genomic region. Moreover the position of the monitored cleavage events – with respect to the associated protein of interest – may provide additional information about higher order chromatin structures. DNA binding proteins tagged with a MNase are cross-linked by formaldehyde addition and nucleic extracts are prepared. The MNase fusion proteins are then activated by addition of calcium. DNA is isolated and subjected to restriction enzyme digest, followed by separation on an agarose gel and Southern blot. By indirect end labeling, cleavage events mediated by the MNase fusion protein, can be mapped at any genomic location of interest.

4.1.1 Preliminary analysis of selected genomic regions

As a proof of principle, three genomic loci that were previously reported to be enriched for H2A.Z at their promoter regions in comparison to the respective open reading frames were analyzed via endogenous MNase digest: MRK1, PRP12 and YDL218W. These loci showed a preferred H2A.Z occupancy at the promoter in ChIP experiments (Zhang et al. 2005). Nucleic extracts of a yeast wildtype strain (NOY505) were subjected to exogenous MNase digestion. DNA was prepared and analyzed as described above. Micrococcal nuclease (MNase) is an endonuclease with little DNA sequence specificity, which is frequently used to analyze nucleosomal protection of DNA. In chromatin, the first sites to be cleaved by the enzyme will be located in the unprotected linker regions, whereas DNA assembled into nucleosomes resists the

attack of the nuclease. MNase digestion thus results in chromatin fragments of characteristic length which get gradually reduced in size in a time course experiment. DNA fragments isolated after MNase digestion of nucleosomal arrays produce a regularly spaced band pattern after agarose gel electrophoresis. After prolonged treatment with MNase, the nuclease trims the DNA projecting from each nucleosome until the entire chromatin preparation has been converted to nucleosome core particles (NCP). The fully trimmed NCP contains 147 bp of DNA and is quite stable. In contrast to ChEC experiments, cleavage of nucleosomal DNA with exogenous MNase summarizes chromatin organization. Signals on autoradiographs do not represent the association of one chromatin interacting factor but give a picture of the nucleosomal distribution at genomic regions of interest. Furthermore, MNase hypersensitive sites can be revealed.

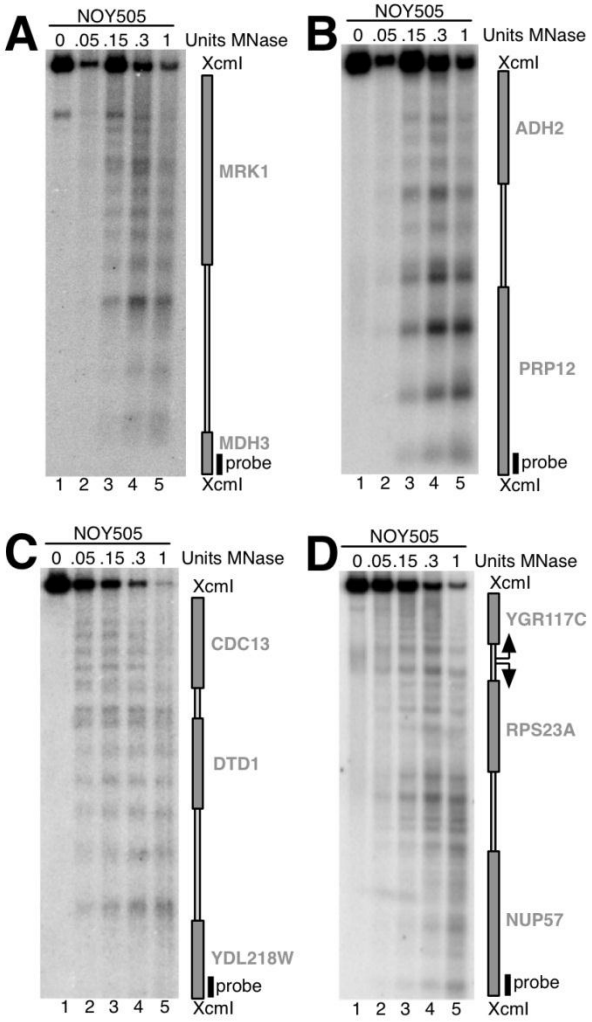

Figure 5: Exogenous MNase digest sites at the investigated loci. Formaldehyde fixed nuclei of wildtype yeast cells NOY505 were incubated with the indicated amounts of MNase at 37°C for 20 minutes. Genomic DNA was isolated and linearized with the restriction enzyme XcmI. The DNA fragments were separated on a 1% agarose gel, blotted onto a nylon membrane and analyzed in a Southern blot by indirect end labeling. Autoradiographs are shown. The schemes on the right side indicate the nucleosome

organization and locations the investigated genomic regions. The binding sites of the individual probes are shown (“probe”)

Figure 5 shows the result for the aforementioned three genomic loci as well as the promoter and open reading frame (ORF) region of the RPS23A gene. Band intensities were not specifically increased in any region, indicating that there were no hypersensitive sites, prone to MNase cuts that would falsely show increased histone incorporation in later experiments. It is interesting though, that the exogenous MNase digestion shows very different patterns for the analyzed loci. At all loci the bands are regularly spaced, but differences between the patterns at all four loci hint at a variety in nucleosomal organization.

4.1.2 Known H2A.Z binding sites can be mapped using Chromatin Endogenous Cleavage analysis (ChEC)

ChEC experiments were conducted from strains expressing H2A or H2A.Z as C-terminal MNase fusion proteins from their respective genomic locations. This allowed a direct comparison of nucleosome organization and differences between canonical and variant nucleosomes at the selected genomic regions (**Figure 6**). H2A-MNase mediated cleavage events were evenly distributed over all genomic regions (panel A-D, lanes 1-5), representing a continuous incorporation of H2A-MNase into chromatin at the inspected loci. Cleavage events from H2A.Z-MNase containing nucleosomes were also detected at all four regions, but an increase of signal intensity – arguing for an increased incorporation of H2A.Z-MNase – was visible at the promoter regions that were previously reported to be enriched for H2A.Z (panel A-C, lanes 6-10, marked with an asterisk) (Zhang et al. 2005).

Analysis of the bi-directional YGR117C/RPS23A promoter (panel D) showed an even distribution of H2A-MNase mediated cleavage events in the intergenic spacer between the 3’ ends of the RPS23A and NUP57 genes (lanes 1-5). DNA cleavage was not detected in the region containing the bi-directional promoter of the YGR117C and RPS23A genes (marked with an asterisk). This result is consistent with a study showing this promoter region to be nucleosome free and bound by the HMG-box protein Hmo1 (Hall et al. 2006).

In contrast, H2A.Z-MNase mediated cleavage was most prominent close to the YGR117/RPS23A promoter (lanes 6-10), suggesting a preferred incorporation of the histone variant into nucleosomes at this location. Taken together, these results confirm the reported preferential association of H2A.Z containing nucleosomes at the

investigated promoter regions and validate ChEC as an alternative method to compare the association of histone molecules and variants at specific gene loci.

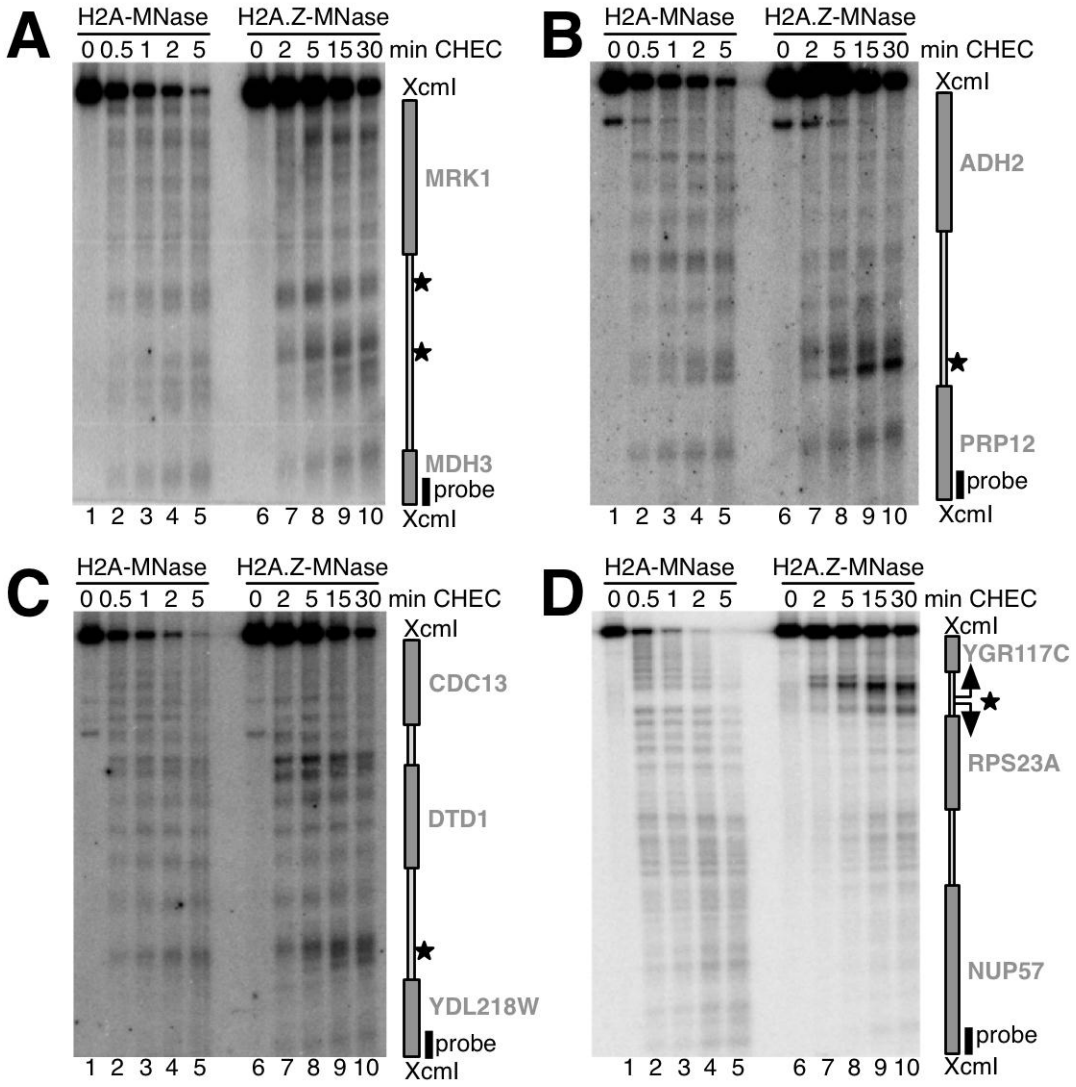

Figure 6 Preferred H2A.Z incorporation at promoters can be visualized by the ChEC method. Formaldehyde fixed nuclei of yeast cells expressing H2A or H2A.Z as MNase fusion proteins were incubated with or without calcium for the times indicated. Genomic DNA was isolated and analyzed by Southern blot and indirect end labeling. The schemes on the right side show the genomic regions investigated. Binding sites of each probe are depicted (“probe”) for all loci. Stronger intensities of bands in the autoradiographs represent an increase of cutting events mediated by the histone-MNase fusion proteins. The increase of cutting events from the H2A.Z-MNase fusion protein correlates with reported H2A.Z enrichment (A-C). Apparent enrichment of H2A.Z at the RPS23A promoter (D) also represents higher H2A.Z occupancy at the promoter as compared to open reading frame regions. Bands of interest are marked with an asterisk.

4.1.3 Core histones are enriched at promoters when they are expressed constitutively

A major difference between canonical and variant histones is their expression pattern throughout the cell cycle. Expression of core histones is strictly limited to S-phase, when newly synthesized DNA has to be compacted and transformed into a nucleosomal structure. Histone variants on the other hand are expressed independently throughout the cell cycle and thus the pool of newly synthesized histone variants is available for incorporation into chromatin outside of S-phase.

To address the influence of constant expression on the deposition of canonical histones, strains were constructed, where the CDS of H2A.Z was replaced with the CDS of H2A-/H2B-/H3- and H4 with a C-terminal MNase tag by homologous recombination. ChEC experiments with these strains expressing the canonical histones under the control of the H2A.Z promoter allowed a comparison of the deposition of canonical histones after constant or S-phase restricted expression.

Results from ChEC experiments with these strains are presented in **Figure 7** along with a complementation control. A time course of cleavage events mediated by H2A-MNase expressed under control of the H2A.Z promoter is presented in panel A. The cleavage events by the MNase fusion protein showed much slower kinetics compared to wildtype H2A experiments (compare indicated time points for H2A-MNase in **Figure 6**), indicating that the expression level of H2A-MNase was reduced under control of the H2A.Z promoter. Moreover, cleavage events of this fusion protein were now strongly enriched around the YGR117C/RPS23A promoter, suggesting an H2A.Z-like incorporation of H2A-MNase into promoter nucleosomes under these conditions.

This effect was not a result of the factual knockout of H2A.Z in the “promoter switch strain”, where the H2A-MNase fusion construct had replaced endogenous H2A.Z. In a control experiment, ChEC was performed with a H2A.Z knockout strain expressing the H2A-MNase fusion from one of the endogenous H2A locations. H2A-MNase expressed under the control of its physiological promoter did not show an enrichment of H2A-MNase mediated cutting events around the YGR117C/RPS23A promoter (**Figure 6D)**. The cleavage pattern was however identical to that of H2A-MNase when H2A.Z was present in the cells (compare with lane 1-5 in **Figure 6D**).

A summary and a direct comparison of the drastic effect of expression timing and expression level on the deposition of canonical histones is shown in panel C. Wildtype histone-MNase mediated cutting patterns are shown in lanes 1-4. For each yeast strain, only one ChEC time point is shown where DNA degradation levels are comparable between the different preparations. H2A.Z-MNase was incubated for 30 minutes, whereas canonical histone-MNase fusion proteins were incubated for only

30 seconds. These different incubation times directly reflect the differing expression levels between canonical and variant histones facilitated by their endogenous promoters. Band intensities were evenly distributed all over the investigated region for all three canonical histones, the enriched H2A.Z-MNase mediated cleavage events were more pronounced in comparison to the canonical histone-MNase fusion proteins in the YGR117C/RPS23A promoter region (compare lane 2 with lanes 1, 3 and 4). Cleavage events mediated by MNase fusions of canonical histones that were expressed from the H2A.Z promoter are shown in lanes 5-8. Surprisingly, cleavage of all MNase fusion proteins was now enriched around the YGR117C/RPS23A promoter, indicating a preferred incorporation of canonical histones in a pattern similar to that of H2A.Z. These results suggest that the preferred incorporation of H2A.Z in nucleosomes encompassing specific promoter regions is not directed by functional or structural aspects of the histone variant. Instead, the expression timing and expression outside of S-phase of the cell cycle seem to be crucial for preferential association of histone molecules with specific chromosomal regions.

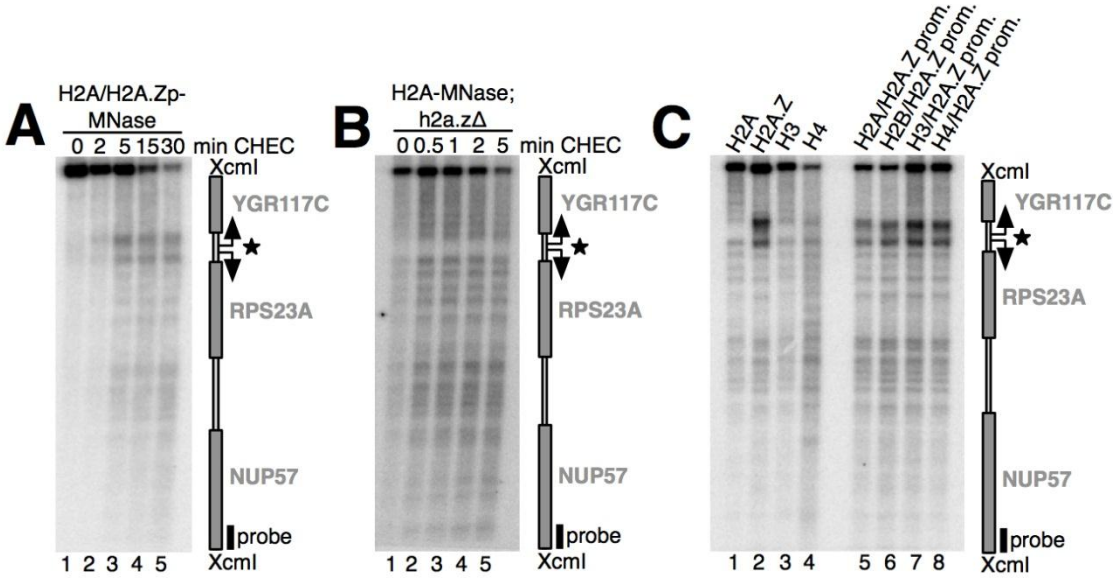

Figure 7: Promoter enrichment of canonical histones upon constitutive expression. Formaldehyde fixed nuclei of yeast cells expressing canonical histones as MNase fusion proteins were incubated with or without calcium for the times indicated. Genomic DNA was isolated and analyzed by Southern blot and indirect end labeling. (A) ChEC analysis of a strain where the CDS of H2A.Z was replaced with the CDS of H2A-MNase. (B) ChEC timecourse of H2A-MNase expressed from its endogenous promoter under h2a.zΔ conditions, incubation times are shown on top. No enrichment of H2A-MNase cleavage events around the bi-directional promoter was observed. (C) Histone-MNase fusion proteins in lanes 1-4 were expressed from their endogenous promoters, histone-MNase fusion proteins in lanes 5-8 were expressed under the control of the H2A.Z promoter. For each strain only one time point was chosen, showing comparable levels of DNA degradation and allowing for a direct comparison of all strains. ChEC incubation time for canonical histones expressed from their endogenous promoters was 30 seconds; incubation time for H2A.Z and canonical histones expressed from the H2A.Z promoter and location was 30 minutes. Different incubation times directly reflect the different expression levels facilitated by the different promoters. Bands of interest are marked with an asterisk.

ChEC experiments presented here suggest that expression timing has an immense influence on nucleosome deposition, since the H2A.Z typical enrichment around the YGR117C/RPS23A promoter could be mimicked by all four canonical histones, when they replaced endogenous H2A.Z and are constitutively expressed at a low level throughout the cell cycle.
Even though the additional H2A.Z knock out in the histone-MNase fusion protein strains did not seem to result in a pronounced phenotype, microscopic analysis of cells with an H2A.Z deletion showed an abnormal morphology (J. Griesenbeck, University of Regensburg, personal communication). It was therefore decided not to work in a h2a.zΔ background in order to prevent artifacts derived from different growth behavior in the mutant situation. Instead, expression cassettes of H2A.Z-/H2A- and H3-MNase under the control of the H2A.Z promoter were genomically integrated in the non-essential URA3 locus. These cells did not show a growth phenotype and were used to repeat the ChEC experiments.

ChEC timecourse experiments in **Figure 8** show for all four loci the previously shown enrichment at the promoter regions of H2A.Z as well as H2A and H3 upon constitutive expression. Albeit overall degradation levels being slightly lower after expression of the MNase fusion proteins from the URA3 locus, the higher signal intensities at promoter regions (marked by asterisks in each panel) were still obvious.

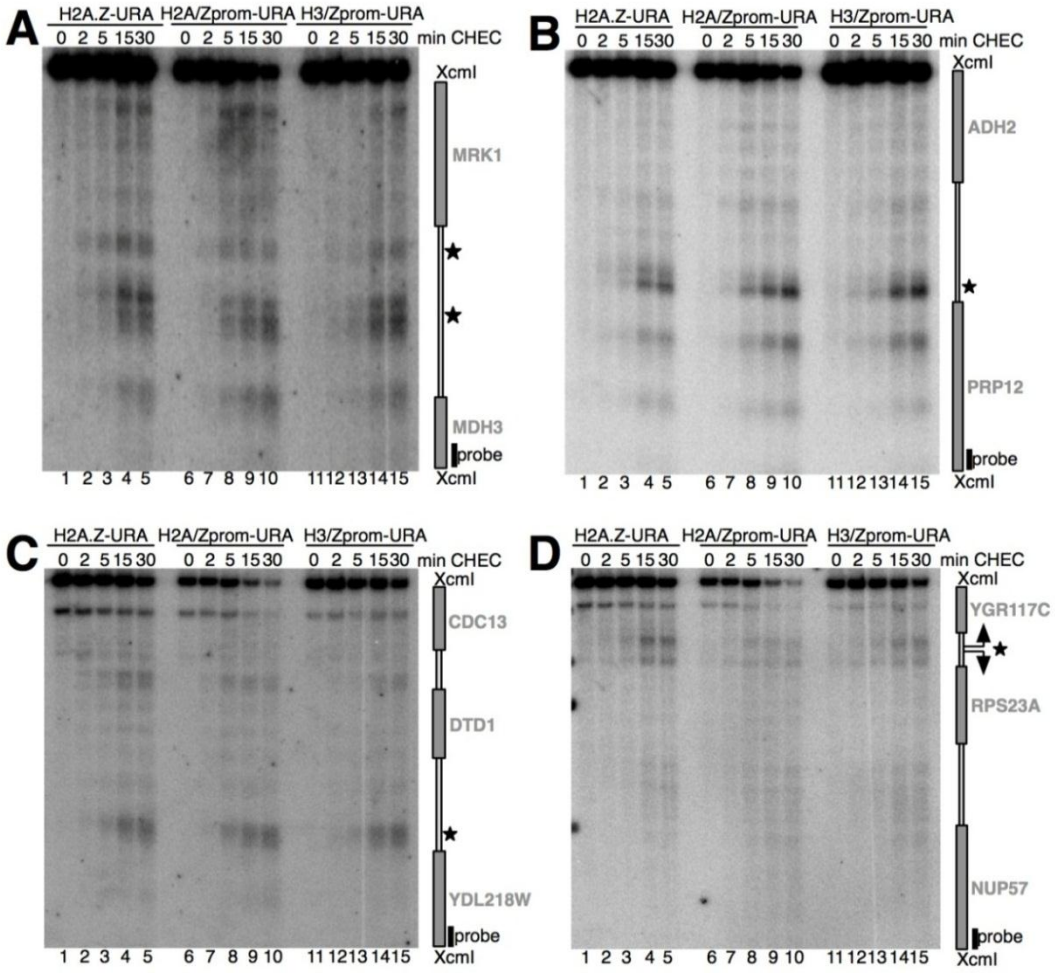

Figure 8: Expression of H2A.Z promoter controlled histone-MNase fusion proteins at the non-essential URA3 locus. In order to avoid a h2a.zΔ background, histone-MNase fusion constructs under the control of the H2A.Z promoter were inserted into the non-essential URA3 locus. Formaldehyde fixed nuclei of yeast cells expressing H2A, H3 or H2A.Z as MNase fusion proteins were incubated with or without calcium for the times indicated. Genomic DNA was isolated and analyzed by Southern blot and indirect end labeling. Cleavage patterns mediated by H2A.Z-MNase, H2A-MNase or H3-MNase, are at all loci identical to the cleavage patterns shown in **Figure 6**. Bands of interest are marked with an asterisk. The investigated genomic regions are depicted on the right hand side.

Figure 9 shows one blot consecutively hybridized with probes detecting the four loci of interest. That way cleavage patterns from H2A-MNase and H2A.Z-MNase expressed from their endogenous promoters and genomic locations were directly compared with H2A.Z, H2A and H3 expressed as MNase fusion proteins controlled by the H2A.Z promoter from the URA3 locus.

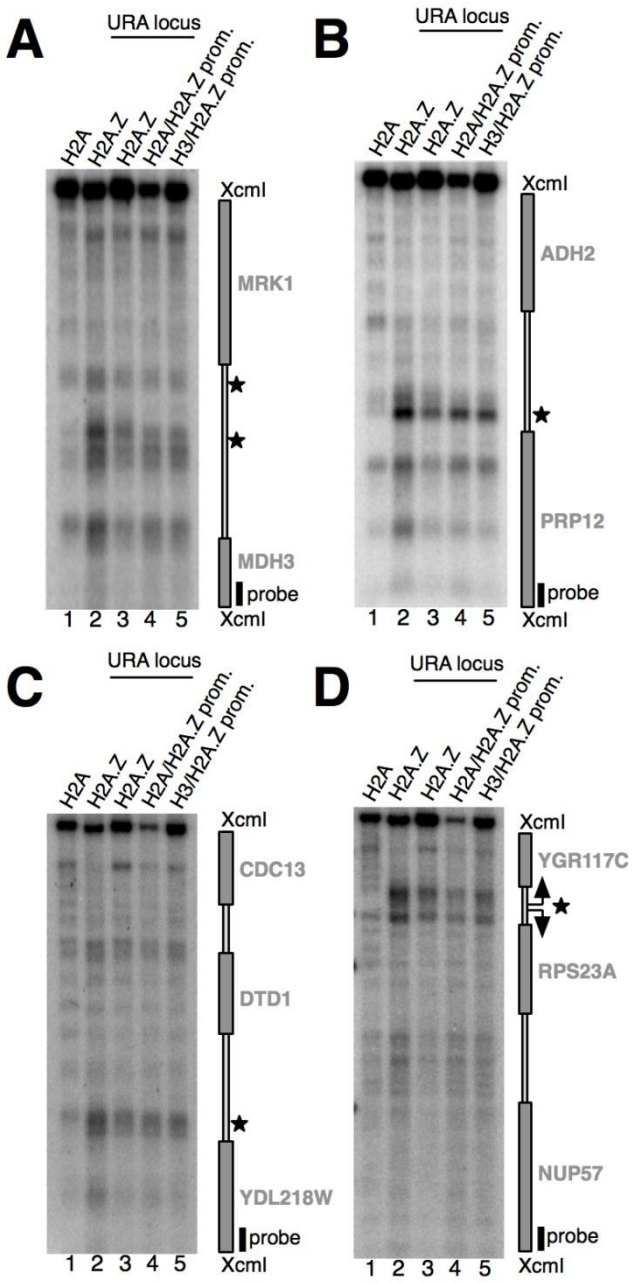

Figure 9: Canonical histones can be deposited into chromatin in an H2A.Z-like distribution pattern, when they are expressed constitutively during the cell cycle. Formaldehyde fixed nuclei of yeast cells expressing H2A, H3 or H2A.Z as MNase fusion proteins were incubated with or without calcium for the times indicated. Genomic DNA was isolated and analyzed by Southern blot and indirect end labeling. For each strain only one time point was chosen with comparable DNA degradation levels. Lanes 1 and 2 show cleavage patterns for H2A-MNase and H2A.Z-MNase each expressed from endogenous promoters and locations. Lanes 3-5 show cleavage patterns for H2A.Z-, H2A- and H3-MNase each expressed under the control of the H2A.Z promoter inserted into the URA3 locus. Schemes on the right show the genomic regions investigated.

H2A-MNase showed a similar cleavage pattern as observed in the previous analyses (**Figure 9A-D**, lane 1; compare with **Figure 6A-D** lanes 1-5), whereas cleavage from the H2A.Z-MNase fusion was enriched at the analyzed promoter regions (A-D, lane 2; marked by asterisks). More importantly, the strains with the integrated expression

cassette of H2A.Z, H2A and H3 under the control of the constitutively active H2A.Z promoter exhibited ChEC patterns almost identical to that of H2A.Z-MNase expressed from its endogenous location (A-D, lanes 3-5) and considerably different than H2A-MNase (compare lanes 4 and 5 with lane 1).

These data suggest that the deposition of H2A.Z into chromatin – at least in part or at certain locations – is not dependent on functional of structural differences between the variant and its canonical counterpart, but is directed by expression timing during the cell cycle and thus may simply depend on the availability of newly synthesized histones outside of S-phase.

4.1.4 H2A.Z is depleted within the ORF region rather than enriched at the promoter

ChEC is an ideal method to get qualitative information about the association of a factor of interest to specific chromosomal locations. However, the analysis of ChEC data is limited in providing quantitative information. Since specific cleavage events can only be observed when the MNase fusion protein binds to a distinct location, it is still possible that ChEC misses protein molecules which do not bind at discrete sites but are rather randomly distributed over a certain region.

Chromatin Immunoprecipitation (ChIP) instead allows relative quantification of the association of a certain factor with genomic DNA. For ChIP analyses the same strains as for ChEC were used, exploiting the 3xHA epitope that is fused to the C-termini of all MNase fusion proteins in this study. **Figure 10** shows relative quantitation of specific DNA regions present in the input fractions and retained on the beads after co-immunoprecipitation (IP) with an antibody recognizing the 3xHA epitope. Fragments from the promoter regions of MRK1, PRP12, YDL218W and RPS23A as well as from the respective open reading frames were efficiently co-precipitated. As expected, the precipitation of DNA fragments from the extracts of the H2A-MNase strains was more efficient compared to the H2A.Z-MNase strains. This is in good correlation with the canonical histone showing higher incorporation levels into chromatin than the histone variant. It is also in agreement with the kinetics of the ChEC experiments, where incubation times with calcium for the H2A-MNase fusion protein were much lower than for H2A.Z-MNase fusion proteins in order to reach comparable degradation of the analyzed restriction enzyme fragments (compare indicated time points in **Figure 6**).

Comparison of co-precipitation of DNA fragments derived from promoter and ORF regions at the MRK1 locus (panel A) showed that H2A precipitated significantly more DNA from the open reading frame than from the corresponding promoter fragment. As

expected, analysis of promoter and ORF fragments with H2A.Z resulted in more efficient co-precipitation of promoter DNA. Interestingly, the amount of DNA precipitated with H2A that was expressed from the H2A.Z promoter was nearly identical to the efficiency observed for H2A.Z. The same result was obtained when histone H3 was expressed under the control of the H2A.Z promoter: precipitation efficiency with H3 was identical to that of H2A.Z under constitutive expression conditions and analysis showed a higher incorporation of constitutively expressed H3 at the promoter (see **Figure 10A**).

These data demonstrate that the preferential incorporation of H2A.Z at the promoter of MRK1 can be mimicked by canonical histones when they are expressed from the constitutive H2A.Z promoter. The presented ChIP analysis of MRK1 strengthens the hypothesis that deposition is not completely protein specific, but instead depends on the expression timing throughout the cell cycle. Moreover, the ChIP data from the MRK1 locus are in agreement with the findings from the Brad Cairns laboratory (Zhang et al. 2005) and also correspond fully with the results from the ChEC experiments, demonstrating the accuracy of the method.

Panels B-D of **Figure 10** show the corresponding ChIP results for the PRP12, YDL218W and RPS23A loci. Co-precipitation of promoter DNA fragments by canonical histones was again significantly reduced upon expression from the H2A.Z promoter, which is in good agreement with the results from the MRK1 locus. However, constitutive expression of H2A and H3 during the cell cycle resulted for the other loci in more efficient co-precipitation of DNA fragments derived from the open reading frames than from the promoter. This tendency was inversed for H2A.Z. At first glance, these findings may be explained by sequence or structure specific incorporation of the histone variant H2A.Z. From the results presented here and the fact that at the promoter itself the precipitated DNA amounts from pulldowns with constitutively expressed H2A and H3 were identical to H2A.Z, it should rather be concluded that H2A.Z is specifically depleted from open reading frames and therefore deposition patterns show the typical promoter enrichment profiles. Any other histone – even when expressed in an H2A.Z-like manner – seems not to be affected by this depletion and therefore shows higher precipitation levels in the open reading frames.

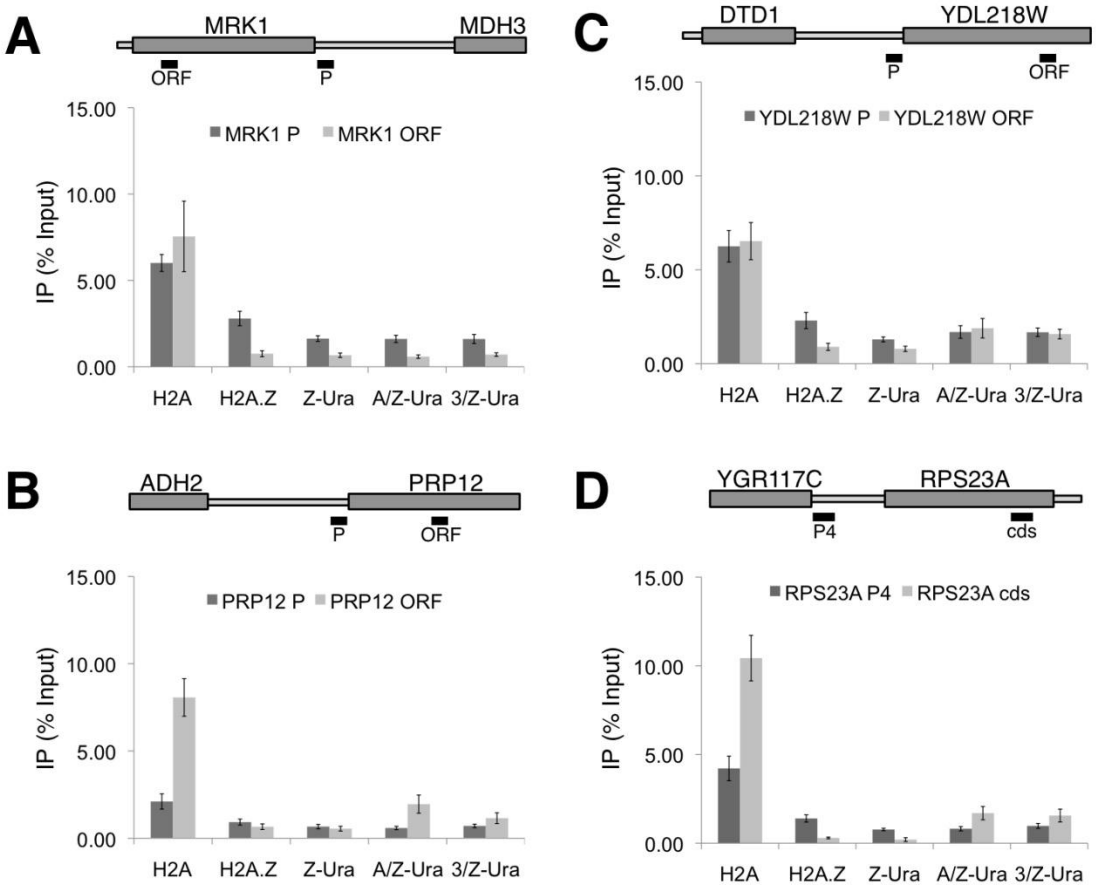

Figure 10: ChIP analyses suggest an ORF specific H2A.Z-depletion instead of targeted promoter enrichment. A scheme of the investigated regions depicting the locations amplified with specific primer pairs in the quantitative PCR (qPCR) analysis of ChIP experiments is shown on top of each panel. Crude extracts from crosslinked yeast cells were subjected to immunoprecipitation with an anti-HA antibody. Specific DNA regions present in the input fractions and retained on the beads after co-immunoprecipitation (IP) were quantified by qPCR. Bars represent total percentage of input DNA retained after IP. Error bars represent standard deviation of triplicates in qPCR reactions. (A-D) ChIP analyses of the indicated genomic loci. Precipitation efficiencies of H2A and H2A.Z are shown, as well as IP efficiencies from H2A.Z, H2A and H3 that where constitutively expressed from the H2A.Z promoter at the URA3 location (termed “Z-Ura”, “A/Z-Ura”, “3/Z-Ura” respectively).

4.1.5 H2A.Z depletion from coding regions might correlate with transcription levels at the respective genes

MRK1 was one exemplary genomic locus with identical incorporation levels of H2A.Z, H2A and H3 at the promoter and ORF when they were expressed under the control of the H2A.Z promoter. How can the observed discrepancies at the other genomic loci in terms of co-precipitation efficiency between promoter and open reading frame fragments be explained? A recent review summarized the whole genome transcription levels of all *S. cerevisiae* genes (von der Haar 2008) including the investigated genes

of this study. MRK1, the only locus showing complete correlation of histone incorporation and expression timing and levels is hardly transcribed under normal growth conditions and no active RNAPII was detected there by ChIP analysis (Mayer et al. 2010). However, PRP12, YDL218W and RPS23A are transcribed under regular conditions and active PolII was found to be associated with these genes as monitored with ChIP experiments presented in the data from Mayer et al.

To further test the possibility of a transcription rate influence, six other genes showing preferred H2A.Z occupancy at the promoter (Guillemette et al. 2005) were analyzed by qPCR (see **Figure 11**). YNL092W, KIN82 and GIT1 (panels A-C) are three genes with low transcription levels, whereas SOL2, PHO5 and YNL116W (panels D-F) are transcribed at higher levels and RNAPII occupancy is also elevated. Interestingly, the transcription level of the analyzed loci seems to influence the histone incorporation.

Panels A-C of **Figure 11** depict the ChIP results for the genes with low transcription rates YNL092W, KIN82 and GIT1. The levels of incorporation of constitutively expressed H2A and H3 at the promoter were almost the same as for H2A.Z. At the YNL092W gene, the promoter fragment was more efficiently co-precipitated than the ORF fragment with constitutively expressed canonical histones H2A and H3. This result is similar to the enrichment of H2A.Z and decisively different than the ORF enrichment exhibited by normal H2A (see panel A). For the KIN82 and GIT1 loci the enrichment of constitutively expressed histones could not be completely mimicked, but the incorporation in the open reading frame was found to be about as high as at the promoter. Replication dependent incorporation of H2A was still more effective in the ORF compared to the promoter region (see panels B and C).

Opposite results were obtained in the ChIP analyses of SOL2, PHO5 and YNL116W (panels D-F). Even though the co-precipitation levels at the promoter were again identical to H2A.Z, constitutively expressed H2A and H3 were significantly enriched in the open reading frame, almost to the same extent as normal H2A.

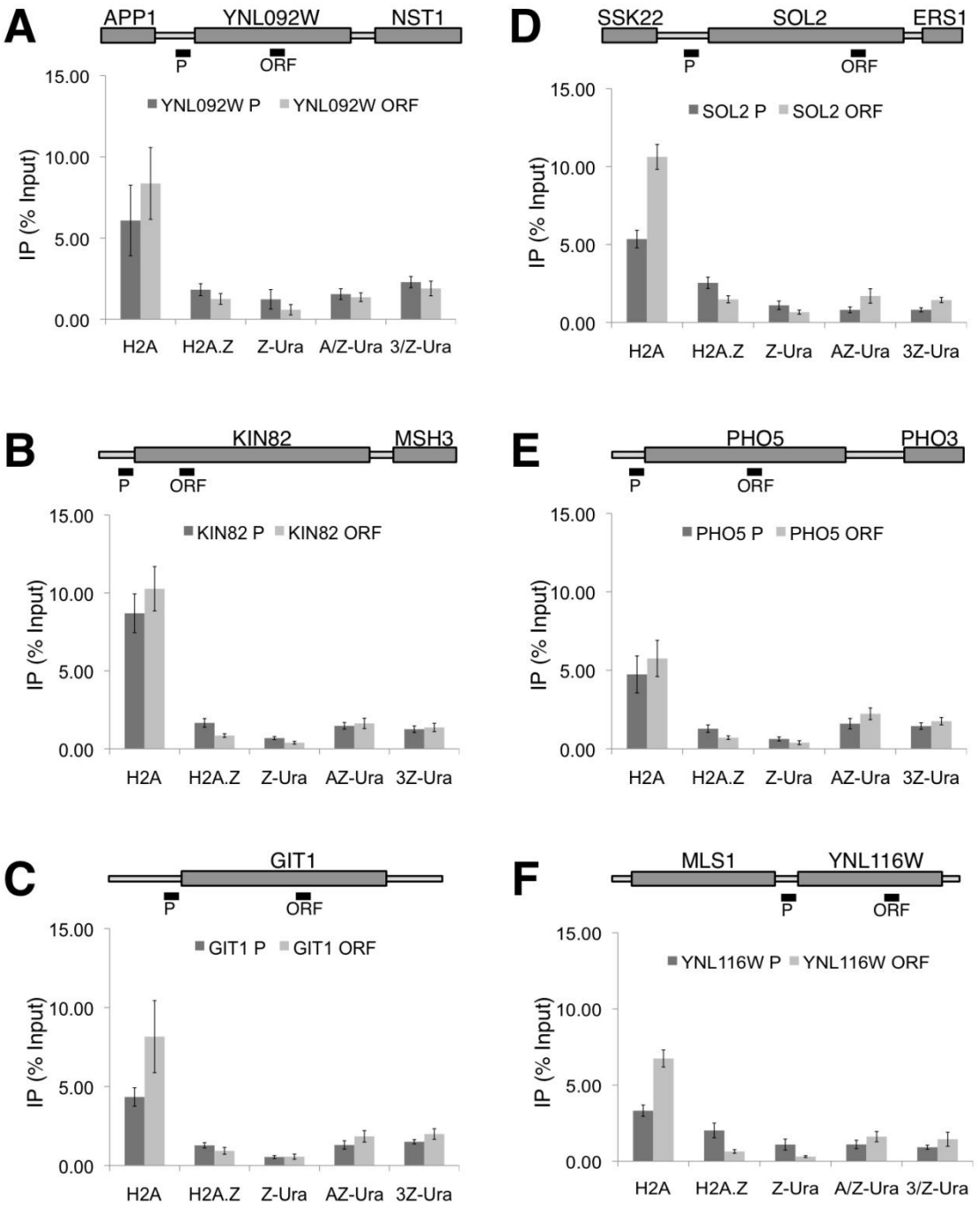

Figure 11: Transcription seems to influence H2A.Z depletion from open reading frames. A scheme of the investigated regions depicting the locations amplified with specific primer pairs in the quantitative PCR (qPCR) analysis of ChIP experiments is shown on top of each panel. Crude extracts from crosslinked yeast cells were subjected to immunoprecipitation with an anti-HA antibody. Specific DNA regions present in the input fractions and retained on the beads after co-immunoprecipitation (IP) were quantified by qPCR. Bars represent total percentage of input DNA retained after IP. Error bars represent standard deviation of triplicates in qPCR reactions. (A-F) ChIP analyses of the indicated genomic loci. Precipitation efficiencies of canonical H2A, H2A.Z are shown, as well as IP efficiencies from H2A.Z, H2A and H3 that where constitutively expressed from the H2A.Z promoter at the URA3 location (termed “Z-Ura”, “A/Z-Ura”, “3/Z-Ura” respectively).

Taken together, these data show a correlation between histone incorporation and histone expression rates as well as a correlation between histone incorporation and transcription rates at the investigated loci. The data can be interpreted in a way that H2A.Z is not specifically targeted to promoters, but instead specifically depleted from open reading frames during RNAPII transcription of the gene. The incorporation levels of H2A.Z at promoters and open reading frames of genes with low transcription levels could be completely mimicked by other histones when they were expressed under the control of the H2A.Z promoter. At loci with high transcription levels and RNAPII occupancy, the amounts of constitutively expressed histones at the promoter stayed the same, but more canonical histones H2A and H3 were found to be incorporated into the ORF of the genes.

Table 3: Overview of transcription influence on histone deposition. The table is based on ChIP-Seq data from Guillemette et al. (2005) concerning H2A.Z promoter enrichment; a summary of transcription rates according to von der Haar (2008); analysis of active RNAPII occupancy from Mayer et al. (2010) and summarizes whether H2A and H2A.Z deposition was similar after constitutive expression. Data can be visualized with the GBrowse function at www.yeastgenome.org

Gene	**H2A.Z promoter enrichment**	**Transcription rate (mRNA level)**	**RNAPII ORF-occupancy**	**Similar H2A and H2A.Z deposition after constitutive expression**
MRK1	Yes	-	- -	Yes
PRP12	Yes	-	o	No
YDL218W	Yes	-	+	No
RPS23A	Yes	++	++	No
YNL092W	Yes	- -	- -	Yes
KIN82	Yes	- -	o	Intermediate
GIT1	Yes	- -	-	Intermediate
SOL2	Yes	+	+	No
PHO5	Yes	+	++	No
YNL116W	Yes	-	+	No

- = low ; - - = very low, + = elevated; ++ = very high; o = intermediate

4.1.6 The H2A.Z deposition pattern is established independently of the SWR complex

Incorporation of H2A.Z into chromatin in *S. cerevisiae* is known to be facilitated by the SWR complex (SWRc) (Krogan et al. 2003; Mizuguchi et al. 2004). Other studies have also shown that one of the proteins within the complex – Bdf1 – is responsible for the recruitment of SWRc to promoters by interacting with bromo-domains of acetylated nucleosomes (Rangasamy et al. 2004).

In order to analyze the effect of SWRc on the deposition patterns of H2A.Z, ChEC experiments were carried out with yeast strains expressing either H2A or H2A.Z as MNase fusion proteins and with a genomic deletion of the SWR1 gene, which encodes the functional ATPase unit of the SWR complex.

The fact that SWRc is predominantly responsible for incorporation of H2A.Z into chromatin is clearly demonstrated in panel A of **Figure 12**. Cleavage patterns mediated by H2A-MNase (lanes 1-5) were observed over the complete RPS23A region and DNA was almost quantitatively digested after 5 min incubation with calcium. On the other hand cleavage of the H2A.Z-MNase fusion protein was strongly reduced (lanes 6-10), corresponding to a decreased incorporation of H2A.Z into nucleosomes in the absence of Swr1p. However, residual cleavage events could be detected, suggesting that a small number of H2A.Z-MNase molecules were still incorporated into chromatin independently of Swr1p.

Panel B shows comparable timepoints of ChEC incubation for both H2A-MNase and H2A.Z-MNase in a Swr1 wildtype background (lanes 1 and 2) or in a swr1Δ background (lanes 3 and 4). The amount of DNA loaded in lane 4 was increased threefold in order to visualize the residual incorporation of H2A.Z in the absence of Swr1p. Comparison of lanes 2 and 4 shows that preferential cleavage events mediated by H2A.Z-MNase were still maintained at the YGR117C/RPS23A promoter independently of Swr1p presence. The incorporation of H2A-MNase was in all cases independent of Swr1p as seen in lanes 1-5 of panel A and lanes 1 and 3 in panel B.

ChEC analysis of a swr1Δ strain expressing H2A-MNase under the control of the H2A.Z promoter and from the H2A.Z location (panel C) showed that deletion of SWR1 had no influence on the incorporation of the constitutively expressed H2A-MNase. Moreover, the observed cleavage pattern around the YGR117C/RPS23A promoter showed the same distribution as H2A.Z-MNase (compare with lanes 2 and 4 in panel B) and was strikingly different from that of H2A-MNase expressed strictly during S-phase (panel A lanes 1-5).

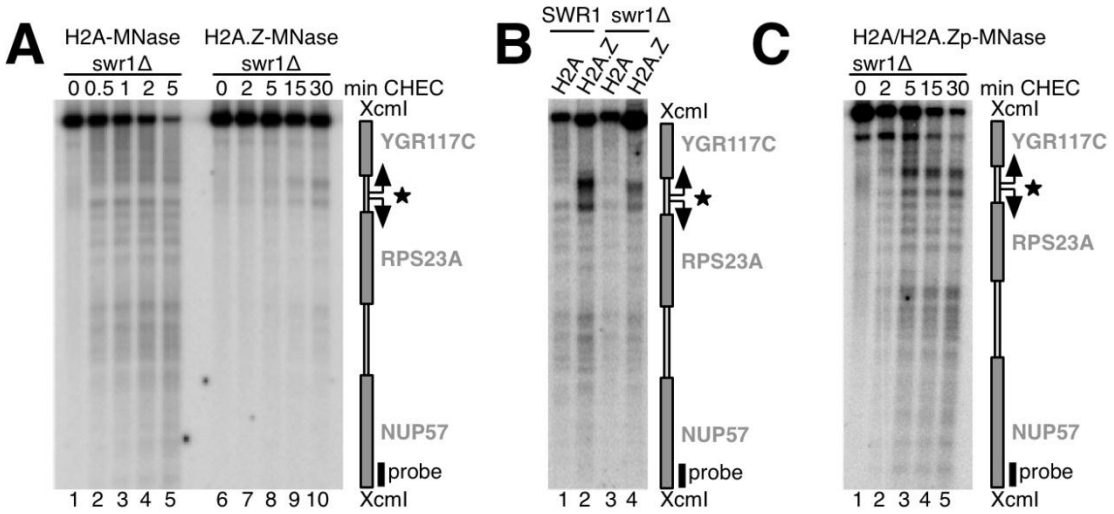

Figure 12: Knock out of Swr1p reduces the level of H2A.Z incorporation into chromatin but does not seem to influence the deposition pattern. Formaldehyde fixed nuclei of yeast cells carrying a knockout of SWR1 and expressing H2A or H2A.Z as MNase fusion proteins were incubated with or without calcium for the times indicated (panel A and C) or in panel B incubation for 30 seconds for H2A-MNase (lanes 1 and 3) and 30 minutes for H2A.Z-MNase (lanes 2 and 4). Genomic DNA was isolated and analyzed by Southern blot and indirect end labeling. For each strain only one time point was chosen with comparable DNA degradation levels. The schemes on the right side show the genomic investigated region. The binding site of the probe is depicted ("probe"). (A) ChEC experiments in swr1Δ strains. Cleavage events mediated by H2A.Z-MNase fusion protein are strongly decreased (lanes 6-10) (B) A threefold increase of DNA loaded onto an agarose gel and then blotted to a nylon membrane visualizes cutting events mediated by H2A.Z-MNase incorporated into nucleosomes in the absence of Swr1p. (C) ChEC analysis of a strain carrying a SWR1 knockout and expressing H2A-MNase under the control of the H2A.Z promoter and from the H2A.Z location.

These data indicate that SWRc is not absolutely required for the specific deposition of H2A.Z and to define a local chromatin structure which allows H2A.Z-like cleavage events in the strain expressing H2A-MNase from the H2A.Z promoter. It is also in good accordance with previously published data that the SWR complex is required for H2A.Z incorporation, but shows that the specific enrichment of this histone variant in certain promoter regions of the genome is maintained without Swr1p.

4.1.7 ChIP analysis of the SWRc influence

In order to analyze the differential association of H2A and H2A.Z with promoter and ORF regions in the absence of Swr1p in a quantitative manner, ChIP experiments were conducted under the same conditions as for the ChEC experiments shown in **Figure 12**. **Figure 13** shows the percentage of DNA fragments after co-immunoprecipitation (IP) of the indicated specific DNA regions.

At the four investigated loci, ChIP analyses did not fully correlate with the ChEC results. The amounts of DNA precipitated with H2A exclusively expressed during S-

phase from the PRP12 and the RPS23A loci (panel B and D) still showed the relative enrichment of H2A within the open reading frame compared to the respective promoter fragment. The ratios of DNA fragments co-precipitated with H2A at the MRK1 and YDL218W promoter and ORF regions (panel A and C) were not fully representing the aforementioned ChEC analyses. The relative enrichment of DNA fragments derived from the promoter and ORF were not differing in the ChIP analysis. This was in contrast to the expected ORF enrichment of DNA precipitated with H2A.

The amounts of DNA precipitated with H2A that was expressed from the H2A.Z promoter ("A/Z switch"), were approximately threefold reduced to those precipitated with H2A expressed under the control of its physiological promoter. The ratios between promoter and ORF fragments were also mimicking the pattern obtained by replication dependently expressed H2A and thus contradicting the findings from ChEC analyses presented in **Figure 12**.

As observed by ChEC, SWRc independent H2A.Z incorporation was greatly reduced, so that no conclusion can be drawn about residual incorporation of H2A.Z in the absence of SWRc.

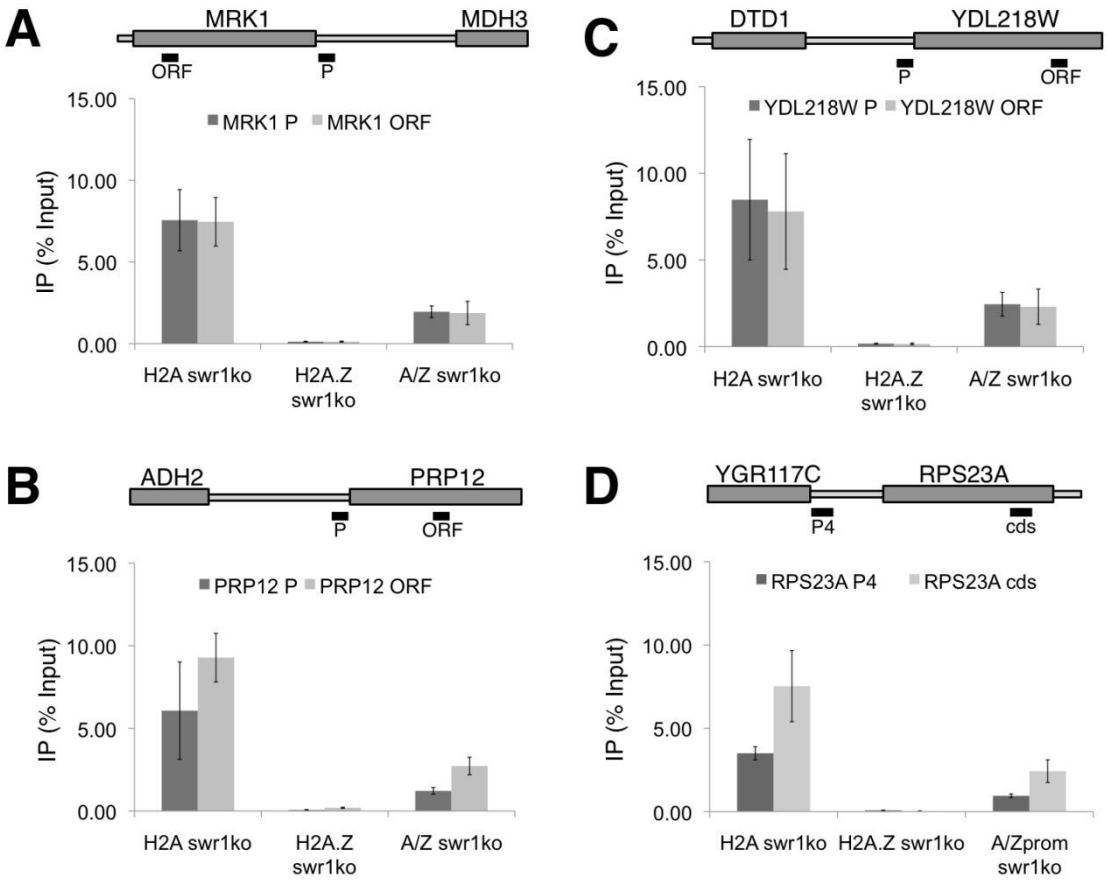

Figure 13: ChIP analyses of swr1Δ strains do not correlate with ChEC results. A scheme of the investigated regions depicting the locations amplified with specific primer pairs in the quantitative PCR (qPCR) analyses of the ChIP experiments is shown on top of each panel. Crude extracts from crosslinked

yeast cells were subjected to immunoprecipitation with an anti-HA antibody. Specific DNA regions present in the input fractions and retained on the beads after co-immunoprecipitation (IP) were quantified by qPCR. Bars represent total percentage of input DNA retained after IP. Error bars represent standard deviation of triplicates in qPCR reactions. (A + C) preferred incorporation of canonical H2A at open reading frames seemed to be disturbed after knockout of Swr1p. (B + D) the pattern of H2A incorporation at the PRP12 and RPS23A loci showed the expected ORF enrichment. In all cases (A-D) the incorporation pattern of constitutively expressed H2A mirrored the pattern of wildtype H2A. The levels of residual H2A.Z incorporation in the absence of Swr1p were drastically reduced so that no conclusions can be drawn from this depiction.

The percentage of co-immunoprecipitated DNA fragments of total input DNA with residually incorporated H2A.Z was below 0.2%. In order to compare the ratios between IP efficiencies from promoter and ORF fragments, the axis scaling from **Figure 13** was changed so that the results for H2A.Z IP in the swr1Δ situation were interpretable.

The findings from this qPCR quantitation were also diverging from the results expected after previous ChEC experiments (see **Figure 14**). Panel D shows the IP percentage of Swr1p independently incorporated H2A.Z at the RPS23A locus. As seen in the ChEC analysis, H2A.Z was still preferentially incorporated at the promoter at this locus. Slight enrichment of H2A.Z at the promoter was also found at the YDL218W locus (panel C). For MRK1 and PRP12 (panels A and B respectively) the pattern changed dramatically and converged more towards the H2A-like incorporation pattern (compare with **Figure 13**, panels A and C, “H2A swr1ko” lane) of equal IP efficiency from MRK1 promoter and ORF fragments (panel A) and clear ORF enrichment for PRP12 fragments (panel B).

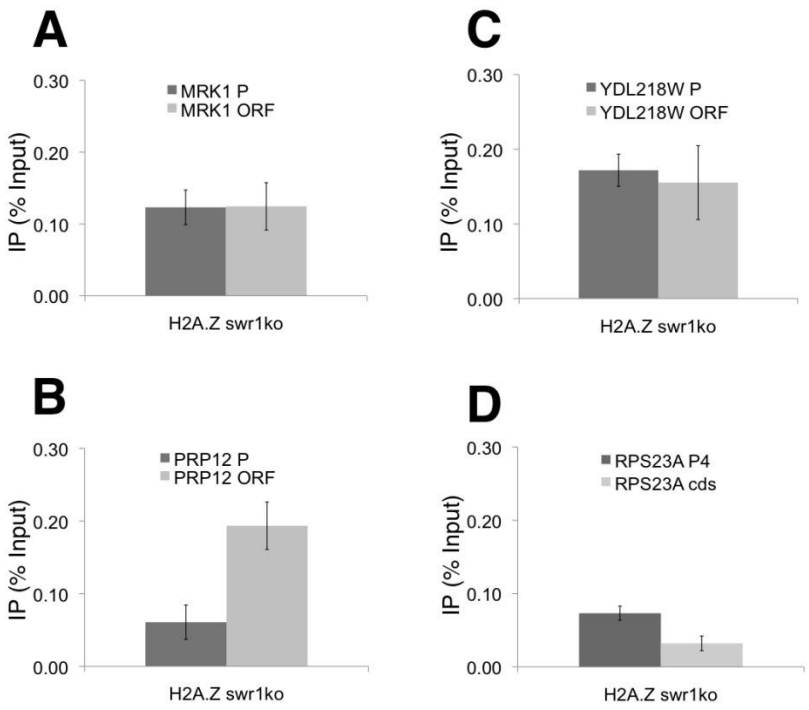

Figure 14: ChIP analyses of H2A.Z under swr1Δ conditions. ChIP quantitation with the values from **Figure 13** is shown with a different scaling of the y-axis in order to make the ratio of promoter to ORF fragments visible. (A + B) At the MRK1 and PRP12 loci, promoter enrichment of H2A.Z looks to be lost upon Swr1 deletion. (C + D) At the YDL218W and the RPS23A promoters H2A.Z is still enriched in the absence of Swr1. Whether ChIP efficiencies this small should be considered relevant is debatable.

The ChIP analysis of residually incorporated H2A.Z in the absence of Swr1p gave ambiguous results. The data indicate that the influence or the mode of action of SWRc is not equal for all loci that were investigated. Two loci still showed promoter enrichment of H2A.Z compared to the respective ORF fragment; two others showed H2A.Z incorporation similar to H2A. Constitutively expressed H2A precipitated DNA fragments from the promoter and ORF regions at the same ratio as H2A that was expressed S-phase dependently.

4.2 Dynamics and positioning of variant nucleosomes

Previous work showed that nucleosomes containing the histone variant H2A.Z occupied different positions on short linear DNA fragments. (Huber 2007).
This project was continued with the aim to test a number of different DNA templates and moreover the influence of remodeling enzymes, as well as the influence of histone variant H3.3 on H2A and H2A.Z containing nucleosomes.

4.2.1 Variant and canonical nucleosomes show similar dynamics during thermal sliding

Four types of recombinant histone octamers were prepared either containing only canonical histones, H2A.Z instead of H2A, H3.3 replacing core histone H3 or containing H2A.Z and H3.3 at the same time.
Nucleosome core particles were assembled on a linear DNA fragment from the mouse mammary tumor virus (MMTV) long terminal repeat containing two major nucleosome positioning sequences (Flaus et al. 1998). Upon assembly the central NucA position is strongly favored, but heating of the nucleosomes results in a quantitative sliding of the nucleosome to the NucB position. This enzyme-independent sliding reaction allows observation of nucleosome dynamics through quantitation of the relative rate at which position NucA is vacated and nucleosomes relocate at position NucB.
To investigate the role of histone variants on the mobility of mononucleosomes, the repositioning thermokinetics of canonical vs. variant nucleosomes were compared. **Figure 15** shows thermal sliding reactions of the four nucleosome types used in this study. Before incubation (time point “0 minutes”) most nucleosomes accumulated at the central position as illustrated in the schemes next to the gel pictures and then quantitatively relocated to the end of the linear DNA fragment, resulting in a faster migrating band in the gel. After four minutes (lanes 2) the bulk of the nucleosomes had already repositioned at the NucB position, after 8 minutes (lanes 3) relocation was completed, where no nucleosomes remain at the center of the DNA fragment. This could be attested to all four types of nucleosomes, showing no considerable influence on nucleosome dynamics of either of the histone variants, nor the combination of both within one nucleosome.

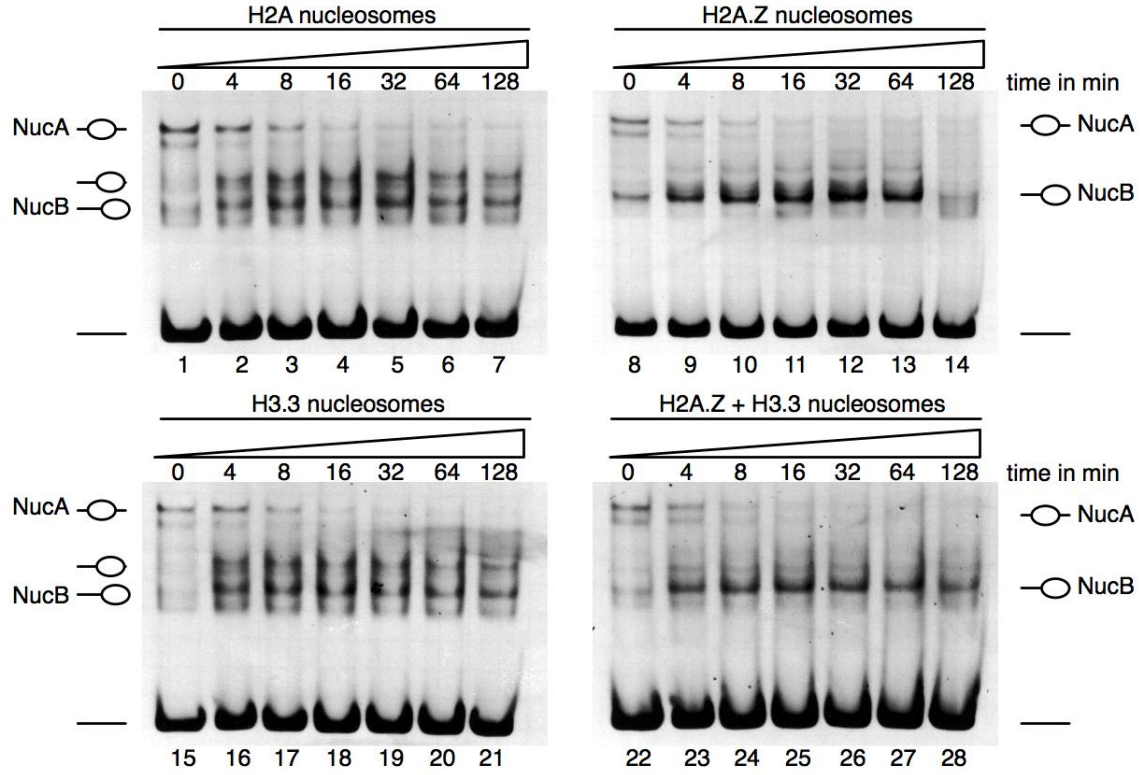

Figure 15: Differential positioning and thermal shift of nucleosomes containing histone variants. Nucleosomes containing either canonical histone octamers ("H2A Nucleosomes") or histone variants H2A.Z, H3.3 or a combination of the two (as depicted above) were reconstituted on a linear DNA fragment from the mouse mammary tumor virus (MMTV) long terminal repeat and incubated at 47°C for the times indicated. Nucleosome positions were analyzed on native 5% polyacrylamide gels and visualized by ethidium bromide staining.

As seen in lanes 1, 8, 15 and 22 of **Figure 15**, all four octamers initially assembled preferentially at the central NucA position. Interestingly, positioning differences were observed during thermal sliding. Nucleosomes containing canonical H2A (lanes 2-7 and 16-21) occupied two different end positions, the indicated NucB position at the end of the DNA fragment as well as another slightly inwards. H2A.Z containing nucleosomes (lanes 9-14 and 23-28) occupied only the NucB position. It can be clearly seen that H3.3 had no influence on the establishment of specific H2A.Z positions during thermal sliding on this particular DNA fragment.

4.2.2 Positioning differences of variant nucleosomes *in vitro*

In order to confirm and extend initial experiments (Huber, 2007), further nucleosome assembly and remodeling reactions were performed. All four types of octamers were assembled into mononucleosomes on two different DNA templates: a fragment from the Hsp70 promoter in *Drosophila melanogaster* (Hamiche et al. 1999) with multiple, well-characterized nucleosome positions; and a fragment from the murine rDNA where

H2A.Z occupies nucleosomes at the spacer promoter (Nemeth et al. 2008). Slight positioning differences were already visible without any chromatin remodeling activity when H2A.Z was present in the nucleosome (**Figure 16** compare lanes 2 and 4 with lane 1).

Results of enzymatic nucleosome remodeling reactions are shown in **Figure 16 A-C lanes 5-8**. Nucleosomes containing H3.3 showed no other positions than canonical nucleosomes (compare lane 3 with lane 1). Remodeling reactions with ACF (see panel A, lanes 5-8) led to a uniform band pattern for all four nucleosome species, as both canonical and variant forms were removed from the end of the linear DNA and relocated at a more central position. Reactions performed with the ISWI remodeler (see panel B, lanes 5-8) seemed to spread nucleosomes evenly over a DNA region between the edge and the middle of the fragment, towards a central position on the DNA, but seemed to retain a significant fraction of H2A.Z containing nucleosomes at the border position (lanes 6 and 8). This H2A.Z specific remodeling did not appear to be inhibited nor intensified by the presence of H3.3 in the nucleosome. A DNA band representing a centrally positioned nucleosome appeared strongest in the H2A.Z containing reaction (lane 6). However, considering the overall weaker band intensities in lane 8, it cannot be ruled out whether this position was occupied at the same level by double variant nucleosomes and thus also argues against an influence of H3.3 on the H2A.Z mediated positioning differences.

Nucleosome sliding reactions with the ATPase SNF2H are shown in panel C. SNF2H moved nucleosomes away from the border and the center of the DNA, relocating them in intermediate positions. Bands on the gel indicated that H2A.Z containing nucleosomes were retained at the border position to a greater extent than canonical and H3.3 nucleosomes (compare lane 5 and 7 with 6 and 8). Nucleosomes containing H2A.Z were also specifically moved toward the center of the DNA (lane 6 and 8) and H3.3 did not seem to influence the specific H2A.Z mediated positioning.

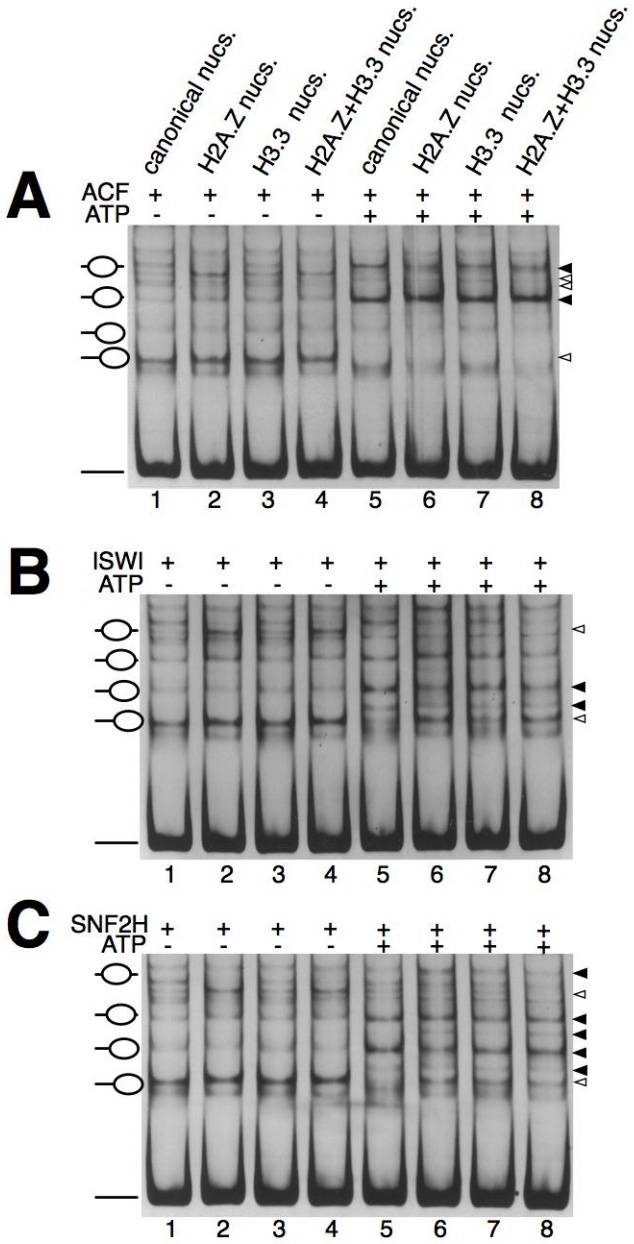

Figure 16: Positioning differences of nucleosomes containing histone variants before and after ATP-dependent chromatin remodeling. Nucleosomes containing either canonical histone octamers ("H2A Nucleosomes") or histone variants H2A.Z, H3.3 or a combination of the two (as depicted above) were reconstituted on a linear DNA fragment from the *Drosophila melanogaster* Hsp70 promoter. Nucleosome positions were analyzed on native 5% polyacrylamide gels and visualized by ethidium bromide staining. All pictures show nucleosome positions in the presence of 150 ng of the indicated chromatin remodeling enzymes (ACF in panel A, ISWI in panel B, SNF2H in panel C) without or with ATP (lanes 1-4 and 5-8 respectively). Nucleosomal positions are depicted on the left hand side. (A, B + C) Nucleosome remodeling with ACF, ISWI and SNF2H respectively. Positioning differences were observed in the presence of H2A.Z. H3.3 presence did not induce differences to either H2A or H2A.Z mediated positioning.

Identical experiments were carried out with nucleosomes reconstituted on a fragment of the murine rDNA spacer promoter (the so called “O2-40/-60” fragment). In a study mentioned above, Nemeth and colleagues found H2A.Z associated with the spacer

promoter of the rDNA from mouse in the region 3000 to 2000 bp upstream of the transcription start site (Nemeth et al. 2008). Preliminary experiments to this work revealed a short fragment (“O2-40/-60”) to cover the region most likely containing H2A.Z in an *in vivo* environment. The same fragment was used to study positioning differences *in vitro*. Results from assembly and remodeling reactions comparing canonical and variant nucleosomes are shown in **Figure 17**. White triangles on the right symbolize nucleosome positions vacated after remodeling, black triangles show new positions that appeared.

Nucleosomes containing H3.3 did not assemble very well on this DNA fragment (see lanes 3-4 and 7-8), making the analysis of a possible H3.3 effect on H2A.Z positioning not reliable. One possible reason for this might be that H3.3 might not occupy this region *in vivo*. Positioning differences mediated by the presence of H2A.Z within the nucleosome were striking on this DNA template. Lanes 1 and 2 in both panels show the initial positions occupied after nucleosome assembly. Border positions were equally occupied by canonical and H2A.Z containing nucleosomes, but only canonical nucleosomes occupied positions more towards the middle of the DNA fragment. Bands representing H2A.Z nucleosomes were preferentially located at the end and in intermediate positions of the fragment and looked less sharp towards the upper regions of the band pattern visualized on the gel.

ATP-dependent nucleosome remodeling with ISWI (panel A) showed a relocation of canonical nucleosomes towards the center of the DNA template (lane 5) whereas H2A.Z containing nucleosomes did not show significant relocation events (lane 6). The nucleosome positions at the end of the DNA fragment are represented by a double band. In the reactions with H2A.Z containing nucleosomes the lower of those two bands lost intensity after the remodeling reaction, while the bands representing intermediate positions of nucleosomes on the DNA gained intensity. The central position however, stayed completely free of variant nucleosomes upon ISWI remodeling. No conclusion can be drawn about the influence of H3.3 on the positioning of H2A.Z containing nucleosomes, since the band intensities are overall too weak (lanes 7 and 8). The specific retention of double variant nucleosomes at one of the end positions and the absence of double variant nucleosomes from the central position (lane 8) might be postulated nonetheless, complementing the findings from experiments on the Hsp70 DNA template.

Nucleosome sliding mediated by the SNF2H remodeling enzyme on the rDNA fragment produced essentially the same results. SNF2H was capable of distributing canonical histones evenly over the spacer promoter fragment (lane 5), but could only move a small fraction of H2A.Z containing nucleosomes away from the end of the DNA (lane

6). Band intensities in lanes 7 and 8 are again too weak to allow for a reliable interpretation, but it can be speculated that double variant nucleosomes also remain quantitatively absent from the center of this DNA fragment.

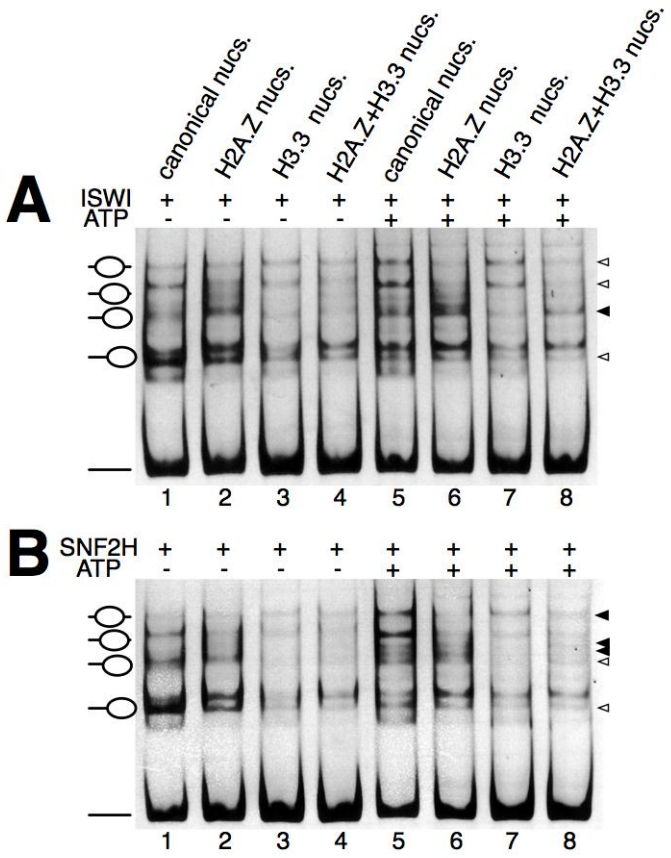

Figure 17: Positioning differences of nucleosomes containing histone variants before and after ATP-dependent chromatin remodeling *in vitro*. Nucleosomes containing either canonical histone octamers ("H2A Nucleosomes") or histone variants H2A.Z, H3.3 or a combination of the two (as depicted above) were reconstituted on a linear DNA fragment from the mouse rDNA spacer promoter (“O2-40/-60”). Nucleosome positions were analyzed on native 5% polyacrylamide gels and visualized by ethidium bromide staining. All pictures show nucleosome positions in the presence of 150 ng of the indicated chromatin remodeling enzymes without or with ATP as depicted. Nucleosomal positions are depicted on the left hand side. (A) ISWI preferentially moves H2A containing nucleosomes to a central position on the linear DNA fragment (lanes 5 and 7) and seems to move H2A.Z containing nucleosomes only slightly away from the end of the DNA (lane 6). (B) SNF2H remodeling shows the same H2A.Z specificity. Nucleosomes containing H3.3 did not assemble very well on this DNA fragment, making the analysis of a possible H3.3 effect on H2A.Z positioning not reliable.

The general conclusion from these *in vitro* experiments is that nucleosomes containing histone variants can occupy different positions on DNA than canonical nucleosomes. ATP dependent remodeling enzymes seem to be capable of recognizing the given content of a nucleosome and can thus exhibit a differentiated specificity depending on the DNA and the nucleosomal context found there. H3.3 did not show a large influence and the H2A.Z mediated differences were not obscured by the second variant.

4.2.3 ChEC shows *in vivo* nucleosome positioning differences

With similar *in vitro* results on positioning of variant nucleosomes (Thakar et al. 2009) and the more extensive findings from the presented *in vitro* studies including differential response of H2A.Z to remodeling enzymes, the project was continued in order to look for a way to visualize *in vivo* nucleosome positioning differences. ChEC was already used for experiments following a different set of questions as presented in the first part of this thesis, a number of different loci were analyzed, again comparing positions of canonical vs. H2A.Z containing nucleosomes. Choosing yeast as a model organism obscured the analysis of the interplay between H2A.Z and H3.3, since yeast only has the H3.3 version of H3.

Results of ChEC analyses comparing the positioning of canonical and H2A.Z containing nucleosomes are presented in **Figure 18**. Panel A depicts band patterns mediated by the H2A-MNase (lanes 1 and 2) and H2A.Z-MNase fusion proteins (lanes 3 and 4) at the GAL locus. The two arrows on the left mark a region in the bidirectional GAL1/GAL10 promoter, where H2A.Z-MNase mediated cleavage events differed from H2A-MNase cuts. The upper arrow points at a nucleosome position that looked to be occupied by canonical nucleosomes; the corresponding H2A.Z containing nucleosome occupied a position slightly further away from the GAL10 gene, resulting in a DNA band on the autoradiograph that is shifted a little downwards. This is not an effect of the running behavior of the gel that could make all DNA bands in lanes 3 and 4 appear to be downshifted, since at the same time most bands representing nucleosome positions run at the same height, exemplarily shown by the lower arrow pointing at the position just downwards of the shifted one.

Panel B highlights findings from the intergenic region between the 5S gene, the enhancer and the 25S gene. At this locus, strong cleavage events mediated by H2A.Z-MNase were positioned differently than cleavage events by H2A-MNase (marked by arrows on the left). Different positioning resulted either in obvious shifts of DNA bands or – as depicted by the topmost arrow – a distribution of the signal over a large area on the autoradiograph, most likely showing that H2A.Z containing nucleosomes at the 3' end of the 25S gene are not strictly positioned, but may occupy multiple alternative positions resulting in the observed broadening of the signal (see lane 2). Canonical nucleosomes (see lane 1) at this position, seemed to be more strictly positioned visualized by H2A-MNase mediated cuts resulting in a sharp band at the 3' end of 25S.

A different cleavage pattern of H2A-MNase and H2A.Z-MNase was observed in the promoter and open reading frame of the rDNA locus (panel C). H2A.Z-MNase induced an additional cut near the 3' end of the 18S gene, suggesting that additional H2A.Z containing nucleosomes occupy a position at the end of the 18S rRNA gene which is

omitted by canonical nucleosomes (upmost arrow, compare lanes 1 and 2). The same phenomenon could be observed within the core element region (CE), indicating positioning differences of H2A-MNase and H2A.Z-MNase containing nucleosomes in this region.

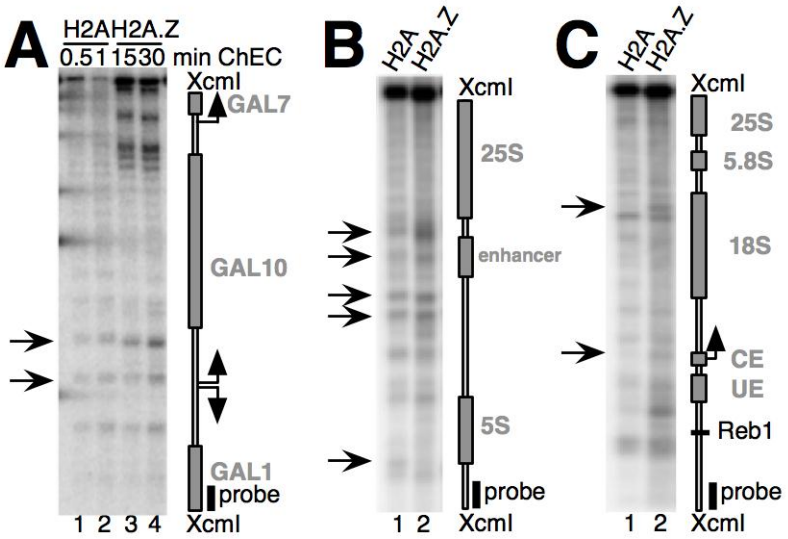

Figure 18: *In vivo* positioning differences are made visible with ChEC analyses. Formaldehyde fixed nuclei of yeast cells expressing H2A or H2A.Z as MNase fusion proteins were incubated with calcium for the times indicated (panel A) and (B+C) for 30 seconds for H2A-MNaseor 30 minutes for H2A.Z-MNase. Genomic DNA was isolated and analyzed by Southern blot and indirect end labeling. The schemes on the right side show the genomic regions investigated. Binding sites of each probe are depicted ("probe"). Bands of interest are marked with arrows. (A) ChEC experiments comparing H2A and H2A.Z containing nucleosomes showed different positions at the bi-directional GAL1/GAL10 promoter. (B) Within the rDNA locus, H2A.Z nucleosomes occupy a number of slightly different positions. (C) H2A.Z nucleosomes occupy two novel positions omitted by canonical nucleosomes.

These experiments demonstrate that variant nucleosomes containing H2A.Z also show positioning differences compared to canonical nucleosomes *in vivo*.

4.2.4 The INO80 complex contributes to nucleosome positioning *in vivo*

The INO80 complex (INO80c) is related to the aforementioned SWR complex, sharing several subunits. The ATPase Ino80p has been implicated to play a role in transcriptional control as well as DNA repair (Shen et al. 2000) and more recently INO80c has been shown to act antagonistically to SWRc and promote the eviction of H2A.Z from chromatin thus regulating the genome wide distribution of this histone variant (Papamichos-Chronakis et al. 2011).

The INO80 gene was knocked out in the yeast strain expressing the H2A.Z-MNase fusion protein to analyze the effect of Ino80p on the incorporation or positioning of

H2A.Z at selected regions of the yeast genome. The observed cleavage events of H2A.Z-MNase in the wildtype and the INO80 deletion mutant in **Figure 19** demonstrate the effects on the positioning of H2A.Z containing promoter nucleosomes which are specifically influenced by Ino80p. Comparison between lane 1 and 2 shows again the preferential occupancy of H2A.Z containing nucleosomes of positions flanking the YGR117C/RPS23A promoter. Lane 3 visualizes that H2A.Z enrichment is maintained upon Swr1p deletion (compare **Figure 12** for a detailed description). Positioning of H2A.Z nucleosomes did not change in the absence of a functional SWR complex. Lane 3 and 4 allow comparison of two ChEC experiments highlighting the cleavage events mediated by H2A.Z-MNase once under swr1Δ (lane 3) and once under ino80Δ (lane 4) conditions. It can be clearly seen that the deletion of the INO80 gene has drastic effects on nucleosome positions at this specific promoter. The two H2A.Z nucleosomes occupying this regulatory region were both shifted towards the YGR117C gene and away from RPS23A, whereas nucleosomes in the intergenic region between RPS23A and NUP57 did not seem to be repositioned at all.

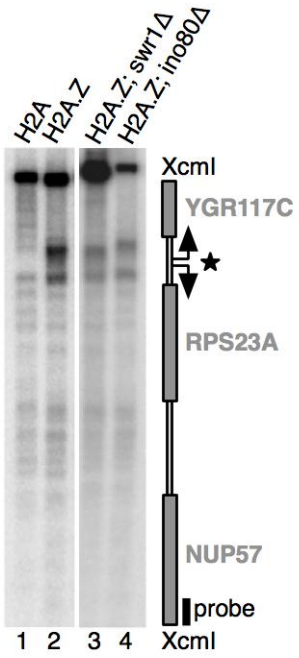

Figure 19: Ino80c is implicated in positioning of H2A.Z. Formaldehyde fixed nuclei of yeast cells expressing H2A or H2A.Z as MNase fusion proteins were incubated with calcium for 30 seconds (H2A) or 30 minutes (H2A.Z). Genomic DNA was isolated and analyzed by Southern blot and indirect end labeling. The schemes on the right side show the genomic regions investigated. Binding site of the probe is depicted ("probe").

These studies addressed for the first time the *in vivo* effect of chromatin remodeling enzymes on histone variant containing nucleosomes. It remains to be seen how INO80 deletion affects other genomic loci, but the findings at the YGR117C/RPS23A promoter may also be observed at other genomic regions.

4.3 Histone H2A C-terminus regulates chromatin dynamics, remodeling and histone H1 binding

This project was carried out in collaboration with the group of Robert Schneider at the Max-Planck Institute for Immunobiology in Freiburg. The work presented here covered the *in vitro* experiments described below and together with *in vivo* data from the Schneider group the results were published in PLoS Genetics in 2010.

4.3.1 Influence of the H2A C-terminal tail on nucleosome assembly and mobility

In this analysis, three different preparations of histone octamers were compared, each containing either two molecules of full-length H2A (129 amino acids) or two molecules of a C-terminal truncation mutant of H2A (122 and 114 amino acids respectively). For the analysis of nucleosome stability and how it is altered upon the deletion of the H2A C-terminus, these octamers were used for assembly of mononucleosomes on a linear DNA fragment containing a central NucA positioning sequence from the mouse mammary tumor virus (MMTV) long terminal repeat (Flaus et al. 2003). As seen in lane 1 of **Figure 20A** initial positions of nucleosomes containing wildtype H2A differed from nucleosomes containing truncated H2A mutants. It was concluded from this that the C-terminal tails of H2A contributes to the selection of specific nucleosome positioning sequences and their stabilization.

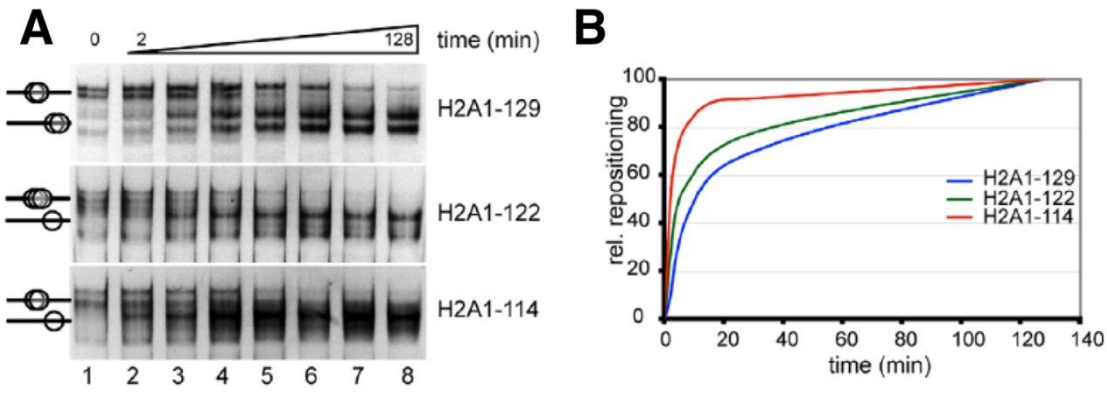

Figure 20: The H2A C-terminal tail is important for nucleosome stability. (A) Differential positioning and thermal shifts of mononucleosomes containing either full length H2A or C-terminal truncation mutants H2A-122 or H2A-114. Mononucleosomes were assembled onto the NucA positioning sequence of the mouse mammary tumor virus (MMTV) long terminal repeat DNA and incubated at 45°C for increasing periods of time. Nucleosome positions were analyzed on a native 5% polyacrylamide gel and visualized by ethidium bromide staining. (B) Quantitation of the relative nucleosome repositioning based on the band intensities.

To determine whether the C-terminal tail of H2A has an influence on the mobility of nucleosomes, the rate of nucleosome relocation after incubation at an increased temperature of 45°C was examined as previously shown for the NucA fragment of the MMTV repeat region (Meersseman et al. 1992; Flaus et al. 1998; Flaus et al. 2003). The H2A-114 mutant containing nucleosomes moved considerably faster away from the center to the so called NucB position located towards the end of the fragment. Nucleosomes containing the H2A-122 showed an increased mobility compared to wildtype H2A containing nucleosomes, but were slower than nucleosomes with the longer deletion. **Figure 20B** shows a quantitation of the nucleosome relocation events represented by increasing or decreasing band intensities in **Figure 20A**, highlighting even more clearly the obvious mobility differences exhibited by the different nucleosomes.

4.3.2 Truncations of the H2A C-terminus affect nucleosome remodeling

With the findings from the thermal mobilization experiments, it seemed even more interesting to investigate the influence of C-terminal deletions of H2A on ATP-dependent remodeling reactions.

Mononucleosomes from all three types of octamers were reconstituted on two different linear DNA fragments: the Hsp70 promoter from *Drosophila melanogaster* (Hamiche et al. 1999), well suited to look for positioning differences and the 601 template (Lowary et al. 1998) to monitor the dynamics of the nucleosomes. Chromatin-remodeling reactions were carried out with recombinant human SNF2H or *Drosophila* ISWI and ACF. All three remodelers belong to the ISWI-family of ATPases. SNF2H is the human orthologue of the *Drosophila* ISWI ATPase and ACF is a complex of the ISWI ATPase and the Acf1 subunit (Langst et al. 2001; Strohner et al. 2005).

Figure 21A shows both the initial positions of the nucleosomes on the Hsp70 fragment as well as positions after ATP dependent remodeling with ISWI, SNF2H and ACF. The complex band pattern in lanes 1 represents the multiple nucleosome positions adopted on this DNA. After incubation with the remodeling enzymes, this pattern changes for all three types of nucleosomes. White triangles on the right symbolize nucleosome positions vacated after remodeling, black triangles show new positions that appeared.

The remodeling efficiency of ISWI and SNF2H was drastically reduced for nucleosomes containing the H2A-114 truncation mutant compared to full length H2A and the H2A-122 mutant. This suggested that amino acids 114-121 are directly involved in controlling remodeling reactions by these two remodelers.

ACF – a complex with higher remodeling efficiency as the two isolated ATPase motor proteins (Eberharter et al. 2004) – was able to reposition even the H2A-114 containing nucleosomes, albeit to a slightly lesser extent than the other types of nucleosomes.

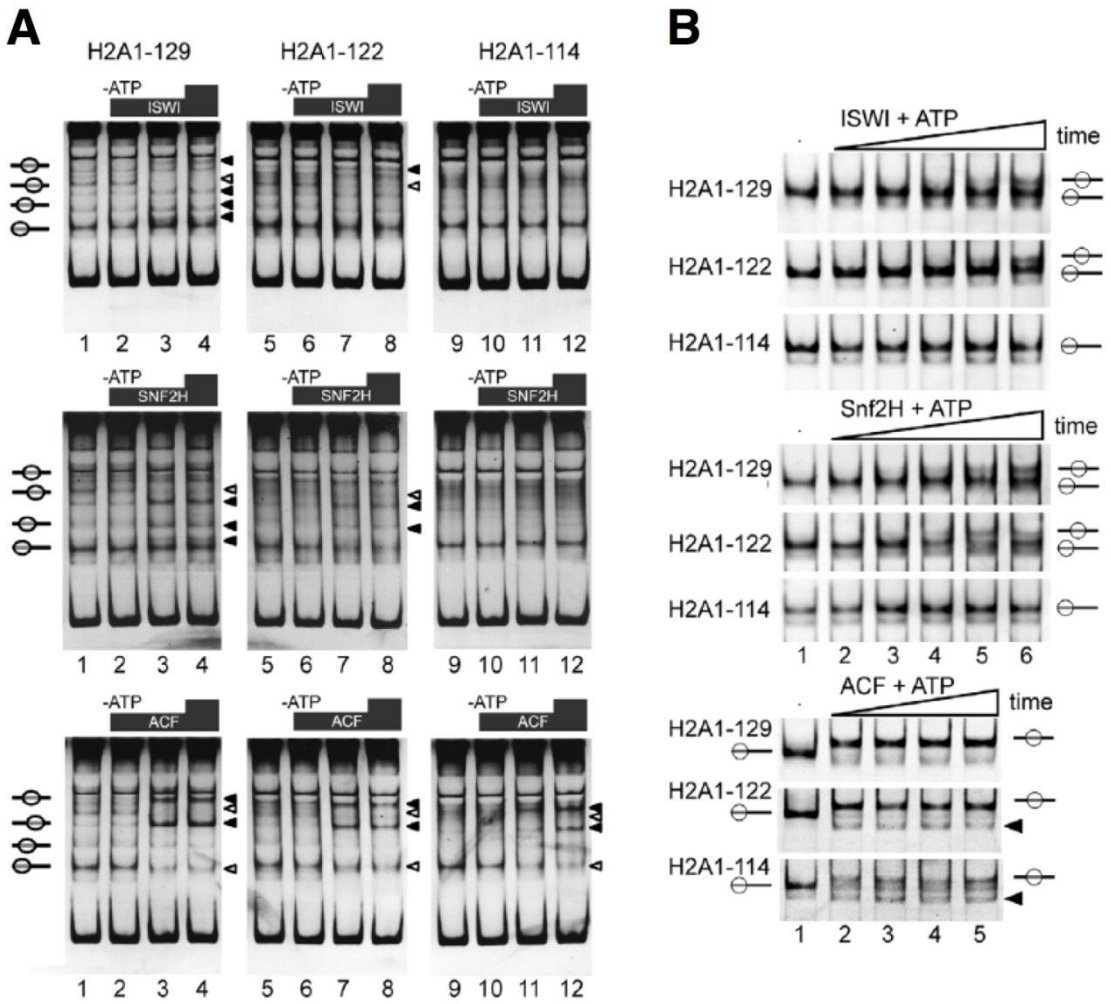

Figure 21: C-terminal truncations of H2A affect chromatin remodeling. (A) In vitro chromatin remodeling assay with mononucleosomes containing full length H2A-129, H2A-122 and H2A-114 assembled on the linear *Drosophila* Hsp70 promoter fragment. Nucleosomes were incubated at 26°C for 60 minutes with the indicated remodeling enzyme with or without ATP. Upper panel: ISWI, middle panel: SNF2H, lower panel: ACF. Lanes 1, 5, 9: reconstituted mononucleosomes. Lanes 2, 6, 10: mononucleosomes and remodeling enzyme, no ATP. Lanes 3, 7, 11 and lanes 4, 8, 12: mononucleosomes and remodeling enzyme + ATP. . Nucleosome positions were analyzed on a native 5% polyacrylamide gel and visualized by ethidium bromide staining. (B) Dynamics of nucleosome remodeling reactions assayed with a 601 remodeling template. Nucleosomes containing full length H2A and the respective C-terminal truncation mutants as indicated on the left, were incubated without (lane 1) or with 100 ng of the indicated remodeling enzymes and ATP (lanes 2-6). The remodeling reactions were incubated for increasing amounts of time (1-40 minutes) and analyzed as described above. Nucleosome positions are depicted on the right hand side: black triangles indicate new nucleosome positions observed with truncations mutants H2A-122 and H2A-114.

To investigate the differences in the remodeling dynamics the remodeling reactions were also analyzed with 601 DNA nucleosomes (**Figure 21B**). As seen on the Hsp70

template, ISWI and SNF2H could efficiently remodel both full length H2A and H2A-122 nucleosomes but were not able to catalyze movement of the H2A-114 containing nucleosomes. ACF, was again capable of relocating even the nucleosomes containing the long truncation form H2A-114 with similar kinetics as wt H2A and H2A-122, however, showing different final positioning patterns.
These data show that the H2A C-terminus is required for the efficient nucleosome remodeling by ISWI and SNF2H; only ACF – a remodeling complex containing two ATPase motor subunits – seems to be able to disregard the missing C-terminal tail. It was also shown – in full correlation with the experiments of thermal mobility – that the C-terminal tail is required for the establishment of specific nucleosome positions on different DNA templates.

4.3.3 The C-terminus of H2A interacts with linker histone H1

In addition to the N-terminal histone tail, a characteristic of all histone molecules, H2A is the only histone bearing a C-terminal tail. Since this tail protrudes from the nucleosome, it suggests a function in the facilitation of protein recruitment.
In order to identify possible interaction candidates, the group of Dr. Robert Schneider in Freiburg performed an unbiased screen in HeLa cells and identified proteins via mass spectrometry. Several peptides originating from either H1.1 or H1.2 could be identified, but no core histones. Via co-immunoprecipitation they identified a direct interaction between H1 and H2A C-terminal tail repeats.
In vitro experiments were then conducted comparing the ability of nucleosomes containing full length H2A and the two truncation mutants to bind H1. A 208 bp DNA fragment containing the 601 positioning sequence was used to assemble mononucleosomes (Thastrom et al. 1999) which were then incubated with rising amounts of H1. As depicted in **Figure 22A,** incubation of nucleosomes containing full length H2A with H1 resulted in a band shift that started to appear at equimolar nucleosome to H1 ratios (lanes 1-6). For nucleosomes containing either the H2A-122 or the even shorter H2A-114 mutants, this H1 interaction was only detected at a much reduced level (compare lanes 7-12 and 13-18 with lanes 1-6 respectively). This led to the assumption that the H2A C-terminus plays an important role in the interaction of nucleosomes with linker histone H1.

The idea arose that the weaker H1 interaction with nucleosomes lacking the H2A C-terminus could result in the formation of a bona fide chromatosome. In order to test this possibility, the H1 binding mode was studied with nuclease digestion experiments.

Figure 22B shows the MNase treated nucleosomes either with or without additional binding of H1. Lanes 1, 4 and 7 show the complete 208bp DNA fragment of an intact mononucleosome, lanes 2, 4 and 8 show the DNA after MNase digestion, reduced to the 147bp protected by the histone octamer. In lane 3 an additional DNA band at approx. 160bp was visible (**Figure 22B** marked by an arrow), the chromatosome stop that transiently blocks MNase digestion. The same effect was visible for the nucleosomes containing the C-terminal truncation mutants of H2A, albeit much weaker. This showed again the lower binding affinity of H1 when the C-terminus of H2A is missing, however proving that the correct binding mode is still maintained.

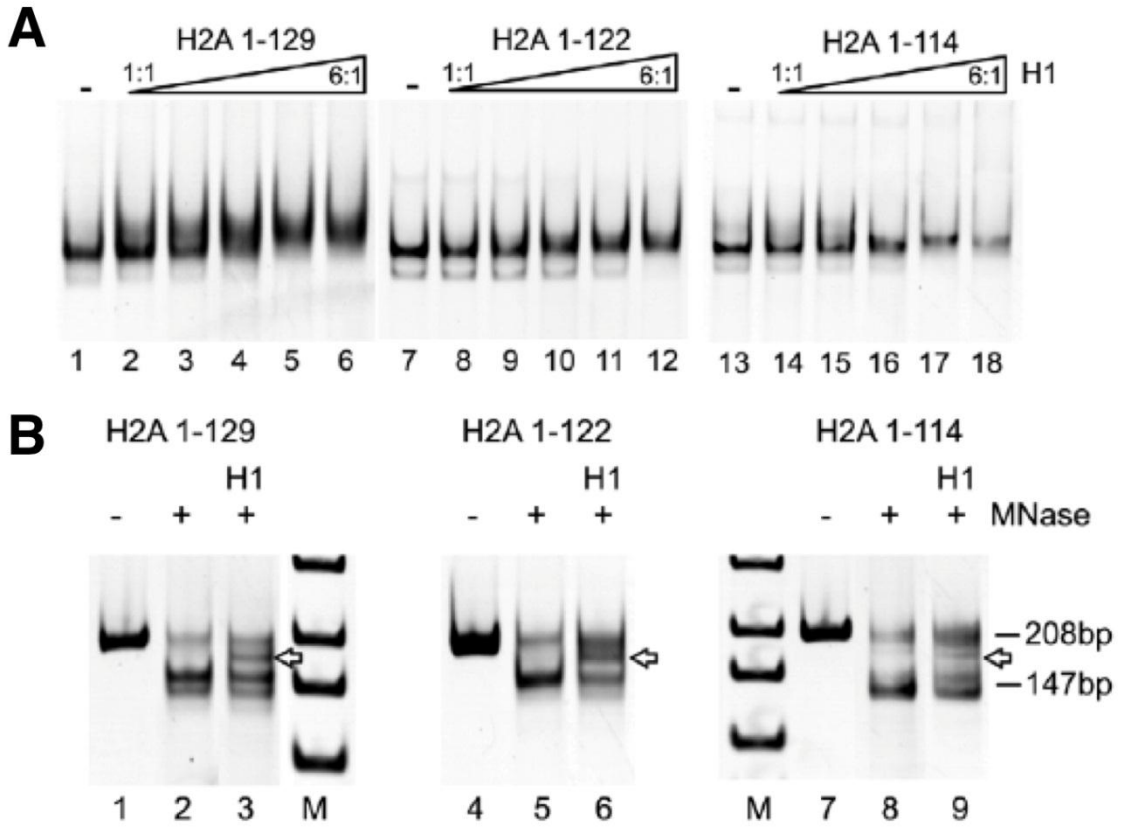

Figure 22: Deletion of the H2A C-terminal tail reduces H1 binding affinity. (A) Binding of H1 to *in vitro* reconstituted mononucleosomes containing either full length H2A (lanes 1-6) or C-terminal truncation mutants H2A-122 (lanes 7-12) or H2A-114 (lanes 13-18). Mononucleosomes were assembled onto a 601 remodeling template, incubated with increasing amounts of H1 (nucleosome to H1 ratios 1:1 – 1:6) and analyzed on native 5% polyacrylamide gels. Nucleoprotein complexes were visualized by ethidium bromide staining. (B) Partial MNase digestions of H1-nucleosome complexes show a chromatosome stop. Nucleosomes and H1-nucleosome complexes (at a molar ratio of 6:1) reconstituted on a 208 bp 601 DNA fragment were incubated under increasing MNase concentrations and the resulting DNA cleavage products were analyzed by native PAGE and ethidium bromide staining next to a DNA standard (M). Positions of the undigested DNA fragment (208 bp), the protected nucleosomal DNA (147 bp) and the chromatosome stop (arrow) are indicated.

5 Discussion

5.1 Mechanisms of H2A.Z deposition

The work presented in this thesis addressed the question whether S-phase coupled vs. constitutive expression can explain the observed incorporation patterns characteristic of H2A.Z *in vivo*. Nucleosome location and deposition were investigated using MNase tagged histones and H2A.Z-like enrichment patterns were observed for constitutively expressed canonical histones under the control of the H2A.Z promoter. This led to the assumption that expression timing plays an important role in histone variant deposition. ChIP analyses of different loci diversified these findings, suggesting a mechanism of random H2A.Z incorporation all over the genome and arguing for transcription as the key factor in establishing distinct H2A.Z occupation patterns.

Several studies have implicated the SWR complex to be responsible for a targeted insertion of H2A.Z at promoters without fully revealing a convincing mechanism for this (Krogan et al. 2003; Kobor et al. 2004; Mizuguchi et al. 2004). However, another study recently proposed an additional deposition mechanism ignoring specific targeting and incorporating H2A.Z randomly over the genome (Hardy et al. 2010). Additionally, a novel computational analysis tool ("Podbat") revealed Swr1p independent deposition events in *Schizosaccharomyces pombe* (Sadeghi et al. 2011).

5.1.1 Transcription is crucial for the establishment of H2A.Z enrichment patterns

Within this work it could be shown that canonical histones mimic H2A.Z deposition patterns when they are expressed under the control of the native H2A.Z promoter.

Chromatin Endogenous Cleavage (ChEC) was used to directly compare the effect of S-phase coupled vs. constitutive expression on the deposition of canonical and variant histones. Cleavage events of H2A.Z-MNase were enriched around selected promoter sites, showing the enrichment of the variant histone in these regions of the yeast genome. Accordingly, no enrichment of H2A-MNase induced cleavage events was observed when it was expressed under control of its native S-phase restricted promoter.

Surprisingly, the effect of constitutive expression on the cleavage of canonical H2A-MNase was considerable. Cleavage of H2A-MNase which was expressed under the control of the H2A.Z promoter was enriched at the same sites as cleavage from H2A.Z-MNase, suggesting a similar incorporation of H2A and H2A.Z when both are constitutively expressed from the H2A.Z promoter. This led to the conclusion that not the functional or structural aspects of the histone variant, but expression timing and level are strong determinants of H2A.Z deposition into chromatin.

Chromatin Immunoprecipitation (ChIP) analyses diversified these findings. IP efficiencies at promoters were identical for H2A.Z and H2A after constitutive expression. Amounts of precipitated DNA from open reading frames however differed considerably, leading to a fraction of loci where ChIP verified enrichment patterns seen by ChEC and a second fraction where results obtained with both methods where contradictory.

Analysis of gene expression data revealed that H2A.Z is present to a relatively high extent at open reading frames of non-transcribed genes (Guillemette et al. 2005; von der Haar 2008). On the other hand, actively transcribed ORFs that are characterized by the presence of active RNAPII subunits (Mayer et al. 2010) were depleted of H2A.Z.

In this work, loci with consistent ChIP and ChEC data, appeared to have a low occupancy of active RNAPII subunits (Mayer et al. 2010) and low levels of mRNA transcription from these loci (von der Haar 2008). At all loci studied here, levels of H2A and H2A.Z at promoter regions depended only on the expression level and timing, differences of histone incorporation observed in the open reading frames, seemed to depend on the interplay of expression timing of the histone and transcriptional activity of the investigated loci.

This led to the suggested model of H2A.Z deposition (**Figure 23**). Therein, H2A.Z is incorporated randomly all over the genome and is specifically depleted from open reading frames during passage of active RNAPII. This is in good accordance with the aforementioned theoretical proposal for a random incorporation mechanism (Hardy et al. 2010) and is a slightly different interpretation of a study proposing two fractions of functionally different H2A.Z (Farris et al. 2005). The authors of the latter study suggest that cells differentiate between promoter H2A.Z and H2A.Z incorporated into coding regions, however, without commenting on how the cellular machinery may carry out this distinction. It remains speculative whether for example posttranslational modifications at different loci could be solely responsible for this distinction or whether another mechanism could be suitable for resolving a delicate problem like this.

The “Place and Erase Model” proposed in this thesis is less complicated and depends largely on a genome wide random incorporation and subsequent transcription for the establishment of specific H2A.Z enrichment patterns. The ChIP data suggest that H2A.Z gets incorporated into chromatin at a certain level, independent of whether it is at the promoter or within the coding region of a given genomic locus. A decrease in histone variant occupancy is seen over transcribed loci, resulting in the typical H2A.Z enrichment at promoters. Since the incorporation levels of H2A.Z could be mimicked with constitutively expressed canonical histones at all promoters and also at the open reading frames of non-transcribed genes, it is suggested that not the incorporation but the transcription-coupled eviction of histones from coding regions takes place in a protein dependent fashion.

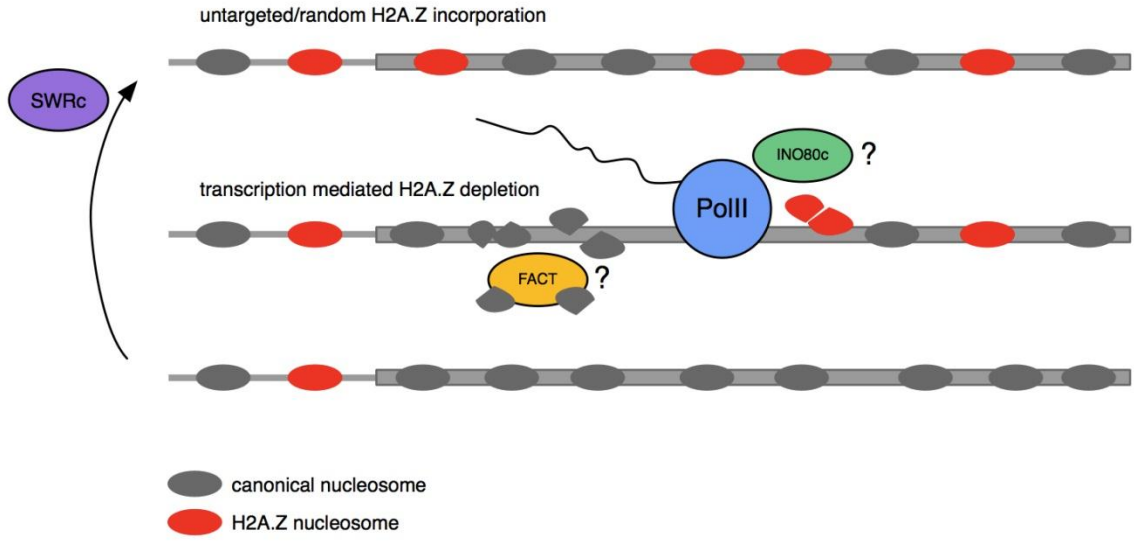

Figure 23: The “Place and Erase Model” of untargeted H2A.Z incorporation. Nucleosomes containing only canonical histones are marked as grey; nucleosomes containing the H2A.Z variant are depicted as red. Random incorporation of H2A.Z nucleosomes over promoters as well as coding regions is shown in the upper graph. Subsequent eviction during transcription elongation and re-incorporation of H2A.Z are schematically presented as discussed in the text.

What is the specific role of H2A.Z if not preferred incorporation at promoters, which is thought to be a marker for transcription initiation but the specific eviction is establishing the promoter enrichment?

It seems possible that a long-discussed decrease in stability of H2A.Z containing nucleosomes (Suto et al. 2000; Abbott et al. 2001; Park et al. 2004; Jin et al. 2007) could be essential for the disruption of nucleosomes during the passage of the RNAPII machinery. It has been shown that h2a.zΔ mutants are hypersensitive to inhibitors of transcriptional elongation (Santisteban et al. 2011) attesting an important role to H2A.Z for the maintenance of transcription in addition to its role in transcription initiation

(Zhang et al. 2005; Jin et al. 2009). Energetically favorable eviction of H2A.Z from coding regions might be followed by a preferred incorporation of canonical H2A during re-assembly of nucleosomes behind the transcriptional machinery. FACT for example has been linked to histone variant exchange mediated by certain posttranslational modifications (Heo et al. 2008), so it is tempting to speculate that specific modifications on evicted H2A.Z prevent it from being re-assembled into chromatin. This would result in a preferred H2A incorporation at transcribed loci that is mediated by FACT.

Besides of an energetically favored eviction, there is also the possibility that eviction of H2A.Z from coding regions is specifically carried out by protein complexes. Two independent studies have provided evidence that the INO80 complex might interact with the transcription elongation machinery (Klopf et al. 2009; Venters et al. 2009). Through its specific exchange activity replacing H2A.Z with H2A (Papamichos-Chronakis et al. 2011), INO80c could also be responsible for H2A.Z eviction from transcribed regions.

5.1.2 The H2A.Z enrichment pattern is established independently of the SWR complex

In this study, the Swr1 protein – the ATPase subunit of the SWR complex – did not turn out to be responsible for the establishment of characteristic H2A.Z enrichment patterns. ChEC analyses of strains with a swr1Δ background showed that H2A.Z incorporation was grossly reduced; however, residual H2A.Z containing nucleosomes were still assembled onto DNA. It could also be shown that these residually incorporated H2A.Z molecules were still enriched around the YGR117C/RPS23A promoter, leading to the hypothesis that the SWR complex is not required for enrichment of this histone variant in nucleosomes encompassing promoter regions.

Canonical H2A expressed constitutively from the H2A.Z promoter in a swr1Δ background was incorporated at the same levels as in the presence of Swr1p. This proved that its incorporation into chromatin is completely independent of Swr1p, but was still enriched at the promoter. The conclusion from these experiments is that the SWR complex is not needed to define a local chromatin structure which allows H2A.Z like cleavage events in the strain expressing H2A from the H2A.Z promoter. This is in good accordance with previously published data that SWRc is required for H2A.Z incorporation (Krogan et al. 2003; Mizuguchi et al. 2004), however, it does not determine the specific enrichment patterns as implicated by others (Koerber et al. 2009).

The mechanism by which SWRc targets H2A.Z to promoters has long been discussed, yet has not been fully resolved. Indirect assumptions have been made on the basis of

two facts: SWRc catalyzes the incorporation of H2A.Z, and SWRc contains Bdf1, a protein which carries two bromodomains shown to interact with acetylated histones, preferentially found at promoters (Matangkasombut et al. 2003; Altaf et al. 2010).
ChIP results in this study, however, showed that the knockout of the Swr1-ATPase does not necessarily suppress the enrichment of H2A.Z at specific promoters regions. Although precipitation efficiencies were very low given the greatly decreased H2A.Z incorporation levels at all investigated loci. Nevertheless some of the promoter regions were enriched for this variant even in the absence of Swr1p. In combination with the ChEC results showing unchanged enrichment of H2A.Z containing nucleosomes in a swr1Δ situation at the YGR117C/RPS23A promoter, these data argue for a SWRc independent mechanism that establishes promoter enrichment of H2A.Z. Undoubtedly, it cannot be excluded that the SWR complex might still contribute to targeting H2A.Z to promoter regions. Both models don't have to be mutually exclusive and it could be possible that they co-exist either being differentiated between different tissues, cell cycle states or between different signaling pathways. It will be interesting to see results of further analyses targeting these questions.

In accordance with the model presented on the basis of this work, an important role for the SWR complex could lie within facilitating repeated rounds of transcription. It has been discussed above that H2A.Z containing nucleosomes are evicted from chromatin over coding regions in a transcription dependent way, rendering RNAPII passage possible because of their lower stability. The re-assembled H2A-containing nucleosomes after one round of transcription are much more stable, constraining further rounds of transcription. Through the exchange activity of the SWR complex, H2A-H2B dimers from these nucleosomes could be exchanged for H2A.Z-H2B dimers, resulting in the less stable nucleosomes, prone to easier disruption during continued rounds of transcriptional elongation. This model would also be in accordance with studies which defined roles for the SWR complex in elongation phenotypes found in h2a.zΔ cells (Santisteban et al. 2011).

5.1.3 Explaining ChEC and ChIP discrepancies

In this work a general correlation between ChEC and ChIP experiments has been observed. ChEC results suggested that timing of histone expression and histone availability might be a factor largely contributing to the preferential deposition of H2A.Z at specific genomic regions. ChIP analyses attenuated this view. ChEC experiments where H2A- and H2A.Z-MNase fusion proteins were expressed from their endogenous promoters correlated completely with the corresponding ChIP analyses. The promoter

switch strains, expressing H2A- and H3-MNase under the control of the H2A.Z promoter were not fully consistent. Differences in ChIP experiments were visible at genes with a high transcription rate, leading to the presented model of transcription-influenced establishment of histone incorporation patterns. Why do ChEC and ChIP results not correlate at loci showing higher transcription rates?

One answer might be that ChEC and ChIP essentially address different things. ChIP gives us an idea about nucleosome density at the analyzed region defined by qPCR primers. Due to the limited resolution of the method of 300 to 500 bp it is not very susceptible to slight changes in nucleosome positioning within a small region of this size. ChEC on the other hand monitors cutting events mediated by protein-MNase fusions at very distinct loci and is thus much more sensitive to the effects of nucleosome redistribution. At transcriptionally inactive loci, the nucleosomes covering these regions are mostly deposited during replication and are thus presumably well positioned. During several rounds of transcription nucleosomes over transcribed regions are more and more misplaced (Weiner et al. 2010). Promoter nucleosomes on the other hand are generally thought to be very precisely positioned (Mavrich et al. 2008), independent of the gene's transcriptional state. This may explain why at the transcriptional silent loci in the presented work, ChEC results showing the promoter enrichment for any constantly expressed histone fully correlated with ChIP data but did not at the higher transcribed loci. Variably placed nucleosomes containing histone-MNase fusion proteins cannot mediate distinct DNA cuts and therefore dilute the signal seen in the autoradiographs thus giving a wrong impression of low protein levels in the ORFs, which then differ from ChIP results.

5.2 Dynamics and positioning of variant nucleosomes

During the work presented here, it could be shown for the first time that nucleosomes containing histone variants exhibit a different behavior in *in vitro* and *in vivo* experiments than nucleosomes containing only canonical histones. Although dynamics in thermal sliding assays did not differ greatly, the influence of H2A.Z incorporation on nucleosome positioning and ATP dependent remodeling was evident.

Positioning differences of nucleosomes are associated with changes in gene expression mediated by changes in promoter accessibility, changes in promoter chromatin architecture and changes in the accessibility of transcription factor binding sites (Tsankov et al. 2010). Therefore the strict regulation and a controlled variation of nucleosome positions are important determinants of all DNA dependent processes.

5.2.1 *In vivo* nucleosome stability might depend on more than pure histone content

Analysis of the contribution of histone variants to nucleosome dynamics in thermal sliding assays did not show an influence of H2A.Z, H3.3 or the simultaneous presence of both histone variants within a nucleosome on the translocation rate from one nucleosome position to another.

Previous studies have been undertaken to answer the question of altered nucleosome stability upon variant incorporation, using a variety of methods and coming to different conclusions. One study used Fluorescence Resonance Energy Transfer and demonstrated that H2A.Z could stabilize nucleosomes (Park et al. 2004). The authors thereby contradicted their own conclusions derived from a previous comparison of NCP crystal structures (Suto et al. 2000), demonstrating that experimental setup must be carefully designed in order to address a biological problem.

Another study used leukemia cell lines stably expressing Flag-tagged histones and the *in vivo* assembled nucleosomes were purified to test their stability upon treatment with different salt concentrations (Jin et al. 2007). The authors found that the influence of H2A.Z alone was not strongly changing salt-dependent nucleosome stability, but only the incorporation of H3.3 rendered nucleosomes extremely sensitive to ionic strength dependent disruption. In their experiments the double variant nucleosomes were the least stable. Contradictory, differences in the stability of H3.3 and H2A.Z containing nucleosomes in comparison to canonical nucleosomes were not observed in the *in vitro* assays of this work.

A biophysical approach with recombinant nucleosomes and ultracentrifugation analysis on the other hand resulted in the proposal that H2A.Z containing nucleosomes are indeed less stable than canonical nucleosomes (Abbott et al. 2001).

The assay presented in this work used a completely different approach which nevertheless was previously used to demonstrate dynamic properties of nucleosomes (Flaus et al. 1998; Flaus et al. 2003). The obtained results with recombinant histones did not show a stabilizing or destabilizing effect of H2A.Z. Together with the varying results found in the literature this most likely suggests that the stability of *in vitro* assembled nucleosomes with varying histone content might be different from the situation *in vivo*. Facilitating or preventing the disruption and movement of nucleosomes is an important check point for cellular mechanisms like transcription. The interplay of different factors, histones and signaling pathways has so far not been fully revealed and it might provide a more comprehensive picture of the influence of histone variants on nucleosomes.

5.2.2 H2A.Z influences nucleosome positioning *in vitro* and *in vivo*

The presented experiments indicate that H2A.Z containing nucleosomes occupy different positions in *in vitro* experiments as well as in the *in vivo* context of *Saccharomyces cerevisiae* chromatin.

Analysis of recombinant mononucleosomes reconstituted on different linear DNA fragments showed in all cases that the H2A.Z containing nucleosomes were positioned slightly different upon assembly. Positions occupied by H3.3 containing nucleosomes on the other hand were identical to canonical nucleosome positions. Positions occupied by double variant nucleosomes containing H2A.Z as well as H3.3 were most similar to the positions of single variant H2A.Z nucleosomes, showing that H2A.Z positioning is dominant over the influence of the histone variant H3.3. Similar results were also reported by another group while this work was in preparation (Thakar et al. 2009). The influence of H2A.Z on nucleosome positioning is fascinating. During nucleosome assembly, an $(H3\text{-}H4)_2$ tetramer is first placed on the DNA, followed by a rapid deposition of H2A-H2B dimers (Li et al. 2012 and referenced therein). This would mean that the $(H3\text{-}H4)_2$ tetramer determines the correct nucleosome position. The fact that variation of the H2A content can alter nucleosome positions shows that the dimers do have a significant influence and initial deposition of the $(H3\text{-}H4)_2$ tetramer does not necessarily represent the final nucleosome position. Histone-DNA interactions on the surface of the nucleosome depend on the structural and physical properties of the

histone octamer. Crystal structure analysis of H2A.Z containing nucleosomes revealed subtle changes in the octamer structure compared to canonical nucleosomes (Suto et al. 2000). Such structural differences lead to altered histone-DNA interactions which might be the cause for differing positions of variant nucleosomes.

In vitro positioning differences were even more evident after ATP-dependent nucleosome remodeling reactions. Interestingly, positioning events varied between different tested remodeling enzymes. Experiments on the *Drosophila melanogaster* Hsp70 promoter fragment showed that remodeling reactions with the ATPases ISWI and SNF2H resulted in a distinctly different occupancy of H2A.Z containing nucleosomes vs. canonical or H3.3 containing nucleosomes.

Remodeling of Hsp70 mononucleosomes with the ACF complex did not result in differentially occupied positions. This “failure” to differentiate between canonical and H2A.Z containing nucleosomes could be due to two different models.

Maybe ACF has a different specificity and simply treats variant nucleosomes in a similar way as canonical nucleosomes. It seems possible that its specificity is not based on the histone content of nucleosomes but rather on the DNA template, thus not discriminating different nucleosomes, but carrying out the sliding reaction as directed by the underlying DNA fragment. On the other hand, the lack of differentiation between canonical and variant nucleosomes could be a phenomenon exclusively observed on this DNA; other DNA templates could very well influence the ACF catalyzed reaction to discriminate between different types of nucleosomes.

A second model could be attested to the fact that the ACF complex contains two ATPase subunits and therefore may exhibit a greater remodeling efficiency than isolated ATPases like ISWI or SNF2H alone (Eberharter et al. 2004; Strohner et al. 2005). Incompleteness of the remodeling reactions carried out by ISWI and SNF2H could explain the relatively similar positioning on the Hsp70 promoter where the observed differences were mostly seen as altered relative occupancy.

Analysis of mononucleosomes reconstituted on a fragment from the murine rDNA spacer promoter was more effective. The observed differences after nucleosome sliding with ISWI and SNF2H were more pronounced and some positions occupied by canonical nucleosomes were left completely free of H2A.Z containing nucleosomes. Taking into account that H2A.Z occupies the mouse rDNA promoter *in vivo*, this argues for a variant specific remodeling pattern instead of plain incompleteness of the ISWI and SNF2H reactions. Unfortunately, ACF was not available for tests on this DNA fragment, so no statement can be made whether its specificity is also only regulated by

this DNA template or whether variant nucleosomes are distinguished by ACF in this DNA context.

Thermal sliding of nucleosomes reconstituted with recombinant histones used in this study showed recombinant variant nucleosomes to be equally stable as canonical nucleosomes. With this in mind, it must be concluded from the chromatin remodeling experiments that at least single ATPases respond differently to an altered histone content of nucleosomes. It cannot be distinguished with these experiments whether the observed differences are the results of different affinities of remodeling enzymes towards histone variant containing nucleosomes or the actual reaction outcome is different. However, the remodeling reactions performed on the mouse rDNA fragment where H2A.Z nucleosomes have been detected *in vivo* (Nemeth et al. 2008) suggest a strong H2A.Z influence on the actual positioning at the end of a remodeling reaction. This influence of a histone variant on nucleosome sliding by chromatin remodeling enzymes could be shown for the first time. In conclusion: nucleosome positions are determined by the underlying DNA sequence in *cis*, chromatin remodeling machines are important *trans*-factors for correct spacing and regulating DNA accessibility and in addition, histone variants can influence both of these determinants. The combinatorial possibilities of interplay between these three factors result in a high complexity of chromatin regulation levels.

Chromatin Endogenous Cleavage complemented the *in vitro* results discussed above and underlined the finding that H2A.Z nucleosomes can exhibit specialized nucleosome positioning. The presented experiments showed for the first time defined differences of *in vivo* positioning of H2A.Z containing vs. canonical nucleosomes. Similar to the *in vitro* experiments, ChEC revealed subtle shifts of H2A.Z nucleosome positions as well as positions exclusively occupied by either canonical or variant nucleosomes. Especially the detection of variant- and canonical-exclusive nucleosome positions suggests that ChEC is a suitable method for such analyses. Conclusions from the appearance of slight shifts, however, should be carefully drawn, as it has been discussed that nucleosomes distributed over a defined region might be slightly re-distributed after transcription and can lead to a reduced signal intensity on autoradiographs and thus falsify the observed results.

5.2.3 The INO80 complex influences nucleosome positions

ChEC analysis of H2A.Z enrichment at the YGR117C/RPS23A promoter in a yeast strain carrying an INO80 deletion showed that the relative intensities of cutting events mediated by the histone-MNase-fusions were not visibly reduced, presumably demonstrating unchanged incorporation levels of histones in the absence of Ino80p.

The positions of the increased cleavage events of H2A.Z-MNase around the YGR117C/RPS23A promoter however clearly changed upon Ino80p deletion, suggesting a role for the INO80 complex in nucleosome positioning *in vivo*.

A recent study by Papamichos-Chronakis and colleagues analyzed the *in vitro* and *in vivo* effects of INO80c on chromatin and made both correlating and conflicting statements compared to the results presented here (Papamichos-Chronakis et al. 2011).

An *in vitro* dimer exchange reaction exclusively evicting H2A.Z and incorporating H2A was observed as well as a lack of transcription induced loss of H2A.Z in the absence of Ino80p. The increase of H2A.Z occupancy over coding regions in an ino80Δ background was not visible in the experiments of the presented work. It can only be speculated, however, why this difference is observed and whether it is due to different experimental setups and ChEC results from this work do not fully represent occupancy levels. It is also not clear, whether their results were obtained with a full deletion of Ino80p or a partial deletion mutant.

The abovementioned study along with several others could demonstrate the *in vitro* nucleosome sliding activity of INO80c (Shen et al. 2000; Chen et al. 2011; Papamichos-Chronakis et al. 2011) without distinguishing between H2A.Z containing and canonical nucleosomes. Not only do the results within this thesis show the *in vivo* influence of INO80c on nucleosome remodeling for the first time, but they also show that the remodeling influence seems to be specifically targeted towards promoter nucleosomes. Positions of nucleosomes over coding regions remain unchanged in the absence of Ino80p. Especially the *in vivo* sliding of promoter nucleosomes might be important to maintain correct promoter positions which are required for transcriptional activation.

Whether INO80c is also capable to distinguish between canonical and H2A.Z containing nucleosomes could not be determined. However, results would be especially interesting and could potentially further strengthen the findings from the *in vitro* experiments where it was shown that remodeling machines seem to be able to not only “read” the underlying DNA context and perform sliding reactions accordingly, but moreover seem to be capable of interpreting the different histone contents of canonical vs. variant nucleosomes.

5.3 Histone H2A C-terminus regulates chromatin dynamics, remodeling and histone H1 binding

It could be demonstrated that the unique C-terminal tail of H2A has a functional role in affecting chromatin structure by modulating nucleosome stability and positioning, regulating ATP-dependent chromatin remodeling and interacting with linker histone H1 implying a role for establishing higher order chromatin structures.
Effects were already observed when studying a smaller truncation mutant, missing only the protruding part of the C-terminus, thus showing that not only the DNA-passing region further upstream plays a crucial role for the characteristic functions.

5.3.1 Dynamics and nucleosome positioning are influenced by the H2A C-terminal tail

Mononucleosomes on linear DNA fragments could be reconstituted with all three types of nucleosomes, demonstrating that the C-terminus is not needed for efficient chromatin assembly. Positioning of mononucleosomes slightly differed between full-length H2A and the truncation mutants, with the greatest differences observed in the H2A-114 truncation mutant.
Thermal shift assays confirmed that the deletion of the C-terminal tail led to a drastic increase in the rate of nucleosome relocation, contradicting a recent study, which attested no general effect to the outermost part of the H2A C-terminus of *Saccharomyces cerevisiae* on chromatin organization (Fink et al. 2007). The reason for these discrepancies is that yeast H2A is most similar not to mammalian H2A but to mammalian H2AX, which differs from canonical H2A in the last 11 amino acids of the C-terminal tail. Furthermore, in the study by Fink and colleagues only the last four amino acids that are not present in mammalian canonical H2A were deleted.

5.3.2 The H2A C-terminal tail is necessary for efficient chromatin remodeling

Among the remodeling machines tested within this study, only ACF was able to efficiently translocate the H2A-114 containing nucleosomes, missing the full C-terminal tail. ATPases ISWI and SNF2H failed to reposition these mutant nucleosomes, despite their decreased stability. This observation was somewhat unexpected but may be best explained by the position of the H2A C-terminus.

ATP-dependent remodeling machines belonging to the ISWI family contact the nucleosomes at the linker DNA and within approx. the first 50 bp of the nucleosomal DNA (Langst et al. 2001). The H2A C-terminus is close to this remodeler-nucleosome contact site and might therefore influence the remodeler-nucleosome interaction and/or their affinity for each other. The isolated ISWI and SNF2H ATPases did not suffice to overcome the missing of the C-terminal tail. The ACF complex however, did not discriminate between the examined nucleosomal substrates. The full ACF complex contains two molecular motors that are linked by the Acf1 subunits and the remodeling activity of its ISWI subunit is largely enhanced (Eberharter et al. 2004; Strohner et al. 2005). Additionally, ACF binds to nucleosomal templates with higher affinity and taken together, these features could help overcome the obstacles for remodeling when the H2A C-terminal tail is missing.
It should be noted that the assay used here, could not distinguish between changes in remodeler-nucleosome affinities and reduced kinetics of the remodeling reaction due to the truncations induced into the different H2A mutants.

Together with *in vivo* data from the group of Robert Schneider, the presented results argue for a specific role of the H2A C-terminal tail in gene expression, stress response and chromatin integrity, mediated through the effects of the tail on chromatin dynamics.

5.3.3 The H2A C-terminus as a new targeting domain for H1?

An unbiased screen identified linker histone H1 as a novel binding partner *in vivo*. Based on this, *in vitro* studies were carried out, demonstrating a decreased binding of H1 to mononucleosomes lacking the H2A C-terminal tail.
Furthermore, at higher molar ratios of H1, a chromatosome could be formed in the absence of the C-terminus, indicating that the H2A C-terminal tail mediates efficient H1 binding, but does not seem to determine the specific binding mode.

The presented interaction with linker histone H1 establishes the C-terminal tail of H2A as a key factor in chromatin dynamics *in vivo*.
In addition, not only its importance for a stable nucleosome structure, but also for nucleosome remodeling point towards a crucial role in targeting nucleosome positioning and regulating chromatin organization.

6 Outlook

6.1 Further experiments on the role of H2A.Z in transcription competent chromatin states

The presented results on H2A.Z deposition led to the conclusion that the observed enrichment of H2A.Z at promoters depends largely on its constitutive expression throughout the cell cycle. ChEC experiments showed that canonical histones could be deposited in a similar manner as H2A.Z when they were expressed under the control of the H2A.Z promoter. ChIP analyses and the interpretation of gene expression data led to the suggested “Place and Erase Model” for H2A.Z deposition. However, transcription coupled eviction of H2A.Z and its replacement with H2A over coding regions could not be directly shown with this work.

Further experiments with the same experimental setup could be carried out. The GIT1 locus may be a prime example for studying H2A.Z depletion upon activation of the gene. Under normal growth conditions the GIT1 gene is not transcribed; the deposition pattern of constitutively expressed H2A was not fully identical with H2A.Z but still very similar. If the proposed model holds true ChIP results should change drastically upon GIT1 activation by growth in medium lacking inositol and phosphate. Subsequently, less H2A.Z should be found in the ORF region, whereas the occupancy of the constitutively expressed H2A within this region should increase.

However, the data gained so far suggest a comprehensive model for H2A.Z deposition and the establishment of its promoter enrichment patterns by transcription elongation. This implicates a role for H2A.Z in maintaining chromatin in a transcription competent state.

6.2 *In vivo* positioning of H2A.Z

The Ino80 ATPase was shown to alter nucleosome positions of H2A.Z containing nucleosomes at the YGR117C/RPS23A promoter.

Further studies would be important to test this activity at other genomic loci. Moreover, it would be desirable to construct a H2A-MNase tagged yeast strain with an INO80 deletion; so far cloning attempts were not successful. This strain would show whether

the INO80 complex can also efficiently move canonical nucleosomes *in vivo* or whether this effect is specific for H2A.Z containing nucleosomes.
In general, large scale sequencing would be very helpful to gather more comprehensive data. An idea would be the establishment of a ChEC-Seq method, combining ChEC experiments with genome-wide sequencing runs. Instead of qualitative analysis of nucleosome movement by Southern blots, repositioning could be analyzed in a quantitative manner depending on the resolution of the sequencing method.

6.3 The C-terminal H2A tail as a new factor in chromatin regulation

The collaboration project was able to show for the first time that the C-terminal tail of H2A has fundamental influence on chromatin structure and stability. The importance of N-terminal histone tails and their modifications has been extensively studied in recent years, but nothing was known about the unique C-terminal H2A tail. The presented results shed light on the influence of the H2A C-terminus and further studies could diversify these findings. Especially the interaction of linker histone H1 with the C-termini of H2A might be interesting to study and could potentially lead to a better understanding of higher order chromatin structures.

7 Material

7.1 Chemicals

All chemicals, reagents and solvents used in this work were *pro analysis* grade (p.a.) and were purchased from the chemicals center at the University of Regensburg. Anything not available there was ordered directly at Merck, Roche, Roth and Sigma. Water was purified with an Elga Purelab Ultra device before use. Radioactive α^{32}P-dATP was ordered from Hartmann-Analytic GmbH.

7.2 Buffers and Media

Unless stated otherwise the solvent is H_2O. The pH value was always measured at room temperature and was adjusted with HCl or NaOH unless indicated otherwise. Stock solutions were prepared according to standard protocols (Sambrook and Russel 2001; LabFAQs, Roche) and stored at room temperature.

LB medium	Tryptone Yeast extract NaCl Agar (for plates)	10 g/l 5 g/l 5g/l 20 g/l
LB-Amp	add Ampicillin from separate stock	50 µg/ml
YPD medium	Yeast extract Peptone Glucose Agar (for plates)	10 g/l 20 g/l 20 g/l 20 g/l
YPG medium	Yeast extract Peptone Galactose Agar (for plates)	10 g/l 20 g/l 20 g/l 20 g/l
YPD-Geneticin / YPG-Geneticin	add Geneticin to YPD / YPG medium	400 mg/l
IR buffer	Tris-HCl pH 8 EDTA	50 mM 20 mM

IRN buffer	Tris-HCl pH 8	50 mM
	EDTA	20 mM
	NaCl	0.5 M
TBE buffer	Tris	90 mM
	Boric acid	90 mM
	EDTA	1 mM
TE buffer	Tris-HCl pH8	10 mM
	EDTA	1 mM
High salt buffer	Tris-HCl pH 7.6	10 mM
	NaCl	2 M
	EDTA	1 mM
	NP40	0.05 %
	β-Mercaptoethanol	1 mM
Low salt buffer	Tris-HCl pH 7.6	10 mM
	NaCl	50 mM
	EDTA	1 mM
	NP40	0.05 %
	β-Mercaptoethanol	1 mM
EX-X buffer	Tris-HCl pH 7.6	20 mM
	KCl	X mM
	$MgCl_2$	1.5 mM
	EGTA	0.5 mM
	Glycerol	10 %
DNA sample buffer (10x)	Tris-HCl pH 7.6	50 mM
	EDTA	10 mM
	Glyerol	50 %
	Bromphenol blue	0.05 %
Upper Tris (4x)	Tris-HCl pH 6.8	0.5 M
	SDS	0.4 %
Lower Tris (4x)	Tris-HCl pH 8.8	1.5 M
	SDS	0.4 %
SDS Electrophoresis buffer (10x)	Tris	250 mM
	Glycine	1.9 M
	SDS	1 %
SDS sample buffer (6x), “Lämmli buffer”	Tris-HCl pH 6.8	350 mM
	SDS	10 %
	Glycerol	30 %
	β-Mercaptoethanol	5 %
	Bromphenol blue	0.2 %
Coomassie staining solution	Coomassie Brilliant Blue G250	1 g/l
	H_2O	45 %
	Methanol	45 %
	Acetic acid	10 %

20 x SSC	NaCl Tri-sodium citrate dehydrate adjust pH to 7	3 M 0.3 M
20 x SSPE	NaCl Sodium dihydrogen phosphate adjust pH to 7.4	3 M 0.2 M 20 mM
ChEC buffer A	Tris-HCl pH 7.4 Spermine Spermidine KCl EDTA	15 mM 0.2 mM 0.5 mM 80 mM 1 mM
ChEC buffer Ag	Tris-HCl pH 7.4 Spermine Spermidine KCl EGTA	15 mM 0.2 mM 0.5 mM 80 mM 0.1 mM
Denature solution	NaOH NaCl	0.5 M 1.5 M
Hybridization buffer	Sodium phosphate pH 7.2 SDS	0.5 M 7 %
Rinse buffer	SSC SDS	3x 0.1 %
Southern wash buffer 1	SSC SDS	0.3x 0.1 %
Southern wash buffer 2	SSC SDS	0.1x 0.1 %
Southern wash buffer 3	SSC SDS	0.1x 1.5 %
Strip-buffer	SSPE SDS	0.1x 0.5 %
MNase buffer	Tris-HCl pH 8 NaCl $CaCl_2$ EDTA EGTA	15 mM 50 mM 1.4 mM 0.2 mM 0.2 mM
ChIP lysis buffer	Hepes pH 7.5 NaCl EDTA EGTA Triton X-100 DOC	50 mM 140 mM 5 mM 5 mM 1% 0.1 %

ChIP wash buffer 1	Hepes pH 7.5 NaCl EDTA Triton X-100 DOC	50 mM 500 mM 2 mM 1 % 0.1 %
ChIP wash buffer 2	Tris-HCl pH 8 LiCl EDTA NP40 DOC	10 mM 250 mM 2 mM 0.5 % 0.5 %
SORB	LiOAc Tris-HCl pH 8 EDTA Sorbitol	100 mM 10 mM 1 mM 1 M
Lit-PEG	LiOAc Tris-HCl pH 8 EDTA PEG 3350 adjust pH to 8; filter sterilize	100 mM 10 mM 1 mM 40 %
Spheroblasting buffer	Sorbitol EDTA	0.9 M 0.1 M
TfbI	KAc $MnCl_2$ KCl_2 Glycerol adjust pH to 5.6 with acetic acid; filter sterilize	30 mM 50 mM 100 mM 15 %
TfbII	MOPS $CaCl_2$ KCl Glycerol adust pH to 7 with NaOH; filter sterilize	10 mM 75 mM 10 mM 15 %
Towbin buffer	Tris SDS Glycine Methanol	25 mM 0.02% 192 mM 20%

7.3 Nucleic acids

7.3.1 Oligonucleotides

All oligonucleotides were purchased from Eurofins MWG Operon and diluted in H_2O or 10 mM Tris-HCl pH 8. Oligonucleotides for PCR reactions and sequencing purposes were designed to show minimal secondary structure or primer dimerization, utilizing the open source online software “Primer3” (accessible via http://primer3.sourceforge.net/). Oligonucleotides named “CHP(number)” or “LP(number)” are deposited within the Längst lab database on addgene (www.lablife.org). Oligonucleotides named with only a number are deposited in the Tschochner lab database (Biochemie3 share server).

CHP / LP primers

Name/ Number	Alternate name	Sequence	Function	Reference
LP29	Ava-601 for	GTTATGTGATGGACCCTATACGC	primer to obtain amplicon “601-Ava” from AvaI digested pUC18-12x601 (together with LP30)	Längst Lab
LP30	Ava-601 rev	GTCGCTGTTCAATACATGCAC	primer to obtain amplicon “601-Ava” from AvaI digested pUC18-12x601 (together with LP29)	Längst Lab
LP31	Not-601 for	GGCCGCCCTGGAGAATC	primer to obtain amplicon “601-Not” from NotI digested pUC18-12x601 (together with LP32)	Längst Lab
LP32	Not-601 rev	GCGTATAGGGTCCATCACATAACC	primer to obtain amplicon “601-Not” from NotI digested pUC18-12x601 (together with LP31)	Längst Lab
LP34	601 NotI frame biotin tagged	LP32 carrying a 5’ biotin tag	primer to obtain amplicon “601-Not” from NotI digested pUC18-12x601 (together with LP31)	Längst Lab/ this work
LP47	Hsp70 for	TGGAATTCGGATCCCACGATAAGC	primer to obtain amplicon “Hsp70” from pUC19 Hsp70 (together with LP48)	Längst Lab
LP48	Hsp70 rev	TAGAATTCAGATCTGAATTGACGTTCC	primer to obtain amplicon “Hsp70” from pUC19 Hsp70 (together with LP47)	Längst Lab
LP49	mDNA_-190for	TATCAGTTCTCCGGGTTGTCAGGTC	primer to obtain amplicon “-190/+90” from pMr974 (together with LP50)	Längst Lab
LP50	mDNA_+90rev	GAATAGGCTGGACAAGCAAAACAGCC	primer to obtain amplicon “-190/+90” from pMr974 (together with LP49)	Längst Lab

CHP1	nucA_for	GATATAAAAGA GTGCTGATTTTT TGAGTAA	primer to obtain amplicon “nucA” from pab485 (together with CHP2)	this work
CHP2	nucA_rev	TTTAAAAATTAC ATCTAGAAAAA GGCG	primer to obtain amplicon “nucA” from pab485 (together with CHP1)	this work
CHP3	974_F1_for	ATAGGGCTACA CAGAAAAACCA TATCTC	primer to obtain amplicon “rDNA_F1” from pMr974 (together with CHP4)	this work
CHP4	974_F1_rev	TTTGTTGTTTTC TGGTGCTCGCT	primer to obtain amplicon “rDNA_F1” from pMr974 (together with CHP3)	this work
CHP5	974_F2_for	GGTGAGTGGCC GGCGGCG	primer to obtain amplicon “rDNA_F2” from pMr974 (together with CHP6)	this work
CHP6	974_F2_rev	CGAGTGGCACA AACGGTCCCCA T	primer to obtain amplicon “rDNA_F2” from pMr974 (together with CHP5)	this work
CHP7	974_F3_for	CGTTTTTGGGT GCCCGAGTCT	primer to obtain amplicon “rDNA_F3” from pMr974 (together with CHP8)	this work
CHP8	974_F3_rev	CATCTCCCTGT ACGACCTCCTT GTT	primer to obtain amplicon “rDNA_F3” from pMr974 (together with CHP7)	this work
CHP9	974_Ovla1_for	GTGAAAGCAAA TCACTATGAAG AGGTACT	primer to obtain amplicon “rDNA_O1” from pMr974 (together with CHP10)	this work
CHP10	974_Ovla1_rev	CGGTGAAAACA GGCAAAATCGT	primer to obtain amplicon “rDNA_O1” from pMr974 (together with CHP9)	this work
CHP11	974_Ovla2_for	CGCCGCCACCC TCCTCTTC	primer to obtain amplicon “rDNA_O2” from pMr974 (together with CHP12)	this work
CH12	974_Ovla2_rev	CTTGTCACCAC TAGGTGTCGCC C	primer to obtain amplicon “rDNA_O2” from pMr974 (together with CHP11)	this work
CHP13	O2for-40	CCCTTACTGTG CTCCCTTCCC	primer to obtain amplicon “O2-40/-60” from pMr974 (together with CHP14)	this work
CHP14	O2rev-60	CGCCGCCACAT TCACTCAC	primer to obtain amplicon “O2-40/-60” from pMr974 (together with CHP13)	this work

Primers within the Tschochner lab database

Name/ Number	**Sequence**	**Function**	**Gene**	**Reference**
Cloning primers				
678	CACGGTGCAACACTCA CTTC	primer to verify URA3 integration upon gene deletion	URA3	Joachim Griesenbeck/ Thomas Wild

1359	CTACCGCGGATACAG GAGCAGGGAGAATTAC GGGAAATGGGAAAGA AAAACTATTCTTCATCG ATGAATTCGAGCTCG	primer to obtain amplicon of pAG37 for deletion of the HTZ1 gene (together with 2117)	HTZ1	Joachim Griesenbeck
2116	TCCATGCTAGATTAGC ACACAGTAA	primer to verify integrity/ deletion of the HTZ1 gene (together with 678)	HTZ1	this work
2117	CGTTAAATTCAATTTCG CACTATAGCCGCACGT AAAAATAACTTAACATA CGTACGCTGCAGGTC GAC	primer to obtain amplicon of pAG37 for deletion of the HTZ1 gene (together with 1359)	HTZ1	this work
2118	GAATTCTAACTGCTCT TTGCATTTTCCAAGTTA TTGCATTACAAGAATAT CGTACGCTGCAGGTC GAC	primer to obtain amplicon of pAG37 for deletion of the SWR1 gene (together with 2119)	SWR1	this work
2119	CTACCGCGGTAGTCC GATTTGGACAACTAAG GCAGCGGTGAAGAGT AGAACCTGGTCCTATC GATGAATTCGAGCTCG	primer to obtain amplicon of pAG37 for deletion of the SWR1 gene (together with 2118)	SWR1	this work
2120	CCTCTATACGATTATTA AGGGAGGG	primer to verify integrity/ deletion of the SWR1 gene (together with 678)	SWR1	this work
2121	GATGGTACCCGTTAAA TTCAATTTCGCACTATA GCCGCACGTAAAAATA ACTTAACATAATGTCC GGTGGTAAAGGTGG	primer to amplify HTA1 CDS from genomic DNA and subsequent subcloning into pAG14 (together with 2122)	HTA1	Joachim Griesenbeck/ this work
2122	AATTAACCCGGGGATC CGTCGACCTGCAGCG TACGATAATTCTTGAG AAGCCTTGG	primer to amplify HTA1 CDS from genomic DNA and subsequent subcloning into pAG14 (together with 2121)	HTA1	Joachim Griesenbeck/ this work
2565	GCTGGGTACCCGTTAA ATTCAATTTCGCACTAT AGCCGCACGTAAAAAT AACTTAACATAATGTC CTCTGCCGCCGAAAA	primer to amplify HTB2 CDS from genomic DNA and subsequent subcloning into pAG14 (together with 2566)	HTB2	this work
2566	TTAACCCGGGGATCCG TCGACCTGCAGCGTAC GAGGCTTGAGTAGAG GAGGAGT	primer to amplify HTB2 CDS from genomic DNA and subsequent subcloning into pAG14 (together with 2565)	HTB2	this work
2567	GCTGGGTACCCGTTAA ATTCAATTTCGCACTAT AGCCGCACGTAAAAAT AACTTAACATAATGGC CAGAACAAAGCAAAC	primer to amplify HHT1 CDS from genomic DNA and subsequent subcloning into pAG14 (together with 2568)	HHT1	this work
2568	TTAACCCGGGGATCCG TCGACCTGCAGCGTAC GATGATCTTTCACCTC TTAATC	primer to amplify HHT1 CDS from genomic DNA and subsequent subcloning into pAG14 (together with 2567)	HHT1	this work

2569	GCTGGGTACCCGTTAAATTCAATTTCGCACTATAGCCGCACGTAAAAATAACTTAACATAATGTCCGGTAGAGGTAAAGG	primer to amplify HHF1 CDS from genomic DNA and subsequent subcloning into pAG14 (together with 2570)	HHF1	this work
2570	TTAACCCGGGGATCCGTCGACCTGCAGCGTACGAACCACCGAAACCGTATAAGG	primer to amplify HHF1 CDS from genomic DNA and subsequent subcloning into pAG14 (together with 2569)	HHF1	this work
3245	GGTACCGGGCCCAGCGCCAAGCCATCTTAAAAGCA	primer to amplify histone CDS under control of HTZ1 promoter from pAG14_HTZ/HTA/HHT and subsequent subcloning into pBlueSkript_URA3 after ApaI digest (together with 3246)	HTZ1	this work
3246	GGTACCGGGCCCAGCAAGAGATTAGACGTGAAAGGAGAGA	primer to amplify histone CDS under control of HTZ1 promoter from pAG14_HTZ/HTA/HHT and subsequent subcloning into pBlueSkript_URA3 after ApaI digest (together with 3245)	HTZ1	this work
3259	TCCATATTAGCAAAGCAAGGCTTAAGACATATAGAAGAGCATTTATAGACCGTACGCTGCAGGTCGAC	primer to obtain amplicon of pAG37 for deletion of the INO80 gene (together with 3260)	INO80	this work
3260	GATAGACATTAACTCCGCTTAATGTAAATAACACAATATGAATACCTTTTATCGATGAATTCGAGCTCG	primer to obtain amplicon of pAG37 for deletion of the INO80 gene (together with 3259)	INO80	this work
3261	CGTGCCCAACGTAGTTTCTT	primer to verify integrity/ deletion of the INO80 gene (together with 678)	INO80	this work
3278	GCTGGGTACCGTGAATAAACAACTTCAAAACAAACAAATTTCATACATATAAAATATAAAATGTCAGGAAAAGCTCATGG	primer to amplify HTZ1 CDS from genomic DNA and subsequent subcloning into pAG13 (together with 3279)	HTZ1	this work
3279	TTAACCCGGGGATCCGTCGACCTGCAGCGTACGTTTCTTACTTCCCTTTTTTT	primer to amplify HTZ1 CDS from genomic DNA and subsequent subcloning into pAG13 (together with 3278)	HTZ1	this work
Primers for preparation of Southern blot probes				
1161	CAGGTTATGAAGATATGGTGCAA	primer to obtain template for Southern blot probe preparation (together with 1162)	rDNA	Katharina Merz
1162	AAAATGGCCTATCGGAATACA	primer to obtain template for Southern blot probe preparation (together with 1161)	rDNA	Katharina Merz

1163	TGTTGCTAGATCGCCTGGTA	primer to obtain template for Southern blot probe preparation (together with 1164)	GAL1	Katharina Merz
1164	TTTCCGGTGCAAGTTTCTTT	primer to obtain template for Southern blot probe preparation (together with 1163)	GAL1	Katharina Merz
1167	TGGATCTAATTTACAGCAGCA	primer to obtain template for Southern blot probe preparation (together with 1168)	NUP57	Katharina Merz
1168	CCTGATCCCACTCTTCTTGA	primer to obtain template for Southern blot probe preparation (together with 1167)	NUP57	Katharina Merz
3262	GTCCATGGCGTTCGCGGG	primer to obtain template for Southern blot probe preparation (together with 3263)	MRK1	this work
3263	TTCTTGCGTAGCTCTTTGACC	primer to obtain template for Southern blot probe preparation (together with 3262)	MRK1	this work
3264	CCCAACCCTCAGTGAGACAT	primer to obtain template for Southern blot probe preparation (together with 3265)	PRP12	this work
3265	GGGTTATTGGGTGGACTGGC	primer to obtain template for Southern blot probe preparation (together with 3264)	PRP12	this work
3266	GAAGTTGGTTTTCTTATTACCTCTA	primer to obtain template for Southern blot probe preparation (together with 3267)	YDL218W	this work
3267	TAAGGGATGACGATGGTTGG	primer to obtain template for Southern blot probe preparation (together with 3266)	YDL218W	this work
Primers for qPCR				
2698	GGGGATATATACCCTTAAATTGACG	primer used for qPCR detection of YDL218W promoter region (together with 2699)	YDL218W	Zhang et al. 2005
2699	AAAACCGTAAACTTTCGTACTGAGA	primer used for qPCR detection of YDL218W promoter region (together with 2698)	YDL218W	Zhang et al. 2005
2700	TACTGCTGACAGTCATAGAAGAGCATG	primer used for qPCR detection of YDL218W ORF region (together with 2701)	YDL218W	Zhang et al. 2005
2701	CGGTCCTAACATTGGTGTTATCGTA	primer used for qPCR detection of YDL218W ORF region (together with 2700)	YDL218W	Zhang et al. 2005

2702	ACAGTTCGTAACAACA GCTGGAAGA	primer used for qPCR detection of YNL092W promoter region (together with 2703)	YNL092W	Zhang et al. 2005
2703	TCAGATCCTCACCAAT TTTTGCC	primer used for qPCR detection of YNL092W promoter region (together with 2702)	YNL092W	Zhang et al. 2005
2704	CCTTCTCGTGGATCTT AGCAGAAT	primer used for qPCR detection of YNL092W ORF region (together with 2705)	YNL092W	Zhang et al. 2005
2705	ATCAACAAACGAGCCA GCACATA	primer used for qPCR detection of YNL092W ORF region (together with 2704)	YNL092W	Zhang et al. 2005
2706	TTTCACTTTTCGTCTTG ACGTCC	primer used for qPCR detection of PRP12 promoter region (together with 2707)	PRP12	Zhang et al. 2005
2707	CTGTATAGGCCCGCTA TATTTTGGT	primer used for qPCR detection of PRP12 promoter region (together with 2706)	PRP12	Zhang et al. 2005
2708	ACTTACTCTCGTACTT CACTCGAGCTTC	primer used for qPCR detection of PRP12 ORF region (together with 2709)	PRP12	Zhang et al. 2005
2709	ACAATTCTTGGCAGAA ATGGCAC	primer used for qPCR detection of PRP12 ORF region (together with 2708)	PRP12	Zhang et al. 2005
2710	CAAAGTCGTCCGATGA GGAACTAA	primer used for qPCR detection of MRK1 promoter region (together with 2711)	MRK1	Zhang et al. 2005
2711	GAGATTATTTTCAAGT CCCTTCCCC	primer used for qPCR detection of MRK1 promoter region (together with 2710)	MRK1	Zhang et al. 2005
2712	GCCGCGTGTTGAAATT AAATTCT	primer used for qPCR detection of MRK1 ORF region (together with 2713)	MRK1	Zhang et al. 2005
2713	TCGACCTGGTTTGAGT AATTAGTGG	primer used for qPCR detection of MRK1 ORF region (together with 2712)	MRK1	Zhang et al. 2005
2714	CCTTGCCCCAGTGTAC ACATATATAA	primer used for qPCR detection of YNL116W promoter region (together with 2715)	YNL116W	Zhang et al. 2005
2715	TGCGTTGCTATACTTT CTCGACTTC	primer used for qPCR detection of YNL116W promoter region (together with 2714)	YNL116W	Zhang et al. 2005
2716	CTTGATATATGCTGCA AACCAGCC	primer used for qPCR detection of YNL116W ORF region (together with 2717)	YNL116W	Zhang et al. 2005

2717	GCCAGCCTTTCTTATAATCGGTTC	primer used for qPCR detection of YNL116W ORF region (together with 2716)	YNL116W	Zhang et al. 2005
3017	CACTCCTACCAATAACGGTAACTATTC	primer used for qPCR detection of rDNA promoter region (together with 3016)	rDNA	this work
3018	CAGATGAAAGATGAATAGACATAG	primer used for qPCR detection of rDNA promoter region (together with 3019)	rDNA	this work
3019	TCCATGCCATAACAGGAAAG	primer used for qPCR detection of rDNA promoter region (together with 3018)	rDNA	this work
3020	CATTGGGATGTTACTTTCCTG	primer used for qPCR detection of rDNA promoter region (together with 3021)	rDNA	this work
3021	CCCTTCAGTTTCCCTTTTTC	primer used for qPCR detection of rDNA promoter region (together with 3020)	rDNA	this work
3022	TCTGAAGCGTATTTCCGTCAC	primer used for qPCR detection of rDNA promoter region (together with 3023)	rDNA	this work
3023	CAACCGAAACCAAAACCAAC	primer used for qPCR detection of rDNA promoter region (together with 3022)	rDNA	this work
3024	GTAATGTATGATATCCGTTGGTTTTG	primer used for qPCR detection of rDNA promoter region (together with 3025)	rDNA	this work
3025	AAAATATACCTTTCTCACACAAGAAAT	primer used for qPCR detection of rDNA promoter region (together with 3024)	rDNA	this work
3026	GCAAGTAGCATATATTTCTTGTGTG	primer used for qPCR detection of rDNA promoter region (together with 3027)	rDNA	this work
3027	GGGTAACCCAGTTCCTCACT	primer used for qPCR detection of rDNA promoter region (together with 3026)	rDNA	this work
3028	TCCGTATTTTCCGCTTCC	primer used for qPCR detection of rDNA promoter region (together with 3029)	rDNA	this work
3029	CTCGCCGAGAAAAACTTCA	primer used for qPCR detection of rDNA promoter region (together with 3028)	rDNA	this work

3030	CGCTAAGATTTTTGGAGAATAGC	primer used for qPCR detection of rDNA promoter region (together with 3031)	rDNA	this work
3031	CCCCCTCCCATTACAAACT	primer used for qPCR detection of rDNA promoter region (together with 3030)	rDNA	this work
3032	GCGACAGAGAGGGCAAAAG	primer used for qPCR detection of rDNA promoter region (together with 3033)	rDNA	this work
3033	CTTCAACTGCTTTCGCATGA	primer used for qPCR detection of rDNA promoter region (together with 3032)	rDNA	this work
3268	TCTCACCGACATTACTATTTGAAC	primer used for qPCR detection of YGR117C promoter region (together with 3269)	YGR117C	this work
3269	CAAACATAACGGTCTGGAAGATAC	primer used for qPCR detection of YGR117C promoter region (together with 3268)	YGR117C	this work
3270	CAATTGGGGCTAAATCATCG	primer used for qPCR detection of YGR117C promoter region (together with 3271)	YGR117C	this work
3271	CGCTAGAAGACTTGCAGAGTG	primer used for qPCR detection of YGR117C promoter region (together with 3270)	YGR117C	this work
3272	GCTTGACGATGCTCTTGAC	primer used for qPCR detection of YGR117C promoter region (together with 3273)	YGR117C	this work
3273	TTACTTTCGTCAGCTACTGGATACC	primer used for qPCR detection of YGR117C promoter region (together with 3272)	YGR117C	this work
3274	CGCTGTCTCCCTTATGAATG	primer used for qPCR detection of YGR117C promoter region (together with 3275)	YGR117C	this work
3275	TGGCTGACAATTCTACTTCCAG	primer used for qPCR detection of YGR117C promoter region (together with 3274)	YGR117C	this work
3276	TTGTAGTAAATCCTATCTTCAACGACA	primer used for qPCR detection of YGR117C promoter region (together with 3277)	YGR117C	this work
3277	GCCTTAGAAAAGTCCGATAGTTC	primer used for qPCR detection of YGR117C promoter region (together with 3276)	YGR117C	this work

GIT1_p2_fwd	CCTAGTTTTTCAATCTGGCTATCTT	primer used for qPCR detection of GIT1 promoter region (together with	GIT1	this work
GIT1_p2_rev	CATCTGCTACAACTACATTCATCG	primer used for qPCR detection of GIT1 promoter region (together with	GIT1	this work
GIT1_o2_fwd	GTGCTTCTGGCCATTGAG	primer used for qPCR detection of GIT1 ORF region (together with	GIT1	this work
GIT1_o2_rev	AACCATGTACCACATGTACCAAG	primer used for qPCR detection of GIT1 ORF region (together with	GIT1	this work
PHO5_p2_fwd	TTTGAATTGTCGAAATGAAACG	primer used for qPCR detection of PHO5 promoter region (together with	PHO5	this work
PHO5_p2_rev	GGTAATCTCGAATTTGCTTGCT	primer used for qPCR detection of PHO5 promoter region (together with	PHO5	this work
PHO5_o2_fwd	GCCAACACTTTGAGTGCTTGTA	primer used for qPCR detection of PHO5 ORF region (together with	PHO5	this work
PHO5_o2_rev	GTTCAAACCCTTGTTTTCCTTG	primer used for qPCR detection of PHO5 ORF region (together with	PHO5	this work
KIN82_p_fwd	TTCAGCTATATTGTTCAAGGAGTAACA	primer used for qPCR detection of KIN82 promoter region (together with	KIN82	this work
KIN82_p_rev	GAACCTTGTTTGCAGTAATCCTTAG	primer used for qPCR detection of KIN82 promoter region (together with	KIN82	this work
KIN82_o_fwd	GACGATACATACAGAGCTGTTACAAAG	primer used for qPCR detection of KIN82 ORF region (together with	KIN82	this work
KIN82_o_rev	TCCGGAGAAGAGCTACCTGA	primer used for qPCR detection of KIN82 ORF region (together with	KIN82	this work
SOL2_p_fwd	ACCAAGGCAAGAGAAAAGACC	primer used for qPCR detection of SOL2 promoter region (together with	SOL2	this work
SOL2_p_rev	CCGCCCTATTTAAACCTAATTTC	primer used for qPCR detection of SOL2 promoter region (together with	SOL2	this work

SOL2_o_fwd	GGGTTTGCCGGTAGAGATTC	primer used for qPCR detection of SOL2 ORF region (together with	SOL2	this work
SOL2_o_rev	ACCACCCATGCAAGTTTCTC	primer used for qPCR detection of SOL2 ORF region (together with	SOL2	this work

7.3.2 Plasmids

Name/ Number	Alternate name	Vector backbone	Bacterial resistance	Cloning strategy	Reference
CH1	pET-21a-H2A	*E. coli*, pET21a, T7 promoter	Ampicillin	human H2A inserted in MCS via NdeI+XhoI	Schneider Group, MPI of Immuno-biology, Freiburg
CH2	pET-21a-H2B	*E. coli*, pET21a, T7 promoter	Ampicillin	human H2B inserted in MCS via NdeI+XhoI	Schneider Group, MPI of Immuno-biology, Freiburg
CH3	pET-21a-H3	*E. coli*, pET21a, T7 promoter	Ampicillin	human H3 inserted in MCS via NdeI+XhoI	Schneider Group, MPI of Immuno-biology, Freiburg
CH4	pET-21a-H4	*E. coli*, pET21a, T7 promoter	Ampicillin	human H4 inserted in MCS via NdeI+XhoI	Schneider Group, MPI of Immuno-biology, Freiburg
CH5	pET-3a-H2A.Z	*E. coli*, pET3a, T7 promoter	Ampicillin	unknown	Längst Lab inventory
CH6	ab485		Ampicillin	see Flaus et al., Mol Cell Biol., 2003	Andrew Flaus (Flaus et al., Mol Cell Biol., 2003)
--	pMr974		Ampicillin	unknown	Längst Lab inventory
--	pUC18-12x601	pUC18	Ampicillin		Längst Lab inventory
--	pUC19 Hsp70	pUC19	Ampicillin		Längst Lab inventory

Plasmids within the Tschochner database

Name	Number	Cloning strategy	Function	Reference
pAG13	834	PCR from pKM09 with primers 1356 and 1357 subcloned into pBlueskriptKS after KpnI/SacII digest	genomic MNase tagging by recombination at HTA1 C-terminus	Joachim Griesenbeck
pAG14	835	PCR from pKM09 with primers 1358 and 1359 subcloned into pBlueskriptKS after KpnI/SacII digest	genomic MNase tagging by recombination at HTZ1 C-terminus	Joachim Griesenbeck
pAG37	937	insertion of a SmaI/SacI restricted PCR fragment obtained from pBS1539 (Puig et al., 2001) using primers 1502 and 1503 into SmaI/SacI restricted pKM9	vector for PCR mediated URA cassette KO using S2 and S3 adapter primer	Joachim Griesenbeck
pAG14_HTA1_MN	1226	Amplification of HTA1 CDS from genomic yeast DNA using primers 2121 and 2222. Subcloned into pAG14 after KpnI/AvaI digest	plasmid for genomic integration of a HTA1-MN-3xHA_kanMX6 cassette to replace the CDS of HTZ1	Ulrike Stöckl/ this work
pAG14_HTB2_MN		Amplification of HTB2 CDS from genomic yeast DNA using primers 2565 and 2566. Subcloned into pAG14 after KpnI/AvaI digest	plasmid for genomic integration of a HTB2-MN-3xHA_kanMX6 cassette to replace the CDS of HTZ1	this work
pAG14_HHT1_MN		Amplification of HTA1 CDS from genomic yeast DNA using primers 2567 and 2568. Subcloned into pAG14 after KpnI/AvaI digest	plasmid for genomic integration of a HHT1-MN-3xHA_kanMX6 cassette to replace the CDS of HTZ1	this work
pAG14_HHF1_MN		Amplification of HTA1 CDS from genomic yeast DNA using primers 2569 and 2570. Subcloned into pAG14 after KpnI/AvaI digest	plasmid for genomic integration of a HHF1-MN-3xHA_kanMX6 cassette to replace the CDS of HTZ1	this work

pBluescript_ URA3		Amplification of URA3 gene from genomic yeast DNA using primers 2686 and 2687. Subcloned into pBluescript KS after KpnI/SacII digest	genomic integration at the URA3 locus by recombination	Stephan Hamperl
pBluescript_ URA3_ HTZ1_MN		Amplification from pAG14 using primers 3245 and 3246. Subcloned into pBlueskript_URA3 after ApaI digest	genomic integration of HTZ1-MN_3xHA_kanMX 6 cassette at the URA3 locus	this work
pBluescript_ URA3_ HTA1_MN		Amplification from pAG14-HTA1_MN using primers 3245 and 3246. Subcloned into pBlueskript_URA3 after ApaI digest	genomic integration of pHTZ1_HTA1-MN_3xHA_kanMX 6 cassette at the URA3 locus	this work
pBluescript_ URA3_ HHT1_MN		Amplification from pAG14-HHT1_MN using primers 3245 and 3246. Subcloned into pBlueskript_URA3 after ApaI digest	genomic integration of pHTZ1_HHT1-MN_3xHA_kanMX 6 cassette at the URA3 locus	this work

7.3.3 DNA probes for Southern Blot detection

All probes were prepared with the “Rad Prime Labelling System” from Invitrogen.

Name	**Synthesis**	**Gene**	**Restriction enzyme**	**Probe size**
GAL1	PCR from genomic DNA using primers 1163 and 1164	GAL1-10	XcmI	295 bp
NUP57	PCR from genomic DNA using primers 1167 and 1168	RPS23A	XcmI	253 bp
Prom	PCR from genomic DNA using primers 817 and 818	rDNA	XcmI	250 bp
5S	PCR from genomic DNA using primers 1161 and 1162	rDNA	XcmI	250 bp
MRK1	PCR from genomic DNA using primers	MDH3	XcmI	282 bp
PRP12	PCR from genomic DNA using primers	PRP12	XcmI	253 bp
YDL218W	PCR from genomic DNA using primers	YDL218W	XcmI	295 bp

7.4 Enzymes and polypeptides

All enzymes were used under conditions specified by the manufacturer.

Herculase II fusion enzyme	Stratagene / Agilent
T4-DNA-ligase	NEW ENGLAND BIOLABS
Restriction endonucleases	NEW ENGLAND BIOLABS
Zymolyase T100	Seikagaku Corporation

Antibodies

antibody	**origin**	**dilution**	**manufacturer**
3F10 anti-HA	monoclonal rat	1:5000	Roche
goat anti-rat (peroxidase conjugated)	goat	1:2500	Jackson ImmunoResearch

7.5 Organisms

7.5.1 Bacteria

For cloning and protein expression chemically competent XL1-Blue cells from Stratagene or BL21(DE3) from Promega were used respectively.

7.5.2 Yeast strains

Name / Nr.	**Parent**	**Genotype**	**Comment**	**Reference**
NOY505 / #348		mata; ade2-1; ura3-1; trp1-1; leu2-3,112; his3-11; can1-100		Nogi et al., 1993
yKM04 / #620	NOY505	mata; ade2-1; ura3-1; trp1-1; leu2-3,112; his3-11; can1-100; HHT1-MNase-3xHA::KanMX6	obtained by trans-formation with KpnI/SacII restricted pKM15	Katharina Merz
yKM25 / #879	NOY505	mata; ade2-1; ura3-1; trp1-1; leu2-3,112; his3-11; can1-100; HHF2-MNase-3xHA::KanMX6	obtained by trans-formation with PCR product (1154/1155) from pKM9	Katharina Merz
yR28 / #954	NOY505	mata; ade2-1; ura3-1; trp1-1; leu2-3,112; his3-11; can1-100; HTZ1-MNase-3xHA::KanMX6	obtained by trans-formation with KpnI/SacII restricted pAG14	Hannah Götze

yR30 / #956	NOY505	mata; ade2-1; ura3-1; trp1-1; leu2-3,112; his3-11; can1-100; HTA1-MNase-3xHA::KanMX6	obtained by trans-formation with KpnI/SacII restricted pAG13	Hannah Götze
yR115 / #1763	NOY505	mat_alpha; ade5; ura3-52; trp1-289; leu2-112; his7-2; htz1Δ::HTA1-MNase-3xHA_KanMX6	obtained by transformation of KpnI/SacII restricted pAG14_HTA1-MNase	Ulrike Stöckl / this work
yCH1	yR30	mata; ade2-1; ura3-1; trp1-1; leu2-3,112; his3-11; can1-108; HTA1-MNase_3xHA_KanMX6; swr1Δ::URA3	obtained by trans-formation with PCR product (2118/2119) from pAG37	this work
yCH2	yR28	mata; ade2-1; ura3-1; trp1-1; leu2-3,112; his3-11; can1-100; HTZ1-MNase-3xHA::KanMX6; swr1Δ::URA3	obtained by trans-formation with PCR product (2118/2119) from pAG37	this work
yCH3	yR30	mata; ade2-1; ura3-1; trp1-1; leu2-3,112; his3-11; can1-100; HTA1-MNase-3xHA::KanMX6; htz1Δ::URA3	obtained by trans-formation with PCR product (1359/2117) from pAG37	this work
yCH4	NOY505	mata; ade2-1; ura3-1; trp1-1; leu2-3,112; his3-11; can1-100; htz1Δ::HTB2-MNase-3xHA_KanMX6	obtained by transformation of KpnI/SacII restricted pAG14_HTB2-MNase	this work
yCH5	NOY505	mata; ade2-1; ura3-1; trp1-1; leu2-3,112; his3-11; can1-100; htz1Δ::HHT1-MNase-3xHA_KanMX6	obtained by transformation of KpnI/SacII restricted pAG14_HHT1-MNase	this work
yCH6	NOY505	mata; ade2-1; ura3-1; trp1-1; leu2-3,112; his3-11; can1-100; htz1Δ::HHF1-MNase-3xHA_KanMX6	obtained by transformation of KpnI/SacII restricted pAG14_HHF1-MNase	this work
yCH7	yR28	mata; ade2-1; ura3-1; trp1-1; leu2-3,112; his3-11; can1-100; HTZ1-MNase-3xHA::KanMX6; ino80Δ::URA3	obtained by transformation with PCR product (3259/3260) from pAG37	this work
yCH8	NOY505	mata; ade2-1; ura3-1; trp1-1; leu2-3,112; his3-11; can1-100 ura3::pHTZ1_HTZ1-MNase-3xHA::KanMX6	obtained by transformation of SbfI restricted pBluescript_URA3_ HTZ1_MN	this work
yCH9	NOY505	mata; ade2-1; ura3-1; trp1-1; leu2-3,112; his3-11; can1-100 ura3::pHTZ1_HTA1-MNase-3xHA::KanMX6	obtained by transformation of SbfI restricted pBluescript_URA3_ HTA1_MN	this work
yCH10	NOY505	mata; ade2-1; ura3-1; trp1-1; leu2-3,112; his3-11; can1-100 ura3::pHTZ1_HHT1-MNase-3xHA::KanMX6	obtained by transformation of SbfI restricted pBluescript_URA3_ HHT1_MN	this work

7.6 Software and online tools

7.6.1 Software

Application	Source
Adobe Photoshop CS3	Adobe Systems Incorporated
Adobe Illustrator CS3	Adobe Systems Incorporated
Äkta Unicorn V5.01	Amersham Biosciences
Endnote X3	Thomson Reuters
Imagereader FLA-3000	Fujifilm
MAC OS X	Apple Inc.
Microsoft Office for MAC 2008 / Microsoft Office 2010	Microsoft
Multi Gauge V3.0	Fujifilm
NanoDrop ND1000	PeqLab
NetWare Browser 2	Novell, Inc.
OmniGraffle Professional 5	The Omni Group
Rotor Gene 6	Corbett Lifescience (QIAGEN)
Vector NTI 11	Invitrogen
Windows XP / 7	Microsoft

7.6.2 Online tools

Application	Source
Primer 3	http://primer3.sourceforge.net/
Netprimer	http://www.premierbiosoft.com/netprimer/index.html
Addgene	http://www.lablife.org
Reverse Complement	http://www.bioinformatics.org/sms/rev_comp.html
NEB double digest finder	http://www.neb.com/nebecomm/DoubleDigestCalculator.asp
Protein database	http://www.uniprot.org/
Protein analysis tools	http://expasy.org/

7.7 Consumables

Consumable	Supplier
Amicon Ultra 4 / Amicon Ultra 15 (MWCO 10,000)	Millipore
Cryo Tube Vials	Nunc
Culture tubes (13 ml)	Sarstedt
Dialysis Membrane (MWCO 6-8,000)	Spectrum Laboratories
Durapore filter (PVDF, 0,22µm)	Millipore
Filter Tips 10 µl; 20 µl; 200 µl; 1000 µl	Sarstedt
Gel cassettes 1 mm	Invitrogen
Glass beads (∅ 0.75-1 mm)	Roth
Glass Pasteur pipettes 150 mm; 230 mm	Brand
Immobilon Transfer Membranes	Millipore
Inoculation loops (1 µl)	Sarstedt
Latex gloves	Roth
Nickel-NTA-agarose	QIAGEN
Nitrile gloves	VWR
Nitrocellulose membrane (GSWP, 0,22µM)	Millipore
Parafilm “M” Laboratory Film	Pechiney
PCR tubes 0.1 ml (for qPCR)	LBF Labortechnik
PCR tubes 0.2 ml	Biozym Scientific
PCR tubes 8x0.2 ml strips	Kisker Biotech
Petri dishes	Sarstedt
Pipette tips 10 µl; 20 µl; 200 µl; 1000 µl	Sarstedt
Plastic cuvettes 10x4x45 mm	Sarstedt
Positive TM membrane	Q-biogene
PVDF membrane (Immobilon)	Millipore
Reaction tubes 1.5 ml; 2 ml	Sarstedt
Reaction tubes black 1,5 ml	Roth
Reaction tubes siliconised 1.5 ml	Biozym Scientific
Reaction tubes with screw cap 1 ml; 2 ml	Sarstedt
Serological pipettes 2 ml; 5 ml; 10 ml; 25 ml	Sarstedt
Serological pipettes 50 ml	Greiner bio-one

Tubes with screw cap 15 ml; 50 ml (“Falcon tubes”)	Sarstedt
Whatman paper 0.36 mm	Macherey-Nagel

7.8 Apparatus

Instrument	**Manufacturer**
37°C incubator	Heraeus Instruments
37°C plate incubator	Memmert
-80°C freezer	Sanyo
Agarose gel chambers	University of Regensburg
ÄKTA purifier	GE Healthcare
Autoclave	Varioklav; Zirbus
BAS cassette 2040	Fujifilm
BAS-III imaging plate	Fujifilm
Centrifuge 1-14	Sigma
Centrifuge 3-16K	Sigma
Centrifuge 4-15	Sigma
Centrifuge 5415R	Eppendorf
Centrifuge Centrikon T-324	Kontron Instruments
Electrophoresis Power Supply	Amersham Biosciences
Elgastat Maxima	Elga Process Water
Eraser	Raytest
Fluorescence Image Reader FLA-3000/-5000	Fujifilm
GelMax	Intas
Gel shaker Polymax 1040	Heidolph
Hybridization oven	PeqLab
Hybridization tubes	Bachofer, Rettberg
Ice machine	Ziegra
Image Reader LAS-3000	Fujifilm
Incubators	Memmert
Magnetic stirrer MR 3001	Heidolph

Magnetic stirrer MR Hei-Mix L	Heidolph
Micro-centrifuge II	Neolab
Microwave	Sharp
Movex Mini-Cell Gel Chamber	Invitrogen
Nanodrop ND-1000 Spectrophotometer	PeqLab
PCR cycler	PeqLab
pH meter	Knick
Photometer Ultraspec 3100 pro	Amersham Biosciences
Pipetboy comfort	IBS Integra Biosciences
Pipetman pipettes P2; P10; P20; P200; P1000	Gilson
Pumpdrive 5001	Heidolph
Roto-Shake Genie	Scientific Industries
Rotor Gene RG-3000	Corbett Research
Safe Imager	Acculab / Invitrogen / Sartorius
Semidry Transfer blotter	PeqLab
Shaker Unimax 2010	Heidolph
Shake incubators Multitron/Minitron	Infors
Sonicator 250	Branson
Speed Vac concentrator	Savant
Stratalinker 1800	Stratagene
Thermomixer compact	Eppendorf
Trans-Blot SD Semi-dry transfer cell	Biorad
Unigeldryer 3545D	Uniequip
Vortex Reax top	Neolab
Water bath Thermomix BU	Braun

8 Methods

8.1 DNA

8.1.1 Enzymatic manipulation of DNA

8.1.1.1 Sequence-specific endonuclease digestion

Restriction enzyme digestion was performed under the conditions specified by New England Biolabs. Control digestions during cloning were performed in a volume of 20 or 50 µl, preparative digestions for yeast transformations in 100 µl. Glycerol was present in the enzyme storage buffer; total glycerol in the reactions should not exceed 5%.

8.1.1.2 DNA ligation

For cloning of insert DNA fragments into vectors, a threefold molar excess of insert to vector was used. To avoid re-ligation of an empty vector, the plasmid was dephosphorylated with Antarctic Phosphatase before ligation.

Ligations were carried out using T4-DNA-Ligase and the corresponding buffer in a total volume of 20 µl. Reactions were either incubated at room temperature for 2 hours or over night at 16°C. 10 µl of the ligation reaction were used for transformation of *E. coli* cells.

8.1.1.3 Polymerase chain reaction

Different PCR reactions were performed depending on the purpose of the amplified DNA. Fragments used for nucleosome assembly were generated with Taq-polymerase. To determine ideal annealing temperatures, a temperature gradient was first run, testing different annealing temperatures. Typical reactions were performed in a volume of 50 µl according to the table below:

10x Taq buffer	5 µl
forward primer 100 µM	1 µl
reverse primer 100 µM	1 µl
dNTPs 10 mM	1 µl
template DNA	50 ng
Taq polymerase	1 µl
water	**ad 50 µl**

For large-scale preparations of nucleosome templates, PCR reactions were scaled up to 10 ml; aliquots of 125 µl were split into reaction tubes. Afterwards single reactions were pooled and DNA was precipitated.

PCR reactions to generate fragments for subsequent cloning into vectors were performed with the Herculase II fusion enzyme (Agilent):

5x Herculase II buffer	20 µl
forward primer 100 µM	2.5 µl
reverse primer 100 µM	2.5 µl
Herculase II dNTPs 0.25 µM	1 µl
template DNA	50 ng (vector) 100-300 ng (genomic DNA)
Herculase II	0.5 µl
water	**ad 100 µl**

8.1.2 Purification of nucleic acids

Plasmid isolation, DNA isolation from agarose gels and PCR purification were all carried out with the respective kits from Invitrogen or QIAGEN. All procedures were performed according to manufacturers' instructions

8.1.2.1 Isolation of genomic DNA from yeast

Cells from a 3 ml overnight culture were harvested and washed once with 500 µl water. Supernatant was discarded and the pellet resuspended in 300 µl spheroblasting buffer. Zymolyase T100 was added (2 µl from a 2% stock solution in water) and cells were incubated for 30 minutes at 37°C. Spheroblasts were pelleted (13.000 rpm, 2 minutes at room temperature) and resuspended in 300 µl IR buffer. SDS was added (50 µl of a 10% stock solution), samples were mixed and incubated at 65°C for 15 minutes. 100 µl of 5 M KOAc were added and the samples were kept on ice for 5 minutes. Samples were centrifuged at 13.000 rpm for 2 minutes. Supernatant was transferred to a new microtube and centrifugation was repeated to eliminate all precipitate. For precipitation of DNA, 300 µl isopropanol were added, samples were mixed and kept on ice for 5-10 minutes. DNA was pelleted at 13.000 rpm for 20 minutes at 4°C. To wash away excess salt, pellets were washed with 70% ethanol. Supernatants were removed completely, pellets were dried and resuspended in 50 µl TE + 0.02 mg/ml RNase. RNA was removed by incubating the samples containing RNase at 37°C for at least 30 minutes.

8.1.2.2 Chloroform-phenol extraction

DNA from aqueous solutions and cell lysates was extracted with chloroform-phenol. An equal volume of a phenol-chloroform-isoamyalcohol mixture (25:24:1) was added to the sample. Mixtures were thoroughly mixed on a vortex and centrifuged for 10 minutes (13.000 rpm, room temperature). The upper, aqueous phase was carefully taken off and transferred to a new microtube without disturbing the intermediate phase of denatured protein.

8.1.2.3 Ethanol precipitation

Samples that did not yet contain at least 250 mM salt, were mixed with an equal volume of IRN buffer. 2.5 volumes of cold ethanol (100%, p.a.) were added, samples were mixed and kept at -20°C for at least one hour. For small amounts of DNA, glycogen was added to facilitate precipitation. DNA was pelleted at 13.000 rpm for 20 minutes at 4°C. To wash away excess salt, pellets were washed with 70% ethanol. Supernatants were removed completely, pellets were dried and resuspended in an appropriate volume of TE or water.

8.1.3 Quantitative and qualitative analysis of nucleic acids

8.1.3.1 UV spectrometry

Concentration of DNA samples was measured with a NanoDrop ND1000 spectrophotometer. Absorption was determined at a wavelength of 260 nm and the concentration was calculated as follows: c [µg/ml] = OD_{260}* 1/sample-volume * 50 µg/ml.

Contamination of the samples with RNA or proteins could be evaluated through the measurement of absorption at 280 nm. For pure DNA the ratio of OD_{260}/OD_{280} should be between 1.8 and 2.0.

8.1.3.2 Agarose-gel electrophoresis

By default, 1% agarose was boiled in 1xTBE, 1/20,000th volume SYBR Safe was added and the solution was cast into a horizontal gel chamber with appropriate gel combs. After solidification, gels were run in 1xTBE as running buffer; 3-5 volts per cm were applied, electrophoresis time depended on the purpose of analysis. Agarose gels for ChEC analysis / Southern blots were 15 cm wide and 20 cm long and were run for 6-7 hours at 100 volts in a Biorad apparatus.

8.1.3.3 Native polyacrylamide gel electrophoresis

Native polyacrylamide gels were prepared with appropriate concentrations of polyacrylamide (5-6% PAA for nucleosome analysis). All components were mixed according to the table below and cast into pre-fixed vertical gel cassettes from Invitrogen with appropriate gel combs.

Volumes for one native PAA gel:

Native PAA gels	**5%**	**6%**
30% Acryl-Bisacrylamide-Mix	1.66 ml	2 ml
5x TBE	800 µl	
20% APS	80 µl	
TEMED	8 µl	
water	ad 10 ml	

After polymerization gels were pre-run in 0.5x TBE for 30-60 minutes at 90 volts to remove unpolymerized polyacrylamide. Electrophoresis was carried out at 85 volts; running time depended on the analyzed samples. To visualize DNA, the gel was incubated in a 0.5x TBE bath containing 0.5 mg/ml ethidiumbromide for 15 minutes and washed twice for 10 minutes in water.

8.1.4 Formaldehyde crosslink

A liquid culture of yeast cells (usually 500 ml) was grown to an OD_{600} of 0.6. Formaldehyde was added to a final concentration of 1% and cells were incubated for another 15 minutes at growth temperature. Crosslinking was stopped by addition of glycine to a concentration of 125 mM and incubation for 5 minutes at 24°C. Cells were harvested (4000 rpm, 10 minutes, 4°C; Centrikon T-324), washed with ice-cold water and resuspended in 1 ml water per OD_{600} 0.1. Aliquots of 1 ml were spun down (13.000 rpm, 2 minutes, 4°C; Eppendorf 5415R), frozen in liquid nitrogen and stored at -80°C.

8.1.5 Preparation of nuclei

An aliquot of formaldehyde fixed yeast cells was thawed on ice. Cells were resuspended in 1 ml of ChEC buffer A + protease inhibitors, spun down (13.000 rpm, 2 minutes, 4°C) and supernatant was removed. This wash step was repeated three times. The pellet was resuspended in 350 µl buffer A + protease inhibitors. Cells were broken with an equal volume of glass beads (∅ 0.75-1 mm, Roth, stored at -20°C) for 10 minutes on a VIBRAX at 4°C. Bottom and top of the microreaction tubes were pierced with a hot needle and placed in a 15 ml falcon tube. Cell lysate was then separated from the glass beads by centrifugation (2000 rpm, 2 minutes, 4°C; Centrikon

T-324). The glass beads remained in the microtube and were discarded. The cell lysate was transferred to a fresh microtube, spun down again (5000 g, 2 minutes, 4°C) and washed once with 1 ml buffer A + protease inhibitors.

8.1.6 Chromatin Endogenous Cleavage (ChEC)

Nuclei were prepared as described above and resuspended in 450 µl of ChEC buffer Ag + protease inhibitors and incubated at 30°C for 2 minutes. One 80 µl aliquot was taken from the well mixed reaction (timepoint “0”), before the reaction was started. The MNase digestion was started by addition of $CaCl_2$ to a final reaction concentration of 2 mM, reaction temperature was usually 30°C but had to be adjusted for different fusion proteins, depending on their abundance in the genome. Aliquots of 80 µl were taken at appropriate time points, usually 2, 5, 15 and 30 minutes. Shorter time points were necessary for high abundance proteins. The reactions were stopped by mixing the 80 µl aliquots with 100 µl of IRN buffer. It was obligatory to mix the samples right before taking aliquots to prevent sedimentation of the nuclei. After completion of the time course, 100 µl of IRN buffer were also added to the 0 minute aliquots. RNA was digested with 2 µl RNase A (stock 20 mg/ml) for 1 h at 37°. Afterwards SDS solution was added to a final concentration of 0.5%, as well as 2 µl of Proteinase K (stock 20 mg/ml) and incubated for 1 h at 56°C. Crosslinking was reversed by incubating the reactions at 65°C for at least 8 hours (usually overnight). DNA was extracted with chlorophorm-phenol, precipitated with ethanol, resuspended in 15 µl water and stored at -20°C.

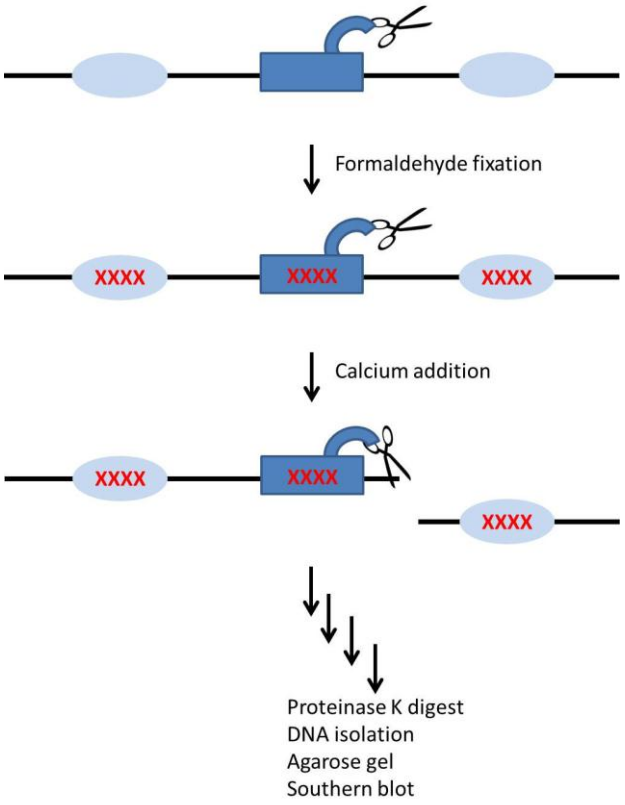

Figure 24: Schematic overview of Chromatin Endogenous Cleavage (ChEC). A MNase tagged protein of interest is depicted as a dark blue rectangle with a pair of scissors, light blue ovals represent neighboring nucleosomes. Formaldehyde fixation is shown as red crosses; calcium addition activates the MNase fusion protein, resulting in DNA cuts in the vicinity of the MNase fusion protein binding site. Subsequent working steps as described in the text are also depicted.

8.1.7 Unspecific endonuclease digestion (MNase)

Nuclei – prepared as above – were washed twice with 500 µl of MNase buffer (16.000 g, 1 minute at 4°C) and the resulting pellet was resuspended in 1 ml of MNase buffer. The suspension was split into five 200 µl aliquots. All aliquots were placed at 37°C for two minutes and then supplemented with 0, 0.05, 0.15, 0.3 and 1 U of MNase. Digestion was carried out at 37°C for 20 minutes and further workup of the DNA was performed as described for ChEC assays in section 8.1.6.

8.1.8 Southern Blot, Hybridization and detection of radioactive probes

8.1.8.1 Southern blot

DNA isolated in ChEC experiments or exogenous MNase digestion reactions was cleaved with XcmI in 27 µl reactions at 37°C over night. Gels (15x20 cm) were cast

with 250 ml of a 1% agarose TBE solution (containing SYBR Safe) and run at 100 V for 6-7 hours.

By southern blot, DNA should be transferred from the gel to a positively charged nylon membrane (Positive TM Membrane, Qbiogen). Before southern blotting, double stranded DNA was denatured by incubating the gel twice for 15 minutes in denaturing solution and subsequently the gel was incubated twice for 15 minutes in transfer buffer, NH_4OAc. DNA was transferred upwards by capillary flow of the transfer buffer through the blotting stack. A blotting stack was assembled as follows (bottom to top): a bridge of thick Whatman paper over a reservoir of transfer buffer, framed with Parafilm slices to prevent bypass of the capillary flow, the gel (turned upside down), the membrane, three thick Whatman papers and a pile of paper towels (ca. 5 cm). All layers except for the paper towels were soaked in transfer buffer before assembly. It had to be assured that no air bubbles formed between any of the layers, to guarantee for full transfer of the DNA. A weight placed on top of the blotting stack assured that the capillary flow was not disrupted.

Southern blot was performed over night at room temperature. Afterwards, the blotting stack was disassembled, the membrane was air-dried and DNA was crosslinked to the membrane (0.3 J/cm^2). Thymine bases were covalently linked to the amino groups of the membrane. Membranes could be stored at room temperature.

8.1.8.2 Preparation of radioactive probes

Radioactive probes for Southern blot hybridization were prepared with the RadPrime DNA Labeling System from Invitrogen and all steps were performed according to the manual. Template DNA was prepared in a separate PCR reaction from genomic yeast DNA. α^{32}P-dATP was ordered from Hartmann-Analytic GmbH.

Shortly, 25 ng of template DNA were denatured for 5 minutes at 95°C and immediately placed on ice. RadPrime buffer, nucleotides – omitting dATP – and 50 µCi α^{32}P-dATP were added and the mixed. For incorporation of radioactive nucleotides, Klenow-Fragment was added and the reaction was placed at 37°C for 10 – 15 minutes. Residual nucleotides were removed by size exclusion spin chromatography (Illustra ProbeQuant G-50 Micro Columns 28903408) and labeling efficiency was determined with a scintillation counter. The eluate from the column was mixed with salmon sperm DNA to reach a final concentration of 100 µg/ml in the hybridization tube (usually 150 µl for a total hybridization volume of 15 ml) and all DNA was denatured for 10 minutes at 95°C. Boiled probes were chilled on ice and then added to the hybridization tubes.

8.1.8.3 Hybridization

Membranes were pre-hybridized for at least 1 hour at hybridization temperature with 50 ml of hybridization buffer per tube. After pre-hybridization, the buffer was discarded and 15 ml fresh, preheated hybridization buffer was poured into the tube. The radioactive probe was mixed with salmon sperm DNA (final concentration in the tube: 100 µg/ml) and boiled for 5 minutes at 95°C and added to the tube.

Hybridization was carried out over night at hybridization temperature on the rotating wheel of a hybridization oven. Up to 6 blots could be stacked into one tube, separated by meshes. Blots should be covered with buffer, stick to the walls of the tube and not roll together.

After hybridization, buffer containing the probe can be stored at -20°C and re-used. Blots were first rinsed with 30 ml rinse buffer and then washed with buffers containing decreasing salt- and rising SDS-concentrations (southern wash buffers 1-3). Washing steps of 15 minutes with 50 ml buffer were repeated twice for each buffer and carried out in the oven at hybridization temperature. After washing, blots were air-dried and stored at room temperature.

8.1.8.4 Detection of radioactive probes

Phosphor-imaging plates (Fujifilm) were first erased in a “Raytest eraser”. Blot membranes were put into cassettes (Fuji), the imaging plate was placed on the membrane (white side down) and the cassette was tightly closed.

Exposure times depended on the intensity of radioactive signal. Imaging plates were scanned with a FujiFilm FLA-5000 phosphor imager.

In order to consecutively hybridize the same blots with different probes, probes had to be removed from the membranes. Therefore, blots were again stacked into hybridization tubes and incubated at least three times for 15 minutes at 80°C with 50 ml of Strip buffer. If radioactivity was still detected on the blots after three rounds of stripping, washing steps were repeated.

8.1.9 Chromatin Immuno Precipitation (ChIP)

ChIP experiments were essentially carried out as described by Hecht and Grunstein (Hecht et al. 1999). Formaldehyde-fixed cells from 50 ml of an exponentially growing yeast culture were washed with 1ml of cold lysis buffer (16,000 g, 1 minute at 4°C) and resuspended in 400 µl of lysis buffer. Cells were broken with an equal volume of glass beads (∅ 0.75-1 mm, Roth, stored at -20°C) for 45 minutes on a VIBRAX at 4°C. Bottom and top of the microreaction tubes were pierced with a hot needle and placed in a 15 ml falcon tube. Cell lysate was then separated from the glass beads by

centrifugation (2000 rpm, 2 minutes, 4°C; Centrikon T-324). The glass beads remained in the microtube and were discarded. DNA was sonicated in a volume of 1 ml lysis buffer using a Branson Sonifier 250 to obtain an average DNA fragment size of 200 to 400 bp. Cell debris was removed by centrifugation (20 min, 13,000 rpm, 4°C). The chromatin extracts were split into three aliquots. A total of 40 µl of each aliquot served as an input control and remained on ice while the other probes were used for immunoprecipitation. 250 µl of each aliquot was incubated for 2 hours at 4°C with 1 µg of a monoclonal anti-HA antibody (3F10; Roche) and 125 µl (slurry) of protein G-Sepharose to enrich the MNase-3xHA-tagged proteins bound by the antibody. After immunoprecipitation, the beads were washed three times with lysis buffer, twice with washing buffer I, and twice with washing buffer II, followed by a final washing step with TE buffer (2,000 rpm, 1 minute at 4°C). 250 µl of IRN buffer were added to the beads as well as to the input samples. DNA was isolated as previously described for ChEC experiments (see section 8.1.6). Both input and IP DNA were suspended in 50 µl of TE buffer and DNA was solved at room temperature for 1 hour shaking in a thermomixer and vortexing.

8.1.10 Quantitative real-time PCR (qPCR)

Quantitative real-time PCR is used to accurately measure the amount of a specific DNA fragment in a given solution, e.g. after enrichment via ChIP. The DNA amount amplified in a qPCR reaction is measured via the intensity of the fluorescence signal of SYBR-Green (Roche), which can only be detected after incorporation of the dye into DNA double helices.

All reactions were performed in a Rotor-Gene RG3000 system (QIAGEN). SYBR-Green was excited at 480 nm and fluorescence was recorded at 510 nm. Data were analyzed with the comparative quantitation module of the RotorGene analysis software. qPCR reactions were performed in 0.1 ml tubes in a total volume of 20 µl. One reaction consisted of 4 µl DNA (in suitable dilutions depending on the region of interest as well as the quality of the immunoprecipitation) and 16 µl of master mix. qPCR master mix consisted of 4 pmol of each the forward and the reverse primer, 0.25 µl of a 1:400,000 SYBR-Green stock solution in DMSO, 0.4 U HotStarTaq-polymerase as well as $MgCl_2$ (final concentration of 2.5 mM in the qPCR reaction), dNTPs (final concentration 0.2 mM in the qPCR reaction) and qPCR buffer. Master mix was split into the reaction tubes in a clean room using filter tips, DNA was added at the regular working bench. All steps were performed on ice.

8.2 Manipulation of *Escherichia coli*

8.2.1 Liquid culture

A 5 ml liquid culture of LB medium containing the appropriate antibiotic was inoculated with a single clone from a LB-agar plate. The culture was grown over night at 37°C and then used for further purposes.

8.2.2 Glycerol stock

Glycerol stocks for long-term storage of *E. coli* cells were prepared from fresh over night liquid cultures. 600 µl from the liquid culture were mixed with 300 µl 100% sterile glycerol, mixed well, transferred to a sterile microreaction tube with screw cap and stored at -80°C.

8.2.3 Preparation of chemically competent bacteria

For a pre-culture 50 ml of SOB medium were inoculated from a glycerol stock and incubated overnight at 37°C. A 200 ml culture was inoculated to an OD_{600} of 0.2 and grown at 37°C until the OD_{600} had reached 0.5-0.6. Cells were harvested in falcon tubes at 4500 rpm for 10 minutes at 4°C and supernatant was removed completely. Each 50 ml pellet was resuspended in 15 ml TfbI and incubated on ice for 20 minutes. Cells were spun down again at 4500 rpm for 10 minutes at 4°C, resuspended in 4 ml of TfbII for the complete 200 ml culture and incubated on ice for 10-20 minutes. Cells were split into 50 µl aliquots and stored at -80°C. All steps had to be carried out rapidly and on ice.

8.2.4 Transformation of competent bacteria

An aliquot (usually 50 µl) of chemically competent *E. coli* cells was thawed on ice. 100 ng of plasmid DNA or 10 µl of a ligation reaction were added to the cells and mixed carefully. Cells were kept on ice for another 5 minutes. Heat shock was carried out at 42°C for 45 seconds, followed by another 5 minutes on ice. To allow for the expression of the resistance gene, 500 µl of LB or SOC medium were added to the transformed bacteria and they were incubated at 37 °C for 30 minutes. 50 and 200 µl of the suspension were plated on agar plates supplemented with the appropriate antibiotics and incubated at 37 °C overnight.

8.3 Manipulation of *Saccharomyces cerevisiae*

8.3.1 Liquid culture

Liquid cultures of yeast cells were inoculated with a single clone from an agar plate and cultivated at the appropriate growth temperature (30°C). First, pre-cultures were grown in a maximum of 4 ml in plastic tubes (tube volume: 13 ml). Other cultures were grown in Erlenmeyer flasks.

8.3.2 Glycerol stock

2 ml of a fresh overnight culture were thoroughly mixed with 2 ml sterile 50% glycerol. The mixture was split into two aliquots in cryo tubes with a screw cap. Cells were frozen at -80°C.

8.3.3 Preparation of competent yeast cells

A 50 ml culture of yeast cells was grown to exponential phase. The cells were pelleted (500 g, 5 minutes at room temperature) and washed with 25 ml sterile water and once with 5 ml SORB. Cells were then resuspended in 500 µl SORB and transferred to a sterile microreaction tube and pelleted again. The supernatant was removed completely, the cells were taken up in 360 µl SORB and the tube was put on ice. 40 µl single stranded salmon sperm DNA (boiled for 5 minutes at 95°C) were added and mixed thoroughly. Aliquots of 50 µl were transferred to sterile microreaction tubes and immediately put at -80°C for storage.

8.3.4 Transformation of competent yeast cells

Aliquots of competent yeast cells were thawed on ice. DNA was added and carefully mixed with the cells. Six volumes of PEG were added and the mixture was incubated for 30 minutes at room temperature. $1/9^{th}$ of total volume (cells+DNA+PEG) of pure sterile DMSO was added. Heat shock was carried out at 42°C for 15 minutes and cells were pelleted (500 g, 2 minutes at room temperature). For auxotrophic markers (uracil), cells were resuspended in 200 µl of selective media and immediately plated on selective plates. For resistance markers (geneticin), cells were resuspended in 3 ml YPD / YPAD and incubated for 2-3 hours at 30°C, then resuspended in selective media and plated on selective plates. Transformed yeast cells with a geneticin marker were replica-plated to verify positive clones.

8.3.5 Establishment of knock out strains

Target knock out genes were replaced with a URA3 cassette via homologous recombination. PCR reactions for amplification of the knock out cassette were performed with primers consisting of a 5' sequence complementary to regions immediately upstream (forward primer) or downstream (reverse primer) of the target gene and a 3' sequence complementary to the S3 (forward primer) or S2 (reverse primer) adapters. PCR reactions of 100 µl were performed with a proof-reading enzyme (Herculase II) with pAG37 serving as template. The PCR product was precipitated with ethanol, DNA resuspended in 10 µl water and transformed into competent yeast cells. Successful transformants were screened for uracil auxotrophy.

8.3.6 Establishment of MNase fusion strains for histones expressed under the control of the H2A.Z promoter

PCR reactions for amplification of a target gene were carried out with overhang primers. These primers were comprised of a 5' restriction enzyme recognition site (forward primer: KpnI; reverse primer: AvaI), followed by a sequence complementary to the H2A.Z-upstream adapter (forward primer) and the S3 adapter of pKM9 (reverse primer; binding site immediately after the MNase-3xHA-KanMX cassette) and a 3' sequence complementary to the respective target gene (forward primer: 50 bp from the start codon; reverse primer: 50 bp immediately before the stop codon) PCR reactions of 100 µl were performed with a proof-reading enzyme (Herculase II) with genomic yeast DNA serving as template. The PCR product was purified with the QIAquick PCR purification kit (QIAGEN) and digested with KpnI/AvaI. After another PCR purification step the PCR product was cloned into pAG14 and transformed into competent *E. coli* cells. After verification of correct cloning, Midi preps were prepared. The cassette containing the H2A.Z promoter region, followed by a histone-MNase-3xHA-KanMX fusion cassette was excised from the plasmid via KpnI/SacII restriction enzyme digest, precipitated from the reaction and subsequently transformed into competent yeast cells. Successful transformants were screened for geneticin resistance.

8.4 Protein-biochemical methods

8.4.1 Denaturing protein extraction from yeast cells

Depending on the abundance of the protein of interest, 0.5-3 ml of an overnight culture were pelleted in microreaction tubes (16,000 g for 5 minutes at 4°C) and resuspended in 1 ml of ice cold water. 150 µl of pre-treatment solution were added, samples were mixed and incubated on ice for 15 minutes. Proteins were precipitated by addition of

150 µl 55% TCA and incubation on ice for 10 minutes and pelleted at 16.000 g for 10 minutes at 4°C. Supernatant was completely removed and the pellet was resuspended in 100 µl of 1x Lämmli buffer. Because of the TCA precipitation, the pH of the suspension was usually too low and the color of the sample was yellow. Thus the pH of the samples had to be neutralized with ammonia gas until the color turned to dark blue again. Proteins were denatured by boiling the samples at 95°C for 10 minutes, insoluble cell particles were pelleted at 16,000 g for 2 minutes at room temperature. A suitable volume of the soluble fraction was analyzed by Western blot.

8.4.2 SDS-polyacrylamide gel electrophoresis

Proteins were separated by vertical, discontinuous SDS-PAGE according to their molecular weight. The discontinuous system consisted of a lower separating gel and an upper stacking gel.

SDS gels of different polyacrylamide concentrations were prepared according to the scheme below (volumes are calculated for one gel cassette).

Volumes for one SDS gel:

Separating gel	**6%**	**10%**	**17%**
30% Acryl-Bisacrylamide-Mix	1.2 µl	2 µl	3.4 µl
4x Lower Tris buffer	1.5 ml		
20% APS	30 µl		
TEMED	6 µl		
water	**ad 10 ml**		

Stacking gel	**5%**
30% Acryl-Bisacrylamide-Mix	250 µl
4x Upper Tris buffer	380 µl
20% APS	7.5 µl
TEMED	1.5 µl
water	**ad 1.5 ml**

Gels were run at 45 mA in 1x SDS running buffer until the bromophenol band had reached the lower border of the gel; electrophoresis time depended on the polyacrylamide percentage and size of the proteins of interest.

8.4.3 Coomassie staining of SDS polyacrylamide gels

To visualize protein bands separated on SDS polyacrylamide gels, gels were fixed and stained in one step for at least 30 minutes on a slowly rocking platform with Coomassie Blue staining solution and then destained by boiling water in a microwave and incubation for 5 minutes in the hot water. Boiling steps were repeated until destaining

was complete. Gels were scanned and subsequently dried on Whatman paper for 1.5 hours at 80°C using a slab gel drier.

8.4.4 Western blot, semi-dry

After SDS-PAGE proteins are negatively charged and can be transferred to a polyvinylidene difluoride (PVDF) membrane.

An SDS gel was run as described in section 8.4.2 with pre-stained marker. After electrophoresis, the gel was incubated in Towbin buffer for 10 minutes. The membrane was first wet in methanol and then soaked in Towbin buffer. A total of six Whatman papers were also soaked in Towbin buffer.

The blot was assembled as follows: three Whatman papers were put on the blot apparatus. The membrane was placed on top of the paper stack, any air bubbles were removed, as they prevent a constant flow of the electric flux. The gel was carefully placed on top of the membrane, again without air bubbles. To complete the blot sandwich, three more Whatman papers were placed on top of the stack. Proteins were transferred for 1 hour 20 minutes at 24 V. After blotting, the bands from the pre stained marker should be visible on the membrane.

8.4.5 Immunodetection of proteins

The membrane was blocked for 30 minutes in 1x PBS/0.2% Tween (PBST) supplemented with 5% dry skimmed milk at room temperature to prevent unspecific binding of the antibody. The primary antibody, directed against the protein of interest, was appropriately diluted in 1x PBST (5-6 ml for one membrane to be completely covered) and incubated with the membrane for 1 hour at room temperature. The membrane was washed three times for 10 minutes at room temperature with 1x PBST.

The secondary antibody – coupled to horseradish peroxidase – was diluted in 1x PBST and also incubated with the membrane for 1 hour at room temperature. The membrane was again washed three times with 1x PBST and once with water.

The western blot was developed with the BM chemiluminescence blotting substrate from Roche. Now the horseradish peroxidase catalyzed the oxidation of diacylhydrazides via an activated intermediate that decays to the ground state by emission of light in the visible range. This chemiluminescence was detected with a LAS-3000 fluorescence reader (FUJIFILM). Protein marker bands were marked with a fluorescence pen.

8.4.6 Expression and purification of recombinant histones

The protocols for expression and purification of recombinant histones and subsequent reconstitution of histone octamers was adapted from the protocol by Karolin Luger (Luger et al. 1999).

8.4.6.1 Preparative expression of recombinant histones

Coding sequences for human histones were cloned into the pET21a expression vector (kind gift from the Robert Schneider Lab, MPI Freiburg). Preparative expressions were carried out in a culture volume of 1 l (LB-Amp medium). Cells (expression strain BL21 (DE3)) were grown to an OD_{600} of 0.6 and gene expression was induced by addition of IPTG to a final concentration of 2 mM. Expression time depended on the histone type (2 hours for H3, H3.3 and H4; 3 hours for H2A, H2B, H2A.Z). Bacteria were harvested by centrifugation (rotor A6.9, 6,000 rpm, 20 minutes at 4°C), pellets were resuspended in 25 ml wash buffer, frozen in liquid nitrogen and stored at -80°C.

8.4.6.2 Purification of inclusion bodies

Histones were purified via inclusion bodies. Cell suspensions were thawed and cells were lysed by sonification (large tip, 70% amplitude, pulse 5 seconds on, 5 seconds off, on ice). Inclusion bodies were pelleted (rotor A8.24, 18,000 rpm, 20 minutes at 4°C), washed once with 25 ml triton-wash buffer and twice with 25 ml wash buffer. Supernatants were discarded and the drained pellet could be stored at -20°C.

For unfolding of inclusion bodies, 1 ml of DMSO was added to the frozen pellet. After thawing, the suspension was homogenized as much as possible with a few ml of unfolding buffer. The volume was then adjusted to 25 ml, DTT was added to a final concentration of 10 mM and the suspension was incubated for 30-60 minutes on a rotating wheel at room temperature. Cell debris was pelleted (rotor A8.24, 18,000 rpm, 20 minutes at 4°C), the supernatant was transferred to a pre-wet dialysis membrane (MWCO 6-8 kDa) and dialyzed against an appropriate volume of SAU-buffer containing 200 mM NaCl (SAU-200) at 4°C. Dialysis buffer was changed twice after at least one hour and a final dialysis step was done overnight. The protein solution was either stored at -20°C or directly used for ion-exchange chromatography.

8.4.6.3 Ion-exchange chromatography

Dialyzed protein samples were centrifuged at 16,000 g for 20 minutes at 4°C to remove any particles which would subsequently clog the pumps of the ÄKTA system.

Test runs were carried out with 1 ml of each sample to determine the ideal salt concentration for elution of the proteins from the ion-exchange column (HiTrap SP FF, 1 ml). Therefore, a linear gradient from 0.2 – 1 M salt was applied with a flow rate of

1 ml/min, elution of the protein was monitored at 280 nm and peak fractions were analyzed on 17% SDS polyacrylamide gels.

For large scale purifications, a step gradient was applied with the elution step at the previously determined salt concentration. Up to 70 mg protein sample could be loaded onto the column, thus elution fractions were relatively concentrated. Peak fractions were pooled and dialyzed against an appropriate volume of water supplemented with 2 mM β-mercaptoethanol. Protein aliquots of 1 mg were frozen in liquid nitrogen and stored at -80°C.

8.4.7 Reconstitution of histone octamers

Histone aliquots were lyophilized and dissolved in unfolding buffer to a concentration of 2 mg/ml and incubated for at least 30 minutes and no longer than 3 hours at room temperature on a rotating wheel. Equimolar amounts of all four core histones were mixed and concentration was adjusted to 1 mg/ml. The mixture was transferred to a pre-wet dialysis membrane (MWCO 6-8 kDa) and dialyzed against an appropriate volume of refolding buffer at 4°C. Buffer was changed twice after at least one hour and a final dialysis step was done overnight.

8.4.7.1 Purification of histone octamers by gel-filtration

Reconstitution mixes were removed from the dialysis membrane and the samples were concentrated to a volume of approximately 1.5 ml with Amicon Ultra Centrifugal Filter Units (Millipore, MWCO: 10 kDa). The concentrated sample was centrifuged to remove any precipitate (16,000 g, 20 minutes at 4°C) and the supernatant was loaded onto an equilibrated HiLoad 16/60 Superdex 200 pg column. Isocratic elution with refolding buffer was carried out at a flow rate of 1 ml/min and elution was monitored at 280 nm. Peak fractions were analyzed on 17% SDS polyacrylamide gels: high molecular weight aggregates eluted after a retention volume of about 45-48 ml, histone octamers between 65-68 ml and (H2A-H2B) dimers around 84 ml.

Octamer fractions were pooled and protein concentration was adjusted to 1 mg/ml with Amicon Ultra Centrifugal Filter Units (Millipore, MWCO: 10 kDa). After analysis of the octamers on a 17% SDS polyacrylamide gel, the samples were mixed with an equal volume of 100% glycerol and stored at -20°C.

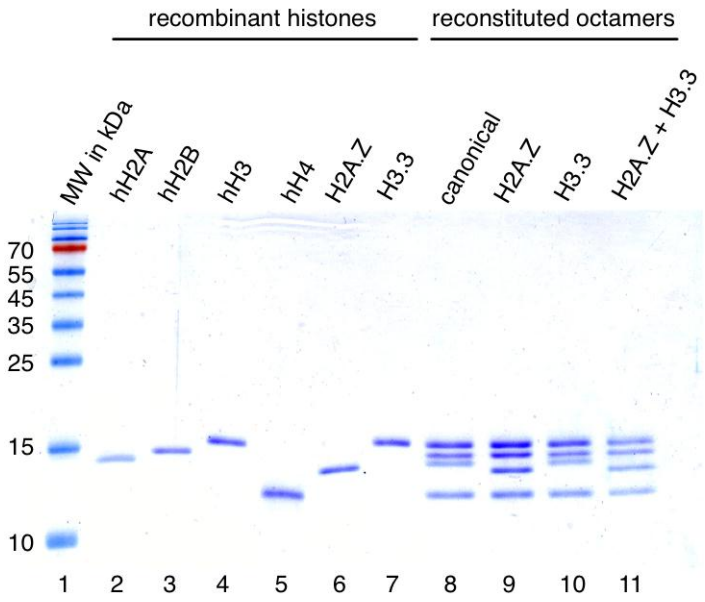

Figure 25: Purified recombinant histones and reconstituted histone octamers. Human histones loaded in lanes 2-7 were expressed and purified as described in section 8.4.6. The histone octamers shown in lanes 8-11 were reconstituted according to section 8.4.7; histone content of the respective octamers is depicted above. Proteins were analyzed on a denaturing 17% polyacrylamide gel; a molecular weight marker was loaded (lane 1).

8.4.8 Chromatin reconstitution

Nucleosomes were reconstituted with linear DNA fragments and purified histone octamers via the salt gradient dialysis method (Rhodes et al. 1989). Assembly reactions were performed in the lid of siliconized microreaction tubes. A hole was melted into the lid – the so-called O-ring – and the bottom of the tube was cut off. Lid and tube were separated by a dialysis membrane (MWCO 6-8 kDa; pre-wet in High salt buffer) and placed in a Styrofoam floater. The floater was placed in a 3 l beaker containing 300 ml High salt buffer and a magnetic stirrer. Air bubbles between buffer and dialysis membrane were removed with a bent Pasteur pipette and assembly reaction mixtures were transferred into the lids of the dialysis tubes.

For specific formation of nucleosomes, the salt concentration was gradually lowered from 2 M to 227 mM by addition of 3 l low salt buffer at a flow rate of 200 ml (overnight at room temperature) and constant stirring.

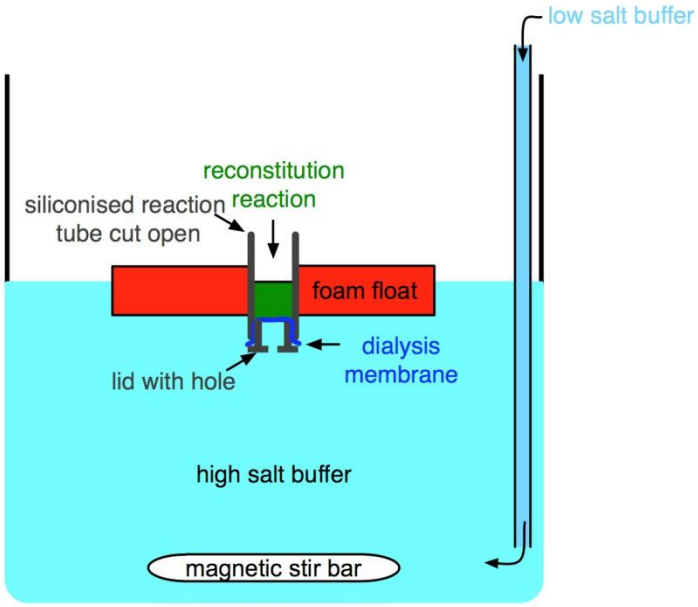

Figure 26: Schematic overview of the experimental setup for salt gradient dialysis. (adapted from diploma thesis Sonja Völker)

First, test assemblies were performed to determine the optimal histones to DNA ratio. A typical test assembly mix contained 4 µg of DNA and rising amounts of histone octamers, starting at a ratio of histones : DNA of 0.2, in a total volume of 40 µl high salt buffer supplemented with BSA in a final concentration of 200 ng/µl. To avoid unspecific nucleosome formation, the reactions also contained 250 ng of a plasmid (usually pCMV14) as competitor DNA. After completion of the dialysis, assembly reactions were carefully removed from the dialysis set up, transferred to siliconized reaction tubes and stored at 4°C.

To visualize nucleosome assembly, approximately 300 ng of each reaction were analyzed on a native polyacrylamide gel (see section 8.1.3.3).

After determination of the optimal histones to DNA ratio, multiple assembly reactions were done and pooled.

8.4.9 Mobilization of nucleosomes

8.4.9.1 Thermophoretic mobility shift assay

Thermal mobilization of nucleosomes was performed as described by Flaus et al. (Flaus et al. 2003).

Shortly, 300 ng of nucleosomes were incubated in a total volume of 20 µl, supplemented with 50 mM Tris-HCl pH 7.6, at different temperatures for 2 hours.

Nucleosome positions were analyzed on a native polyacrylamide gel (see section 8.1.3.3).

8.4.9.2 Nucleosome remodeling assay

A nucleosome remodeling assay visualized the mobilization of mononucleosomes catalyzed by ATP-dependent remodeling enzymes.

Typical remodeling reactions consisted of 300 ng of reconstituted mononucleosomes and rising amounts of remodeling enzyme in an Ex-Buffer system to adjust the salt concentration to 90-100 mM in a total volume of 10 µl. The mix was supplemented with 1 mM ATP and incubated at 26°C for 90 minutes. Reactions were stopped by the addition of 1 µg of plasmid DNA (usually pCMV14) and further incubation at 26°C for 5 minutes.

Nucleosome positions were visualized by native gel electrophoresis as described in section 8.1.3.3.

9 Bibliography

Abbott, D. W., V. S. Ivanova, X. Wang, W. M. Bonner and J. Ausio (2001). "Characterization of the stability and folding of H2A.Z chromatin particles: implications for transcriptional activation." The Journal of biological chemistry **276**(45): 41945-41949.

Adkins, M. W., S. R. Howar and J. K. Tyler (2004). "Chromatin disassembly mediated by the histone chaperone Asf1 is essential for transcriptional activation of the yeast PHO5 and PHO8 genes." Mol Cell **14**(5): 657-666.

Ahmad, K. and S. Henikoff (2002). "The histone variant H3.3 marks active chromatin by replication-independent nucleosome assembly." Mol Cell **9**(6): 1191-1200.

Akhmanova, A., K. Miedema and W. Hennig (1996). "Identification and characterization of the Drosophila histone H4 replacement gene." FEBS Lett **388**(2-3): 219-222.

Albert, I., T. N. Mavrich, L. P. Tomsho, J. Qi, S. J. Zanton, S. C. Schuster and B. F. Pugh (2007). "Translational and rotational settings of H2A.Z nucleosomes across the Saccharomyces cerevisiae genome." Nature **446**(7135): 572-576.

Allshire, R. C. and G. H. Karpen (2008). "Epigenetic regulation of centromeric chromatin: old dogs, new tricks?" Nat Rev Genet **9**(12): 923-937.

Altaf, M., A. Auger, J. Monnet-Saksouk, J. Brodeur, S. Piquet, M. Cramet, N. Bouchard, N. Lacoste, R. T. Utley, L. Gaudreau and J. Cote (2010). "NuA4-dependent acetylation of nucleosomal histones H4 and H2A directly stimulates incorporation of H2A.Z by the SWR1 complex." J Biol Chem **285**(21): 15966-15977.

Badis, G., E. T. Chan, H. van Bakel, L. Pena-Castillo, D. Tillo, K. Tsui, C. D. Carlson, A. J. Gossett, M. J. Hasinoff, C. L. Warren, M. Gebbia, S. Talukder, A. Yang, S. Mnaimneh, D. Terterov, D. Coburn, A. Li Yeo, Z. X. Yeo, N. D. Clarke, J. D. Lieb, A. Z. Ansari, C. Nislow and T. R. Hughes (2008). "A library of yeast transcription factor motifs reveals a widespread function for Rsc3 in targeting nucleosome exclusion at promoters." Mol Cell **32**(6): 878-887.

Bednar, J., R. A. Horowitz, S. A. Grigoryev, L. M. Carruthers, J. C. Hansen, A. J. Koster and C. L. Woodcock (1998). "Nucleosomes, linker DNA, and linker histone form a unique structural motif that directs the higher-order folding and compaction of chromatin." Proc Natl Acad Sci U S A **95**(24): 14173-14178.

Belotserkovskaya, R., S. Oh, V. A. Bondarenko, G. Orphanides, V. M. Studitsky and D. Reinberg (2003). "FACT facilitates transcription-dependent nucleosome alteration." Science **301**(5636): 1090-1093.

Bernstein, E. and S. B. Hake (2006). "The nucleosome: a little variation goes a long way." Biochem Cell Biol **84**(4): 505-517.

Birch, J. L., B. C. Tan, K. I. Panov, T. B. Panova, J. S. Andersen, T. A. Owen-Hughes, J. Russell, S. C. Lee and J. C. Zomerdijk (2009). "FACT facilitates chromatin transcription by RNA polymerases I and III." EMBO J **28**(7): 854-865.

Boeger, H., J. Griesenbeck, J. S. Strattan and R. D. Kornberg (2003). "Nucleosomes unfold completely at a transcriptionally active promoter." Mol Cell **11**(6): 1587-1598.

Bonisch, C., K. Schneider, S. Punzeler, S. M. Wiedemann, C. Bielmeier, M. Bocola, H. C. Eberl, W. Kuegel, J. Neumann, E. Kremmer, H. Leonhardt, M. Mann, J. Michaelis, L. Schermelleh and S. B. Hake (2012). "H2A.Z.2.2 is an alternatively spliced histone H2A.Z variant that causes severe nucleosome destabilization." Nucleic Acids Res.

Boyarchuk, E., R. Montes de Oca and G. Almouzni (2011). "Cell cycle dynamics of histone variants at the centromere, a model for chromosomal landmarks." Curr Opin Cell Biol **23**(3): 266-276.

Brandt, W. F., W. N. Strickland, M. Strickland, L. Carlisle, D. Woods and C. von Holt (1979). "A histone programme during the life cycle of the sea urchin." Eur J Biochem **94**(1): 1-10.

Bruno, M., A. Flaus, C. Stockdale, C. Rencurel, H. Ferreira and T. Owen-Hughes (2003). "Histone H2A/H2B dimer exchange by ATP-dependent chromatin remodeling activities." Mol Cell **12**(6): 1599-1606.

Cao, R., L. Wang, H. Wang, L. Xia, H. Erdjument-Bromage, P. Tempst, R. S. Jones and Y. Zhang (2002). "Role of histone H3 lysine 27 methylation in Polycomb-group silencing." Science **298**(5595): 1039-1043.

Carr, A. M., S. M. Dorrington, J. Hindley, G. A. Phear, S. J. Aves and P. Nurse (1994). "Analysis of a histone H2A variant from fission yeast: evidence for a role in chromosome stability." Mol Gen Genet **245**(5): 628-635.

Celona, B., A. Weiner, F. Di Felice, F. M. Mancuso, E. Cesarini, R. L. Rossi, L. Gregory, D. Baban, G. Rossetti, P. Grianti, M. Pagani, T. Bonaldi, J. Ragoussis, N. Friedman, G. Camilloni, M. E. Bianchi and A. Agresti (2011). "Substantial histone reduction modulates genomewide nucleosomal occupancy and global transcriptional output." PLoS Biol **9**(6): e1001086.

Chakravarthy, S., Y. Bao, V. A. Roberts, D. Tremethick and K. Luger (2004). "Structural characterization of histone H2A variants." Cold Spring Harb Symp Quant Biol **69**: 227-234.

Chen, L., Y. Cai, J. Jin, L. Florens, S. K. Swanson, M. P. Washburn, J. W. Conaway and R. C. Conaway (2011). "Subunit organization of the human INO80 chromatin remodeling complex: an evolutionarily conserved core complex

catalyzes ATP-dependent nucleosome remodeling." J Biol Chem **286**(13): 11283-11289.

Clapier, C. R. and B. R. Cairns (2009). "The biology of chromatin remodeling complexes." Annu Rev Biochem **78**: 273-304.

Clarkson, M. J., J. R. Wells, F. Gibson, R. Saint and D. J. Tremethick (1999). "Regions of variant histone His2AvD required for Drosophila development." Nature **399**(6737): 694-697.

Corpet, A. and G. Almouzni (2009). "Making copies of chromatin: the challenge of nucleosomal organization and epigenetic information." Trends Cell Biol **19**(1): 29-41.

Cremer, T., K. Kupper, S. Dietzel and S. Fakan (2004). "Higher order chromatin architecture in the cell nucleus: on the way from structure to function." Biol Cell **96**(8): 555-567.

Deal, R. B., C. N. Topp, E. C. McKinney and R. B. Meagher (2007). "Repression of flowering in Arabidopsis requires activation of FLOWERING LOCUS C expression by the histone variant H2A.Z." Plant Cell **19**(1): 74-83.

Dechassa, M. L., A. Sabri, S. Pondugula, S. R. Kassabov, N. Chatterjee, M. P. Kladde and B. Bartholomew (2010). "SWI/SNF has intrinsic nucleosome disassembly activity that is dependent on adjacent nucleosomes." Mol Cell **38**(4): 590-602.

Dhillon, N. and R. T. Kamakaka (2000). "A histone variant, Htz1p, and a Sir1p-like protein, Esc2p, mediate silencing at HMR." Mol Cell **6**(4): 769-780.

Dhillon, N., M. Oki, S. J. Szyjka, O. M. Aparicio and R. T. Kamakaka (2006). "H2A.Z functions to regulate progression through the cell cycle." Mol Cell Biol **26**(2): 489-501.

Dion, M. F., T. Kaplan, M. Kim, S. Buratowski, N. Friedman and O. J. Rando (2007). "Dynamics of replication-independent histone turnover in budding yeast." Science **315**(5817): 1405-1408.

Draker, R. and P. Cheung (2009). "Transcriptional and epigenetic functions of histone variant H2A.Z." Biochemistry and cell biology = Biochimie et biologie cellulaire **87**(1): 19-25.

Dryhurst, D., T. Ishibashi, K. L. Rose, J. M. Eirin-Lopez, D. McDonald, B. Silva-Moreno, N. Veldhoen, C. C. Helbing, M. J. Hendzel, J. Shabanowitz, D. F. Hunt and J. Ausio (2009). "Characterization of the histone H2A.Z-1 and H2A.Z-2 isoforms in vertebrates." BMC Biol **7**: 86.

Durant, M. and B. F. Pugh (2007). "NuA4-directed chromatin transactions throughout the Saccharomyces cerevisiae genome." Mol Cell Biol **27**(15): 5327-5335.

Eberharter, A., I. Vetter, R. Ferreira and P. B. Becker (2004). "ACF1 improves the effectiveness of nucleosome mobilization by ISWI through PHD-histone contacts." EMBO J **23**(20): 4029-4039.

Eirin-Lopez, J. M., R. Gonzalez-Romero, D. Dryhurst, T. Ishibashi and J. Ausio (2009). "The evolutionary differentiation of two histone H2A.Z variants in chordates (H2A.Z-1 and H2A.Z-2) is mediated by a stepwise mutation process that affects three amino acid residues." BMC Evol Biol **9**: 31.

Eisen, J. A., K. S. Sweder and P. C. Hanawalt (1995). "Evolution of the SNF2 family of proteins: subfamilies with distinct sequences and functions." Nucleic Acids Res **23**(14): 2715-2723.

English, C. M., M. W. Adkins, J. J. Carson, M. E. Churchill and J. K. Tyler (2006). "Structural basis for the histone chaperone activity of Asf1." Cell **127**(3): 495-508.

Faast, R., V. Thonglairoam, T. C. Schulz, J. Beall, J. R. Wells, H. Taylor, K. Matthaei, P. D. Rathjen, D. J. Tremethick and I. Lyons (2001). "Histone variant H2A.Z is required for early mammalian development." Curr Biol **11**(15): 1183-1187.

Fan, J. Y., D. Rangasamy, K. Luger and D. J. Tremethick (2004). "H2A.Z alters the nucleosome surface to promote HP1alpha-mediated chromatin fiber folding." Mol Cell **16**(4): 655-661.

Farris, S. D., E. D. Rubio, J. J. Moon, W. M. Gombert, B. H. Nelson and A. Krumm (2005). "Transcription-induced chromatin remodeling at the c-myc gene involves the local exchange of histone H2A.Z." J Biol Chem **280**(26): 25298-25303.

Fedor, M. J., N. F. Lue and R. D. Kornberg (1988). "Statistical positioning of nucleosomes by specific protein-binding to an upstream activating sequence in yeast." J Mol Biol **204**(1): 109-127.

Fink, M., D. Imholz and F. Thoma (2007). "Contribution of the serine 129 of histone H2A to chromatin structure." Mol Cell Biol **27**(10): 3589-3600.

Flaus, A., D. M. Martin, G. J. Barton and T. Owen-Hughes (2006). "Identification of multiple distinct Snf2 subfamilies with conserved structural motifs." Nucleic Acids Res **34**(10): 2887-2905.

Flaus, A. and T. Owen-Hughes (2003). "Dynamic properties of nucleosomes during thermal and ATP-driven mobilization." Mol Cell Biol **23**(21): 7767-7779.

Flaus, A. and T. J. Richmond (1998). "Positioning and stability of nucleosomes on MMTV 3'LTR sequences." J Mol Biol **275**(3): 427-441.

Fritsch, O., G. Benvenuto, C. Bowler, J. Molinier and B. Hohn (2004). "The INO80 protein controls homologous recombination in Arabidopsis thaliana." Mol Cell **16**(3): 479-485.

Gasser, R., T. Koller and J. M. Sogo (1996). "The stability of nucleosomes at the replication fork." J Mol Biol **258**(2): 224-239.

Gaykalova, D. A., V. Nagarajavel, V. A. Bondarenko, B. Bartholomew, D. J. Clark and V. M. Studitsky (2011). "A polar barrier to transcription can be circumvented by remodeler-induced nucleosome translocation." Nucleic Acids Res **39**(9): 3520-3528.

Gerard, A., S. Koundrioukoff, V. Ramillon, J. C. Sergere, N. Mailand, J. P. Quivy and G. Almouzni (2006). "The replication kinase Cdc7-Dbf4 promotes the interaction of the p150 subunit of chromatin assembly factor 1 with proliferating cell nuclear antigen." EMBO Rep **7**(8): 817-823.

Groth, A., W. Rocha, A. Verreault and G. Almouzni (2007). "Chromatin challenges during DNA replication and repair." Cell **128**(4): 721-733.

Grove, G. W. and A. Zweidler (1984). "Regulation of nucleosomal core histone variant levels in differentiating murine erythroleukemia cells." Biochemistry **23**(19): 4436-4443.

Guillemette, B., A. R. Bataille, N. Gevry, M. Adam, M. Blanchette, F. Robert and L. Gaudreau (2005). "Variant histone H2A.Z is globally localized to the promoters of inactive yeast genes and regulates nucleosome positioning." PLoS Biol **3**(12): e384.

Guo, X. W., J. P. Th'ng, R. A. Swank, H. J. Anderson, C. Tudan, E. M. Bradbury and M. Roberge (1995). "Chromosome condensation induced by fostriecin does not require p34cdc2 kinase activity and histone H1 hyperphosphorylation, but is associated with enhanced histone H2A and H3 phosphorylation." EMBO J **14**(5): 976-985.

Hall, D. B., J. T. Wade and K. Struhl (2006). "An HMG protein, Hmo1, associates with promoters of many ribosomal protein genes and throughout the rRNA gene locus in Saccharomyces cerevisiae." Mol Cell Biol **26**(9): 3672-3679.

Hamiche, A., R. Sandaltzopoulos, D. A. Gdula and C. Wu (1999). "ATP-dependent histone octamer sliding mediated by the chromatin remodeling complex NURF." Cell **97**(7): 833-842.

Hardy, S. and F. Robert (2010). "Random deposition of histone variants: A cellular mistake or a novel regulatory mechanism?" Epigenetics **5**(5): 368-372.

Hartley, P. D. and H. D. Madhani (2009). "Mechanisms that specify promoter nucleosome location and identity." Cell **137**(3): 445-458.

Hecht, A. and M. Grunstein (1999). "Mapping DNA interaction sites of chromosomal proteins using immunoprecipitation and polymerase chain reaction." Methods Enzymol **304**: 399-414.

Heo, K., H. Kim, S. H. Choi, J. Choi, K. Kim, J. Gu, M. R. Lieber, A. S. Yang and W. An (2008). "FACT-mediated exchange of histone variant H2AX regulated by phosphorylation of H2AX and ADP-ribosylation of Spt16." Mol Cell **30**(1): 86-97.

Hermann, A., H. Gowher and A. Jeltsch (2004). "Biochemistry and biology of mammalian DNA methyltransferases." Cell Mol Life Sci **61**(19-20): 2571-2587.

Hermann, A., R. Goyal and A. Jeltsch (2004). "The Dnmt1 DNA-(cytosine-C5)-methyltransferase methylates DNA processively with high preference for hemimethylated target sites." J Biol Chem **279**(46): 48350-48359.

Hou, H., Y. Wang, S. P. Kallgren, J. Thompson, J. R. Yates, 3rd and S. Jia (2010). "Histone variant H2A.Z regulates centromere silencing and chromosome segregation in fission yeast." J Biol Chem **285**(3): 1909-1918.

Ioshikhes, I. P., I. Albert, S. J. Zanton and B. F. Pugh (2006). "Nucleosome positions predicted through comparative genomics." Nat Genet **38**(10): 1210-1215.

Jensen, K., M. S. Santisteban, C. Urekar and M. M. Smith (2011). "Histone H2A.Z acid patch residues required for deposition and function." Mol Genet Genomics **285**(4): 287-296.

Jenuwein, T. and C. D. Allis (2001). "Translating the histone code." Science **293**(5532): 1074-1080.

Jiang, C. and B. F. Pugh (2009). "Nucleosome positioning and gene regulation: advances through genomics." Nat Rev Genet **10**(3): 161-172.

Jin, C. and G. Felsenfeld (2007). "Nucleosome stability mediated by histone variants H3.3 and H2A.Z." Genes Dev **21**(12): 1519-1529.

Jin, C., C. Zang, G. Wei, K. Cui, W. Peng, K. Zhao and G. Felsenfeld (2009). "H3.3/H2A.Z double variant-containing nucleosomes mark 'nucleosome-free regions' of active promoters and other regulatory regions." Nat Genet **41**(8): 941-945.

Kalocsay, M., N. J. Hiller and S. Jentsch (2009). "Chromosome-wide Rad51 spreading and SUMO-H2A.Z-dependent chromosome fixation in response to a persistent DNA double-strand break." Mol Cell **33**(3): 335-343.

Kamakaka, R. T. and S. Biggins (2005). "Histone variants: deviants?" Genes & development **19**(3): 295-310.

Kaplan, C. D., L. Laprade and F. Winston (2003). "Transcription elongation factors repress transcription initiation from cryptic sites." Science **301**(5636): 1096-1099.

Kaplan, N., T. R. Hughes, J. D. Lieb, J. Widom and E. Segal (2010). "Contribution of histone sequence preferences to nucleosome organization: proposed definitions and methodology." Genome Biol **11**(11): 140.

Kaplan, N., I. Moore, Y. Fondufe-Mittendorf, A. J. Gossett, D. Tillo, Y. Field, T. R. Hughes, J. D. Lieb, J. Widom and E. Segal (2010). "Nucleosome sequence preferences influence in vivo nucleosome organization." Nat Struct Mol Biol **17**(8): 918-920; author reply 920-912.

Keogh, M. C., T. A. Mennella, C. Sawa, S. Berthelet, N. J. Krogan, A. Wolek, V. Podolny, L. R. Carpenter, J. F. Greenblatt, K. Baetz and S. Buratowski (2006). "The Saccharomyces cerevisiae histone H2A variant Htz1 is acetylated by NuA4." Genes Dev **20**(6): 660-665.

Khorasanizadeh, S. (2004). "The nucleosome: from genomic organization to genomic regulation." Cell **116**(2): 259-272.

Klopf, E., L. Paskova, C. Sole, G. Mas, A. Petryshyn, F. Posas, U. Wintersberger, G. Ammerer and C. Schuller (2009). "Cooperation between the INO80 complex and histone chaperones determines adaptation of stress gene transcription in the yeast Saccharomyces cerevisiae." Mol Cell Biol **29**(18): 4994-5007.

Kobor, M. S., S. Venkatasubrahmanyam, M. D. Meneghini, J. W. Gin, J. L. Jennings, A. J. Link, H. D. Madhani and J. Rine (2004). "A protein complex containing the conserved Swi2/Snf2-related ATPase Swr1p deposits histone variant H2A.Z into euchromatin." PLoS Biol **2**(5): E131.

Koerber, R. T., H. S. Rhee, C. Jiang and B. F. Pugh (2009). "Interaction of transcriptional regulators with specific nucleosomes across the Saccharomyces genome." Mol Cell **35**(6): 889-902.

Kornberg, R. D. (1974). "Chromatin structure: a repeating unit of histones and DNA." Science **184**(4139): 868-871.

Kornberg, R. D. and L. Stryer (1988). "Statistical distributions of nucleosomes: nonrandom locations by a stochastic mechanism." Nucleic Acids Res **16**(14A): 6677-6690.

Krogan, N. J., K. Baetz, M. C. Keogh, N. Datta, C. Sawa, T. C. Kwok, N. J. Thompson, M. G. Davey, J. Pootoolal, T. R. Hughes, A. Emili, S. Buratowski, P. Hieter and J. F. Greenblatt (2004). "Regulation of chromosome stability by the histone H2A variant Htz1, the Swr1 chromatin remodeling complex, and the histone acetyltransferase NuA4." Proc Natl Acad Sci U S A **101**(37): 13513-13518.

Krogan, N. J., M. C. Keogh, N. Datta, C. Sawa, O. W. Ryan, H. Ding, R. A. Haw, J. Pootoolal, A. Tong, V. Canadien, D. P. Richards, X. Wu, A. Emili, T. R. Hughes, S. Buratowski and J. F. Greenblatt (2003). "A Snf2 family ATPase complex required for recruitment of the histone H2A variant Htz1." Mol Cell **12**(6): 1565-1576.

Kumar, S. V. and P. A. Wigge (2010). "H2A.Z-containing nucleosomes mediate the thermosensory response in Arabidopsis." Cell **140**(1): 136-147.

Langst, G. and P. B. Becker (2001). "ISWI induces nucleosome sliding on nicked DNA." Mol Cell **8**(5): 1085-1092.

Langst, G., P. B. Becker and I. Grummt (1998). "TTF-I determines the chromatin architecture of the active rDNA promoter." EMBO J **17**(11): 3135-3145.

Langst, G., E. J. Bonte, D. F. Corona and P. B. Becker (1999). "Nucleosome movement by CHRAC and ISWI without disruption or trans-displacement of the histone octamer." Cell **97**(7): 843-852.

Lavelle, C. (2007). "Transcription elongation through a chromatin template." Biochimie **89**(4): 516-527.

Li, Q., R. Burgess and Z. Zhang (2012). "All roads lead to chromatin: Multiple pathways for histone deposition." Biochim Biophys Acta **1819**(3-4): 238-246.

Liu, X., B. Li and GorovskyMa (1996). "Essential and nonessential histone H2A variants in Tetrahymena thermophila." Mol Cell Biol **16**(8): 4305-4311.

Lorch, Y., J. W. LaPointe and R. D. Kornberg (1987). "Nucleosomes inhibit the initiation of transcription but allow chain elongation with the displacement of histones." Cell **49**(2): 203-210.

Lowary, P. T. and J. Widom (1998). "New DNA sequence rules for high affinity binding to histone octamer and sequence-directed nucleosome positioning." J Mol Biol **276**(1): 19-42.

Luger, K., A. W. Mader, R. K. Richmond, D. F. Sargent and T. J. Richmond (1997). "Crystal structure of the nucleosome core particle at 2.8 A resolution." Nature **389**(6648): 251-260.

Luger, K., T. J. Rechsteiner and T. J. Richmond (1999). "Expression and purification of recombinant histones and nucleosome reconstitution." Methods in molecular biology (Clifton, N J) **119**: 1-16.

Luk, E., A. Ranjan, P. C. Fitzgerald, G. Mizuguchi, Y. Huang, D. Wei and C. Wu (2010). "Stepwise histone replacement by SWR1 requires dual activation with histone H2A.Z and canonical nucleosome." Cell **143**(5): 725-736.

Luk, E., N. D. Vu, K. Patteson, G. Mizuguchi, W. H. Wu, A. Ranjan, J. Backus, S. Sen, M. Lewis, Y. Bai and C. Wu (2007). "Chz1, a nuclear chaperone for histone H2AZ." Mol Cell **25**(3): 357-368.

Lusser, A. and J. T. Kadonaga (2003). "Chromatin remodeling by ATP-dependent molecular machines." Bioessays **25**(12): 1192-1200.

Madigan, J. P., H. L. Chotkowski and R. L. Glaser (2002). "DNA double-strand break-induced phosphorylation of Drosophila histone variant H2Av helps prevent radiation-induced apoptosis." Nucleic Acids Res **30**(17): 3698-3705.

Malik, H. S. and S. Henikoff (2003). "Phylogenomics of the nucleosome." Nat Struct Biol **10**(11): 882-891.

Maresca, T. J. and R. Heald (2006). "The long and the short of it: linker histone H1 is required for metaphase chromosome compaction." Cell Cycle **5**(6): 589-591.

Matangkasombut, O. and S. Buratowski (2003). "Different sensitivities of bromodomain factors 1 and 2 to histone H4 acetylation." Mol Cell **11**(2): 353-363.

Mavrich, T. N., I. P. Ioshikhes, B. J. Venters, C. Jiang, L. P. Tomsho, J. Qi, S. C. Schuster, I. Albert and B. F. Pugh (2008). "A barrier nucleosome model for statistical positioning of nucleosomes throughout the yeast genome." Genome Res **18**(7): 1073-1083.

Mayer, A., M. Lidschreiber, M. Siebert, K. Leike, J. Soding and P. Cramer (2010). "Uniform transitions of the general RNA polymerase II transcription complex." Nat Struct Mol Biol **17**(10): 1272-1278.

Meersseman, G., S. Pennings and E. M. Bradbury (1992). "Mobile nucleosomes--a general behavior." EMBO J **11**(8): 2951-2959.

Millar, C. B., F. Xu, K. Zhang and M. Grunstein (2006). "Acetylation of H2AZ Lys 14 is associated with genome-wide gene activity in yeast." Genes & development **20**(6): 711-722.

Mizuguchi, G., X. Shen, J. Landry, W. H. Wu, S. Sen and C. Wu (2004). "ATP-driven exchange of histone H2AZ variant catalyzed by SWR1 chromatin remodeling complex." Science **303**(5656): 343-348.

Narlikar, G. J., M. L. Phelan and R. E. Kingston (2001). "Generation and interconversion of multiple distinct nucleosomal states as a mechanism for catalyzing chromatin fluidity." Mol Cell **8**(6): 1219-1230.

Nemeth, A., S. Guibert, V. K. Tiwari, R. Ohlsson and G. Langst (2008). "Epigenetic regulation of TTF-I-mediated promoter-terminator interactions of rRNA genes." EMBO J **27**(8): 1255-1265.

Olins, A. L. and D. E. Olins (1974). "Spheroid chromatin units (v bodies)." Science **183**(4122): 330-332.

Orphanides, G., T. Lagrange and D. Reinberg (1996). "The general transcription factors of RNA polymerase II." Genes Dev **10**(21): 2657-2683.

Papamichos-Chronakis, M., J. E. Krebs and C. L. Peterson (2006). "Interplay between Ino80 and Swr1 chromatin remodeling enzymes regulates cell cycle checkpoint adaptation in response to DNA damage." Genes Dev **20**(17): 2437-2449.

Papamichos-Chronakis, M. and C. L. Peterson (2008). "The Ino80 chromatin-remodeling enzyme regulates replisome function and stability." Nat Struct Mol Biol **15**(4): 338-345.

Papamichos-Chronakis, M., S. Watanabe, O. J. Rando and C. L. Peterson (2011). "Global regulation of H2A.Z localization by the INO80 chromatin-remodeling enzyme is essential for genome integrity." Cell **144**(2): 200-213.

Park, Y.-J., P. N. Dyer, D. J. Tremethick and K. Luger (2004). "A new fluorescence resonance energy transfer approach demonstrates that the histone variant H2AZ stabilizes the histone octamer within the nucleosome." The Journal of biological chemistry **279**(23): 24274-24282.

Park, Y. J., J. V. Chodaparambil, Y. Bao, S. J. McBryant and K. Luger (2005). "Nucleosome assembly protein 1 exchanges histone H2A-H2B dimers and assists nucleosome sliding." J Biol Chem **280**(3): 1817-1825.

Pickart, C. M. (2001). "Ubiquitin enters the new millennium." Mol Cell **8**(3): 499-504.

Poccia, D. L. and G. R. Green (1992). "Packaging and unpackaging the sea urchin sperm genome." Trends Biochem Sci **17**(6): 223-227.

Raisner, R. M., P. D. Hartley, M. D. Meneghini, M. Z. Bao, C. L. Liu, S. L. Schreiber, O. J. Rando and H. D. Madhani (2005). "Histone variant H2A.Z marks the 5' ends of both active and inactive genes in euchromatin." Cell **123**(2): 233-248.

Rando, O. J. and H. Y. Chang (2009). "Genome-wide views of chromatin structure." Annu Rev Biochem **78**: 245-271.

Rangasamy, D., L. Berven, P. Ridgway and D. J. Tremethick (2003). "Pericentric heterochromatin becomes enriched with H2A.Z during early mammalian development." EMBO J **22**(7): 1599-1607.

Rangasamy, D., I. Greaves and D. J. Tremethick (2004). "RNA interference demonstrates a novel role for H2A.Z in chromosome segregation." Nat Struct Mol Biol **11**(7): 650-655.

Redon, C., D. Pilch, E. Rogakou, O. Sedelnikova, K. Newrock and W. Bonner (2002). "Histone H2A variants H2AX and H2AZ." Curr Opin Genet Dev **12**(2): 162-169.

Reinke, H. and W. Horz (2003). "Histones are first hyperacetylated and then lose contact with the activated PHO5 promoter." Mol Cell **11**(6): 1599-1607.

Rhodes, D. and R. A. Laskey (1989). "Assembly of nucleosomes and chromatin in vitro." Methods Enzymol **170**: 575-585.

Ridgway, P., K. D. Brown, D. Rangasamy, U. Svensson and D. J. Tremethick (2004). "Unique residues on the H2A.Z containing nucleosome surface are important for Xenopus laevis development." J Biol Chem **279**(42): 43815-43820.

Ridgway, P., D. Rangasamy, L. Berven, U. Svensson and D. J. Tremethick (2004). "Analysis of histone variant H2A.Z localization and expression during early development." Methods Enzymol **375**: 239-252.

Rippe, K., A. Schrader, P. Riede, R. Strohner, E. Lehmann and G. Langst (2007). "DNA sequence- and conformation-directed positioning of nucleosomes by chromatin-remodeling complexes." Proc Natl Acad Sci U S A **104**(40): 15635-15640.

Sadeghi, L., C. Bonilla, A. Stralfors, K. Ekwall and J. P. Svensson (2011). "Podbat: a novel genomic tool reveals Swr1-independent H2A.Z incorporation at gene coding sequences through epigenetic meta-analysis." PLoS Comput Biol **7**(8): e1002163.

Santisteban, M. S., M. Hang and M. M. Smith (2011). "Histone variant H2A.Z and RNA polymerase II transcription elongation." Mol Cell Biol **31**(9): 1848-1860.

Santos-Rosa, H., R. Schneider, B. E. Bernstein, N. Karabetsou, A. Morillon, C. Weise, S. L. Schreiber, J. Mellor and T. Kouzarides (2003). "Methylation of histone H3 K4 mediates association of the Isw1p ATPase with chromatin." Mol Cell **12**(5): 1325-1332.

Sarcinella, E., P. C. Zuzarte, P. N. Lau, R. Draker and P. Cheung (2007). "Monoubiquitylation of H2A.Z distinguishes its association with euchromatin or facultative heterochromatin." Mol Cell Biol **27**(18): 6457-6468.

Schmid, M., T. Durussel and U. K. Laemmli (2004). "ChIC and ChEC; genomic mapping of chromatin proteins." Mol Cell **16**(1): 147-157.

Schones, D. E., K. Cui, S. Cuddapah, T. Y. Roh, A. Barski, Z. Wang, G. Wei and K. Zhao (2008). "Dynamic regulation of nucleosome positioning in the human genome." Cell **132**(5): 887-898.

Schwabish, M. A. and K. Struhl (2004). "Evidence for eviction and rapid deposition of histones upon transcriptional elongation by RNA polymerase II." Mol Cell Biol **24**(23): 10111-10117.

Segal, E., Y. Fondufe-Mittendorf, L. Chen, A. Thastrom, Y. Field, I. K. Moore, J. P. Wang and J. Widom (2006). "A genomic code for nucleosome positioning." Nature **442**(7104): 772-778.

Shen, X., G. Mizuguchi, A. Hamiche and C. Wu (2000). "A chromatin remodelling complex involved in transcription and DNA processing." Nature **406**(6795): 541-544.

Shimada, K., Y. Oma, T. Schleker, K. Kugou, K. Ohta, M. Harata and S. M. Gasser (2008). "Ino80 chromatin remodeling complex promotes recovery of stalled replication forks." Curr Biol **18**(8): 566-575.

Simic, R., D. L. Lindstrom, H. G. Tran, K. L. Roinick, P. J. Costa, A. D. Johnson, G. A. Hartzog and K. M. Arndt (2003). "Chromatin remodeling protein Chd1 interacts with transcription elongation factors and localizes to transcribed genes." EMBO J **22**(8): 1846-1856.

Smith, A. P., A. Jain, R. B. Deal, V. K. Nagarajan, M. D. Poling, K. G. Raghothama and R. B. Meagher (2010). "Histone H2A.Z regulates the expression of several classes of phosphate starvation response genes but not as a transcriptional activator." Plant Physiol **152**(1): 217-225.

Smith, S. and B. Stillman (1989). "Purification and characterization of CAF-I, a human cell factor required for chromatin assembly during DNA replication in vitro." Cell **58**(1): 15-25.

Sogo, J. M., H. Stahl, T. Koller and R. Knippers (1986). "Structure of replicating simian virus 40 minichromosomes. The replication fork, core histone segregation and terminal structures." J Mol Biol **189**(1): 189-204.

Srinivasan, S., J. A. Armstrong, R. Deuring, I. K. Dahlsveen, H. McNeill and J. W. Tamkun (2005). "The Drosophila trithorax group protein Kismet facilitates an early step in transcriptional elongation by RNA Polymerase II." Development **132**(7): 1623-1635.

Stargell, L. A., J. Bowen, C. A. Dadd, P. C. Dedon, M. Davis, R. G. Cook, C. D. Allis and M. A. Gorovsky (1993). "Temporal and spatial association of histone H2A variant hv1 with transcriptionally competent chromatin during nuclear development in Tetrahymena thermophila." Genes Dev **7**(12B): 2641-2651.

Strahl, B. D. and C. D. Allis (2000). "The language of covalent histone modifications." Nature **403**(6765): 41-45.

Straube, K., J. S. Blackwell, Jr. and L. F. Pemberton (2010). "Nap1 and Chz1 have separate Htz1 nuclear import and assembly functions." Traffic **11**(2): 185-197.

Strohner, R., M. Wachsmuth, K. Dachauer, J. Mazurkiewicz, J. Hochstatter, K. Rippe and G. Langst (2005). "A 'loop recapture' mechanism for ACF-dependent nucleosome remodeling." Nat Struct Mol Biol **12**(8): 683-690.

Studitsky, V. M., G. A. Kassavetis, E. P. Geiduschek and G. Felsenfeld (1997). "Mechanism of transcription through the nucleosome by eukaryotic RNA polymerase." Science **278**(5345): 1960-1963.

Stuwe, T., M. Hothorn, E. Lejeune, V. Rybin, M. Bortfeld, K. Scheffzek and A. G. Ladurner (2008). "The FACT Spt16 "peptidase" domain is a histone H3-H4 binding module." Proc Natl Acad Sci U S A **105**(26): 8884-8889.

Suto, R. K., M. J. Clarkson, D. J. Tremethick and K. Luger (2000). "Crystal structure of a nucleosome core particle containing the variant histone H2A.Z." Nature structural biology **7**(12): 1121-1124.

Svotelis, A., N. Gevry and L. Gaudreau (2009). "Regulation of gene expression and cellular proliferation by histone H2A.Z." Biochemistry and cell biology = Biochimie et biologie cellulaire **87**(1): 179-188.

Talbert, P. B. and S. Henikoff (2010). "Histone variants--ancient wrap artists of the epigenome." Nat Rev Mol Cell Biol **11**(4): 264-275.

Thakar, A., P. Gupta, T. Ishibashi, R. Finn, B. Silva-Moreno, S. Uchiyama, K. Fukui, M. Tomschik, J. Ausio and J. Zlatanova (2009). "H2A.Z and H3.3 histone variants affect nucleosome structure: biochemical and biophysical studies." Biochemistry **48**(46): 10852-10857.

Thastrom, A., P. T. Lowary, H. R. Widlund, H. Cao, M. Kubista and J. Widom (1999). "Sequence motifs and free energies of selected natural and non-natural nucleosome positioning DNA sequences." J Mol Biol **288**(2): 213-229.

Thatcher, T. H. and M. A. Gorovsky (1994). "Phylogenetic analysis of the core histones H2A, H2B, H3, and H4." Nucleic Acids Res **22**(2): 174-179.

Thiriet, C. and J. J. Hayes (2005). "Replication-independent core histone dynamics at transcriptionally active loci in vivo." Genes Dev **19**(6): 677-682.

Treand, C., I. du Chene, V. Bres, R. Kiernan, R. Benarous, M. Benkirane and S. Emiliani (2006). "Requirement for SWI/SNF chromatin-remodeling complex in Tat-mediated activation of the HIV-1 promoter." EMBO J **25**(8): 1690-1699.

Tsankov, A. M., D. A. Thompson, A. Socha, A. Regev and O. J. Rando (2010). "The role of nucleosome positioning in the evolution of gene regulation." PLoS Biol **8**(7): e1000414.

van Attikum, H., O. Fritsch, B. Hohn and S. M. Gasser (2004). "Recruitment of the INO80 complex by H2A phosphorylation links ATP-dependent chromatin remodeling with DNA double-strand break repair." Cell **119**(6): 777-788.

Vaquero, A., A. Loyola and D. Reinberg (2003). "The constantly changing face of chromatin." Sci Aging Knowledge Environ **2003**(14): RE4.

Venters, B. J. and B. F. Pugh (2009). "A canonical promoter organization of the transcription machinery and its regulators in the Saccharomyces genome." Genome Res **19**(3): 360-371.

von der Haar, T. (2008). "A quantitative estimation of the global translational activity in logarithmically growing yeast cells." BMC Syst Biol **2**: 87.

Wan, Y., R. A. Saleem, A. V. Ratushny, O. Roda, J. J. Smith, C. H. Lin, J. H. Chiang and J. D. Aitchison (2009). "Role of the histone variant H2A.Z/Htz1p in TBP recruitment, chromatin dynamics, and regulated expression of oleate-responsive genes." Mol Cell Biol **29**(9): 2346-2358.

Wang, A. Y., J. M. Schulze, E. Skordalakes, J. W. Gin, J. M. Berger, J. Rine and M. S. Kobor (2009). "Asf1-like structure of the conserved Yaf9 YEATS domain and role in H2A.Z deposition and acetylation." Proc Natl Acad Sci U S A **106**(51): 21573-21578.

Weber, C. M., J. G. Henikoff and S. Henikoff (2010). "H2A.Z nucleosomes enriched over active genes are homotypic." Nat Struct Mol Biol **17**(12): 1500-1507.

Weiner, A., A. Hughes, M. Yassour, O. J. Rando and N. Friedman (2010). "High-resolution nucleosome mapping reveals transcription-dependent promoter packaging." Genome Res **20**(1): 90-100.

West, M. H. and W. M. Bonner (1980). "Histone 2A, a heteromorphous family of eight protein species." Biochemistry **19**(14): 3238-3245.

Workman, J. L. (2006). "Nucleosome displacement in transcription." Genes Dev **20**(15): 2009-2017.

Wratting, D., A. Thistlethwaite, M. Harris, L. A. Zeef and C. B. Millar (2012). "A conserved function for the H2A.Z C-terminus." J Biol Chem.

Wu, R. S. and W. M. Bonner (1981). "Separation of basal histone synthesis from S-phase histone synthesis in dividing cells." Cell **27**(2 Pt 1): 321-330.

Wu, R. S., S. Tsai and W. M. Bonner (1982). "Patterns of histone variant synthesis can distinguish G0 from G1 cells." Cell **31**(2 Pt 1): 367-374.

Wu, W. H., S. Alami, E. Luk, C. H. Wu, S. Sen, G. Mizuguchi, D. Wei and C. Wu (2005). "Swc2 is a widely conserved H2AZ-binding module essential for ATP-dependent histone exchange." Nat Struct Mol Biol **12**(12): 1064-1071.

Zhang, H., D. N. Roberts and B. R. Cairns (2005). "Genome-wide dynamics of Htz1, a histone H2A variant that poises repressed/basal promoters for activation through histone loss." Cell **123**(2): 219-231.

Zhang, Z., C. J. Wippo, M. Wal, E. Ward, P. Korber and B. F. Pugh (2011). "A packing mechanism for nucleosome organization reconstituted across a eukaryotic genome." Science **332**(6032): 977-980.

Zhou, B. O., S. S. Wang, L. X. Xu, F. L. Meng, Y. J. Xuan, Y. M. Duan, J. Y. Wang, H. Hu, X. Dong, J. Ding and J. Q. Zhou (2010). "SWR1 complex poises heterochromatin boundaries for antisilencing activity propagation." Mol Cell Biol **30**(10): 2391-2400.

Zlatanova, J. and A. Thakar (2008). "H2A.Z: view from the top." Structure **16**(2): 166-179.

Appendix

List of publications

Vogler, C.*, **Huber, C.***, Waldmann, T., Ettig, R., Braun, L., Izzo, A., Daujat, S., Chassignet, I., Lopez-Contreras, A.J., Fernandez-Capetillo, O., Dundr, M., Rippe, K., Längst, G., and Schneider, R. (2010);
Histone H2A C-terminus regulates chromatin dynamics, remodeling, and histone H1 binding. PLoS Genet. 2010 Dec 9; 6(12)

* equal author-contribution

Huber C., Griesenbeck J., Längst G. (2012);
Mechanisms of H2A.Z deposition in *Saccharomyces cerevisiae* – in preparation

Huber C., Griesenbeck J., Längst G. (2012);
In vitro and *in vivo* positioning differences of H2A.Z containing nucleosomes – in preparation

Conferences

June 26th – 29th 2008: The Epigenome – Network of Excellence (NoE) Symposium in Madrid, Spain.

September 12th – 14th 2011: International Symposium “Chromatin Changes in Differentiation and Malignancies” in Gießen.
Title of poster: “Deposition of H2A.Z in *Saccharomyces cerevisiae*”

Acknowledgments – Danksagung

An dieser Stelle möchte ich allen Personen danken, die zum Gelingen dieser Arbeit beigetragen haben.

Bei Prof. Dr. Gernot Längst möchte ich mich für die Vergabe eines interessanten Projektes bedanken und sein Vertrauen dieses „von klein auf“ selbstständig zu bearbeiten. Durch seinen Ideenreichtum schaffte er es immer, den Laboralltag spannend zu gestalten. Weiterhin bedanke ich mich für die Chancen zur Teilnahme an interessanten Tagungen und die Möglichkeit ein Praktikum in Chile zu betreuen.

Herrn Prof. Dr. Klaus Grasser danke ich für die Übernahme des Zweitgutachtens.

Herrn Prof. Dr. Michael Thomm danke ich für die Übernahme des Amtes als Drittprüfer.

PD Dr. Joachim Griesenbeck danke ich recht herzlich für die fachliche und methodische Hilfsbereitschaft, die Einführung in die Welt der Hefen und seine ständige Diskussionsbereitschaft.

Dr. Philipp Milkereit danke ich für seine außerordentliche Fähigkeit sich in kürzester Zeit in fremde Projekte hinein zu denken und sie durch zahlreiche Fragen zu bereichern.

Mein Dank gilt allen Mitgliedern des Lehrstuhls Biochemie III, wo immer eine wirklich außergewöhnliche Arbeitsatmosphäre herrschte. Schee war’s.
Ein großer Dank gebührt an dieser Stelle der AG Griesi für den ausgeübten Pufferkommunismus, mit dem sie mir („von da drüben“) oftmals sehr geholfen haben.

Elisabeth Silberhorn, Regina Gröbner-Ferreira, Christine Lemche-Auerbach, Gisela Pöll, Kristin Hergert, Jan Linnemann und Ulrike Stöckl danke ich für ihre unermüdlichen Versuche eine funktionierende Infrastruktur aufrechtzuerhalten.

Dr. Helen Hoffmeister danke ich für ihren Enthusiasmus, ihre Hilfsbereitschaft und ihre Unterstützung. Unsere manchmal unverständlichen Lachanfälle und unser gemeinsamer Sinn für den Unsinn haben den Laboralltag sehr bereichert.

Virginia Babl, Stephan Hamperl und Manuel Wittner bin ich sehr dankbar für die gegenseitige Arbeitsteilung im Isolab. Ein besonderer Dank an dich, Stephan, dass ich dir jede noch so triviale Frage auch wiederholt stellen durfte, du immer ein offenes Ohr für die großen und kleinen Laborsorgen hattest und mich morgens regelmäßig mit Kaffee versorgt hast.

Den Korrekturlesern: Daniel, Felix und Stephan, vielen Dank für die investierte Zeit und eure Kommentare.

Danke an die ehemaligen „Insassen“ in BIO 4.1.05 und 4.1.33 für so manch feierabendlichen Ratsch, unzählige dumme Sprüche und das gelegentliche Kaffee-Asyl.

Daniel und Lena danke ich für ihre langjährige Freundschaft, ihr Verständnis, ihre Hilfsbereitschaft und Unterstützung, sowie zahlreiche Kletterausflüge, Koch-, Ratsch- und Fußballabende.

Felix, danke für deine Geduld, deine Denkanstöße, dafür dass du meine „Stimme der Vernunft“ bist und besonders für die gemeinsame Zeit außerhalb des Labors.

Meiner Familie habe ich alles zu verdanken! Danke für eure Unterstützung in allen Lebenslagen, euer Vertrauen in mich und dass ich mich auf euch immer verlassen kann.